**Progress Annual Report**

# HPT Annex 54:
# Heat Pump Systems with Low-GWP Refrigerants

## TASKS 1, 2, AND 3

**April 2023**

**Compiled and Edited by**

**Lei Gao, Ph.D., and Yunho Hwang, Ph.D. (Operating Agent)**

**Center for Environmental Energy Engineering**
**Department of Mechanical Engineering**
**University of Maryland**
**College Park, MD 20742, USA**
**Contact: yhhwang@umd.edu ; +1-301-405-5247**

# Executive Summary

The following document presents an all-encompassing and current analysis of the latest research on developing and optimizing heat pump systems using low global warming potential (GWP) refrigerants. It also features a cutting-edge review of the low-GWP refrigerant application to heat pumps and a summary of the industry's collaborative efforts of researchers, engineers, and regulation committees. The report has the following chapters.

Chapter 1 investigates the detailed performance of novel heat exchangers and system design under cold climate conditions or during transient operations, along with a brief yet informative review of low GWP refrigerants. The low GWP refrigerant review highlights the importance of low charge for flammable refrigerants and alternative refrigerants for R-410A.

Chapter 2 presents a thorough and informative update on market status, research, and development efforts in Sweden regarding low GWP refrigerants and their applications in heat pump systems. Three research entities provide detailed progress reports on various aspects, including case studies, design guidelines for component and system optimization, and the impact of design advancements on Life Cycle Climate Performance (LCCP) reduction. The chapter also encompasses several experimental-oriented projects focused on the long-term evaluation of novel heat pump systems utilizing low GWP refrigerants.

Chapter 3 discusses the investigation of the potential replacement of high GWP refrigerants with low GWP refrigerants in heat pumps to reduce greenhouse gas emissions. Task 3 focuses on the impact of changing a heat pump system from an R-410A baseline system to a charge-optimized R-290 system on the LCCP of a heat pump system. The LCCP of both systems was calculated using Pack Calculation Pro, and the indirect emissions were calculated using the IIR-LCCP-Calculation-Tool. The findings show that the charge-optimized R-290 system has better direct $CO_{2e}$ emissions, energy efficiency performance, and a significantly lower LCCP value than the R-410A baseline system. The study supports the replacement of high GWP refrigerants with low GWP refrigerants and highlights the importance of reducing refrigerant charge and improving refrigerant leakage rates.

This report aims to offer an updated and comprehensive review of component research and development involving a review of state-of-the-art technologies, case studies, and design guidelines for optimizing components and systems. The contributions of each chapter's authors are greatly appreciated, as this report would not have been possible without their efforts.

# Table of Contents

# 1 Country Report: United States

**Prepared by:**

**James Tancabel[1], Lei Gao[1], Vikrant Aute[1],Yunho Hwang[1]***

**[1] Center for Environmental Energy Engineering,**
**Department of Mechanical Engineering, University of Maryland,**
**4164 Glenn Martin Hall Bldg., College Park, MD 20742, United States**

*** Corresponding Author, yhhwang@umd.edu**

## 1.1 Optimum Component Designs and Impacts on Emission Reduction

This chapter first provides an in-depth examination of the recent advancements in simulation tools and optimization algorithms, allowing researchers to design high-performance, highly compact air-to-refrigerant heat exchangers (HXs) that do not require fins. Such novel HXs have reduced size, weight, cost, and refrigerant charge compared to current state-of-the-art HXs while maintaining or improving system-level performance. The report presents an HX optimization framework featuring automated CFD and FEA simulations and approximation-assisted optimization for optimizing residential air conditioning systems' condensers for three refrigerants: R-410A, R-32, and R-454B. The optimal HXs achieve at least 20% reductions in airside pressure drop and envelope volume, up to 11% reduction in tube material volume, and more than 40% reduction in tube internal volume while delivering similar capacity to the state-of-the-art baseline HX. The differences between the refrigerant-specific optimal HXs are also discussed in detail to shed light on how the refrigerant choice impacts the final HX designs. Then, one novel refrigeration cycle has been thoroughly investigated for its performance and efficiency. The performance of carbon emissions associated with Heat Pumps (HP) operating under low-temperature conditions. Ultimately, this analysis can inform the design and implementation of more sustainable and environmentally friendly HP systems. Although the idea was initially proposed for cold climates, its potential usefulness extends to a wide range of other applications. The findings of this study provide valuable insights into the potential of these novel cycles as energy-efficient and environmentally friendly alternatives to conventional heating systems.

### 1.1.1 Optimization of novel air-to-refrigerant heat exchangers for lower-GWP refrigerants in air-conditioning systems

#### 1.1.1.1 Background

Air-to-refrigerant heat exchangers (HXs) are fundamental components in all HVAC&R systems. Compact HXs, i.e., HXs with characteristic tube diameters smaller than 6.0 mm [1], are of particular interest to researchers since their intrinsically high heat transfer area to envelope volume ratio can yield significant size reductions. However, these small characteristic diameter tubes do not have adequate primary heat transfer area to achieve the required thermal resistance to satisfy the HX capacity requirements. Thus, compact HXs typically utilize fins to increase the airside heat transfer area and satisfy the thermal resistance requirements. However, fins have inherent drawbacks, including increased airside pressure drop, material consumption, and fouling/frosting potential. Recent research [2] has noted that finless surfaces have a superior airside thermal-hydraulic performance to similarly-sized finned surfaces as the characteristic diameter decreases. Small-diameter, round-tube HXs have also been well-studied throughout the literature [3-6].

More recently, Bacellar et al. [2,7] argued that classical HX design paradigms should evolve to leverage modern computational and manufacturing capabilities. To this end, the authors developed a comprehensive multi-scale analysis and shape-and-topology optimization framework capable of designing finless compact HXs which utilize novel, -small-diameter, non-round tubes. Their methodology was experimentally validated using an additively manufactured proof-of-concept HX design, further strengthening the case for implementing shape optimization and additive manufacturing into HX design ideology.

In a related work, Radermacher et al. [8] suggested that non-round, shape-optimized tube designs may lack the required mechanical strength for pressure- holding, thereby requiring detailed structural analyses to verify pressure-holding capabilities of all candidate geometries. Additionally, Tancabel et al. [9] noted that no air-to-refrigerant HX shape-and-topology optimization studies explicitly considered tube mechanical strength.

In this chapter, we present the application of an HX design optimization methodology which features integrated multi-scale and multi-physics analyses and shape-and-topology optimization [10-11] to optimize a residential air-conditioning (A/C) units' condensers using novel, shape-optimized non-round tubes which can be conventionally (i.e., non-additively) manufactured. We considered three different refrigerants: (i) R-410A (GWP = 2,088), the industry standard for US residential A/C units, (ii) R-32, a lower-GWP (GWP = 677) alternative to R-410A, which is the most popular replacement for R-410A in the EU [12-16], and (iii) R-454B, an even lower-GWP (GWP = 466) alternative to R-410A (compared to R-32) [16-19]. Comparisons between the optimal HX designs for each refrigerant are discussed in detail to show how the refrigerant choice impacts the final HX design.

### 1.1.1.2 Methodology

#### 1.1.1.2.1 Design optimization framework

The HX design optimization framework (Fig. 1) utilizes Approximation-Assisted Optimization (AAO) [20] involving automated Computational Fluid Dynamics (CFD) [21] and Finite Element Analysis (FEA) simulations [10-11], Kriging meta-models [22], and optimization with a multi-objective genetic algorithm (MOGA) [23].

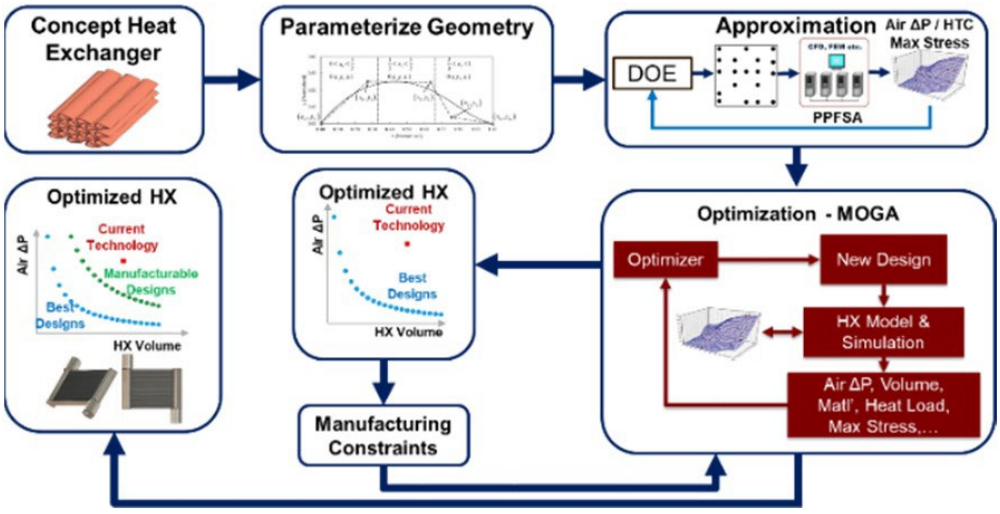


**Figure. 1 Numerical optimization framework.**

#### 1.1.1.2.2 Problem description

High-performance HXs featuring a novel, non-round tubes have been investigated for many applications [10-11, 24]. This research uses the optimization framework to design novel, finless, air-to-refrigerant condensers for residential A/C applications using lower-GWP alternative refrigerants. The baseline HX is a commercially- available, state-of-the-art nominal 5.28 kW (1.5-Ton) tube-fin air-to-R-410A condenser. Three refrigerants are investigated: (i) R-410A, (ii) R-32,

and (iii) R-454B. The inlet conditions for each refrigerant are taken from commercially-available residential A/C units with a nominal 5.28 kW (1.5-Ton) capacity [25]. Sample schematics for a representative tube-fin HX and a finless HX with shape-optimized tubes are shown in Figure 2.

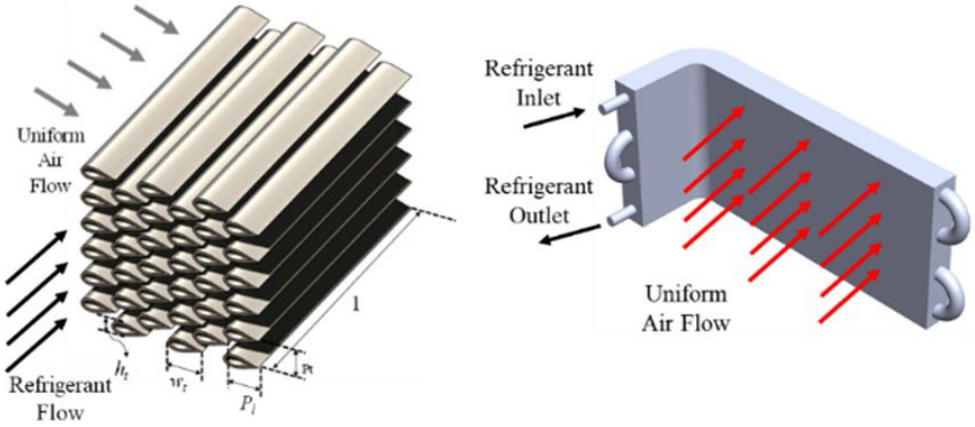


**Figure. 2 (Left) Generic HX with shape-optimized tubes; (Right) Generic multi-pass tube-fin condenser.**

The HXs are in cross-flow, and all HX models assume the following: (i) uniform inlet air velocity on the HX face and (ii) fully-developed, uniform refrigerant flow. The airside thermal-hydraulic performance was predicted using CFD, and the tube-level mechanical performance was computed using FEA. Refrigerant-side performance was computed using existing correlations for single and two-phase flow in small-diameter channels. The framework utilizes fourth-order Non-Uniform Rational B-Splines (NURBS) [26] to represent the novel, non-round tube shapes (Fig. 3). The tube shape considered in this study [2] has been conventionally manufactured in both copper and aluminum. Burst pressure testing and FEA modeling of the copper tubes showed minimal deformation up to 20.0 MPa, validating the tube's structural strength [27]. We, therefore, considered the copper version hereafter.

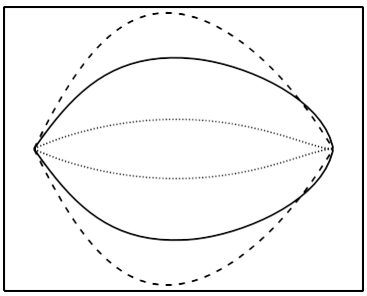

**Figure. 3 Sample non-round tube shapes.**

1.1.1.2.3 Parallel parameterized fluid and structural analysis

It is impractical to simulate an entire multi-variable Design of Experiments (DoE) manually, and thus the entire simulation process must be automated to reduce the computational time burden. To this end, Abdelaziz et al. [21] developed Parallel Parameterized CFD (PPCFD) to automate CFD simulations, resulting in more than 90% engineering time savings. Similarly, Tancabel et al.

[10-11] integrated automated FEA simulations into the PPCFD framework for multi-physics analyses of HXs utilizing shape-and-topology optimized tubes. Their framework was termed Parallel Parameterized Fluid and Structural Analysis (PPFSA).

As mentioned above, the modeling and experimental validation of the copper tube structural integrity eliminates the need to consider the structural component of PPFSA. Thus, it is only necessary to consider the CFD component of PPFSA, which is explained in detail in the following sections. All present analyses utilized the ANSYS® 18.0 platform [28-29]. Geometry and meshing were performed using Gambit® 2.4.6 [28], and all CFD simulations were run using Ansys® Fluent 18.0 [29].

1.1.1.2.4 CFD modeling, post-processing, and uncertainty analysis

The airside CFD computational domain (Fig. 4) was a two-dimensional cross-section of the HX in the depth-wise direction wherein all end effects were negligible, and the working fluid was dry air. In the near-wall region, an inflation layer mesh was employed with a growth ratio of 1.2 to capture the boundary layer physics more accurately. The core mesh was a pave mesh scheme where the average element size was the same as the inflation layer's last row.

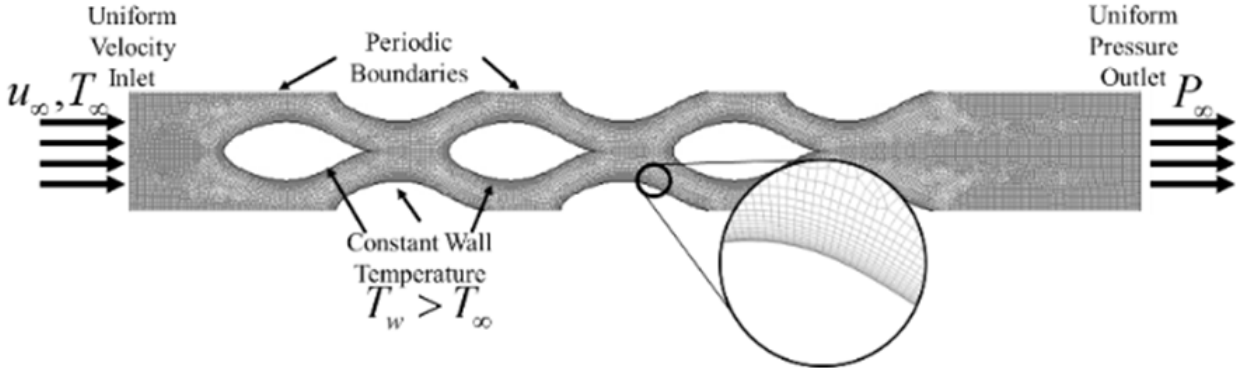


**Figure. 4 Sample CFD domain, mesh, & boundary conditions.**

The left boundary was a uniform velocity and temperature inlet, and the right was a uniform atmospheric pressure outlet. The tube walls were fixed to a constant temperature, and periodic boundaries were applied at the upper and lower domain boundaries. The dry air thermophysical properties were computed using polynomial curve fits as a function of temperature, while the density was computed using the ideal gas law. The realizable k-ε (RKE) model [30] was utilized to model turbulence. The convergence criteria utilized is maximum residuals, and the limits were set to $1e^{-05}$ for continuity and momentum, $1e^{-06}$ for energy, and $1e^{-03}$ for turbulence. If these convergence criteria were not met, but the simulation stabilized to a solution, the simulation was considered converged if the standard deviation of the final 100 iterations was less than 0.5% of the average of those same 100 iterations.

The CFD simulations were utilized to determine the airside thermal-hydraulic performance only, and thus the wall and refrigerant thermal resistances could be neglected. This allows for the airside heat transfer coefficient to be efficiently computed using UA-Log Mean Temperature Difference (UA-LMTD) method as given in equation (1) [31]. In contrast, the airside pressure drop was computed as the difference between the inlet and outlet static pressures, as given in equation (2).

$$\mathrm{hair} = \mathrm{mc_p}\, ln\left[\frac{T_w - T_{in}}{T_w - T_{out}}\right] \qquad (1)$$

$$\delta P_{air} = P_{in} - P_{out} \quad (2)$$

The CFD modeling grid resolution uncertainty was quantified using the Grid Convergence Index (GCI) method [32-35] for all boundary designs using three grid resolutions and a constant refinement ratio of 1.3. The GCI for a given design was computed using the absolute relative difference for a metric of interest (in this case, hair and ΔPair) between two consecutive grid sizes [34-35]. All CFD uncertainty quantification results are tabulated in Table 1.

**Table. 1 CFD uncertainty quantification using GCI.**

| **Metric** | ***hair*** | **Δ*Pair*** |
|---|---|---|
| Designs with GCI ≤ 10% | 96% | 91% |
| Max | 16.5% | 54.6% |
| Average | 0.9% | 1.25 |
| Median | 2.0% | 3.3% |

1.1.1.2.5 Metamodeling

If a new CFD simulation were required for each individual generated by the optimizer during a single optimization run, tens of thousands of CFD simulations would be required. To reduce this computational burden, this research employed approximation-assisted optimization [20], wherein a simplified model, sometimes called a metamodel capable of accurately representing the simulation behavior, was utilized to carry out the optimization. In this case, metamodels were utilized to quickly and efficiently compute the airside thermal-hydraulic performance.

A 5000-sample Design of Experiments (DoE) generated using Latin Hypercube Sampling (LHS) [36] was simulated using PPFSA, and Kriging metamodels [22] were built using 2673 converged samples. The metamodels were then verified by comparing the predicted (metamodel) responses to simulated (CFD) responses for 544 converged random samples. The Metamodel Acceptance Score (MAS) [37] was utilized to quantify the metamodel accuracy. The MAS gives the percentage of predicted responses whose absolute relative error compared to the simulated response was less than a prescribed threshold. The metamodel verification results are summarized in Table 2 and Figure 5.

**Table. 2 Metamodel verification statistics**

| **Metric** | ***hair*** | **Δ*Pair*** |
|---|---|---|
| Mean Absolute Error | 6.30 | 14.27 |
| Root Mean Square Error | 13.51 | 41.70 |
| MAS (10%) | 97.97% | 70.95% |
| MAS (20%) | 99.26% | 90.99% |

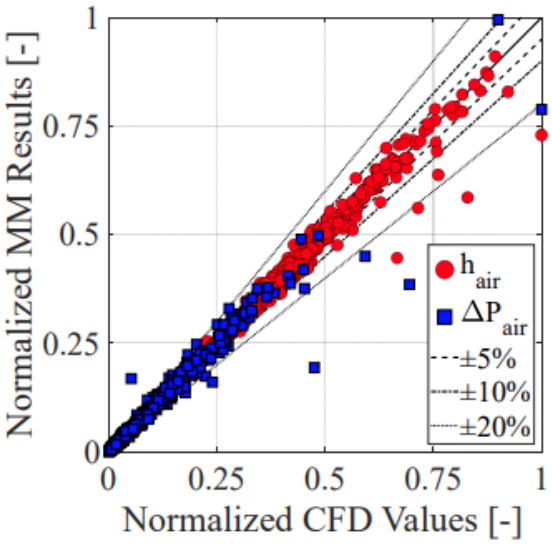


**Figure 5. Metamodel verification results.**

1.1.1.2.6 Multi-Objective Optimization

This research presents the application of a multi-scale and multi-physics analysis with shape-and-topology optimization methodology [2,7,10-11], which leverages a Multi-Objective Genetic Algorithm (MOGA) [23] to model full HXs with novel tube shapes and topologies. Full HX models were built and simulated using an in-house, experimentally-validated air-to-refrigerant HX modeling tool [39]. CFD-based metamodels were utilized to predict the airside thermal-hydraulic performance (hair, ΔPair). Refrigerant-side thermal-hydraulic performance was evaluated using empirical correlations for single- phase flow and (condensing) two-phase flow in small channels (Tab. 3). Refrigerant thermodynamic property calculations utilized NIST REFPROP v10.0 [39] augmented with polynomial curve fits as proposed by Aute and Radermacher [40].

**Table. 3 Thermal-hydraulic performance correlations**

| **Operating Mode** | ***$h_{ref}$ Correlation*** | ***$\Delta P_{ref}$ Correlation*** |
|---|---|---|
| Air | CFD Metamodels | |
| Liquid refrigerant | Gnielinski (1976) [41] | Churchill (1977) [42] |
| Two-phase refrigerant | Shah (2019) [43] | Xu-Fang (2013) [44] |
| Vapor refrigerant | Gnielinski (1976) [41] | Churchill (1977) [42] |

### 1.1.1.3 Optimization Results & Discussion

1.1.1.3.1 Optimization Problem Formulation

This research considered a bi-objective optimization problem as defined in equation (3), where the objectives are to minimize airside pressure drop and HX core envelope volume. The overall objective was to design air-to-refrigerant condensers featuring the novel non-round tube shape,

which was conventionally manufactured in copper as discussed above [25, 27] for three different refrigerants: (i) R-410A, (ii) R-32, and (iii) R-454B. For each refrigerant, the inlet air (temperature, volume flow rate) and refrigerant states (temperature, pressure, mass flow rate) were fixed to that of commercially-available residential units with a nominal 5.28 kW (1.5-Ton) capacity [25].

$$\begin{aligned} &\min \Delta P_{air}, V_{HX} \\ &\text{s.t.} \\ &\Delta P_{air} \le 2.0 \cdot \Delta P_{air,BL} \quad V_{HX} \le V_{HX,BL} \\ &0.5 \le {H_{HX}}/{L_{HX}} \le 2.0 \quad A_f \le A_{f,BL} \\ &\Delta T_{SC,BL} - 1.0\,\mathrm{K} \le \Delta T_{SC} \le \Delta T_{SC,BL} \end{aligned} \tag{3}$$

All optimal HXs have a 60%/40% two-fluid-pass configuration, i.e., the first fluid pass contains 60% of the tubes, and the second fluid pass contains the remaining tubes. The airside pressure drop cannot exceed two times the baseline value, and the HX frontal area cannot exceed the baseline value. Moreover, the HX frontal aspect ratio (height-to-length ratio) was constrained such that the HX was no more than two times as tall as long or vice versa. The HX capacity constraint was considered by constraining the condenser outlet subcooling to be at least the same, but no more than 1.0 K more, compared to the baseline value. Note that the problem statement is sufficiently general, and it is possible to find additional promising designs by examining other pass configurations and removing the HX face area constraint. In total, five (5) design variables were considered: horizontal tube spacing, vertical tube spacing, number of tube banks, number of tubes per bank, and inlet air velocity.

Five separate optimization runs were conducted for each refrigerant (R-410A, R-32, and R-454B). The optimal designs presented in the following sections are the non-dominated set of designs found by combining the output from all optimization runs (for each refrigerant separately) and conducting non-dominated sorting to find the best designs for each refrigerant, respectively. Additional MOGA settings are summarized in Table 4.

**Table. 4 Thermal-hydraulic performance correlations**

| **Type** | Unit | Value |
|---|---|---|
| Optimization runs per refrigerant. | - | 5 |
| Population size | - | 50 |
| Replacement | % | 20 |
| Iterations | - | 300 |

1.1.1.3.2 Optimization Results

Figures 6 – 8 present a summary of the optimization results colored by HX face area (Fig. 6), core material volume (Fig. 7), and core internal volume (Fig. 8). All metrics are normalized with respect to the baseline, and the dashed lines represent the 20%-20% improvement region for each

objective. For the baseline airside pressure drop, the optimal designs for each refrigerant can achieve ~46% reduction in HX core envelope volume, ~30% reduction in HX face area, ~7% in tube material volume, and ~50% reduction in internal tube volume. For the baseline HX core envelope volume, the optimal designs for each refrigerant can achieve ~46% reduction in airside pressure drop, ~9% reduction in HX face area, and ~20% reduction in tube internal volume. However, for those designs, the tube material volume is ~27% greater than the baseline, which would result in significantly higher manufacturing costs. From an environmental standpoint, the significant internal tube volume reductions will correspond to significant charge reductions and thus lower the overall environmental impact. In contrast, the significant face area reductions are highly advantageous to HX manufacturers since face area is directly related to system footprint [25]. These results clearly emphasize that we can use systematic optimization to arrive at highly compact and lighter HX designs for any of the new lower-GWP replacement refrigerants.

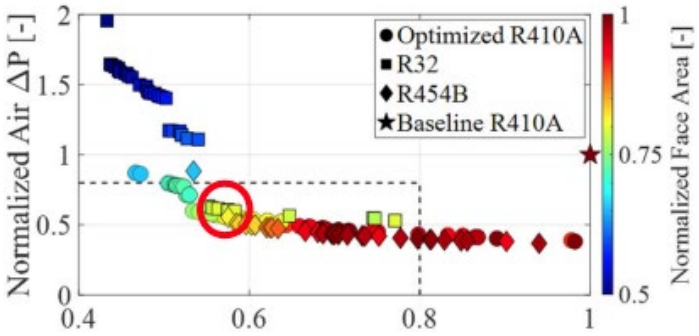


**Figure. 6 Optimization results (Colour: face area).**

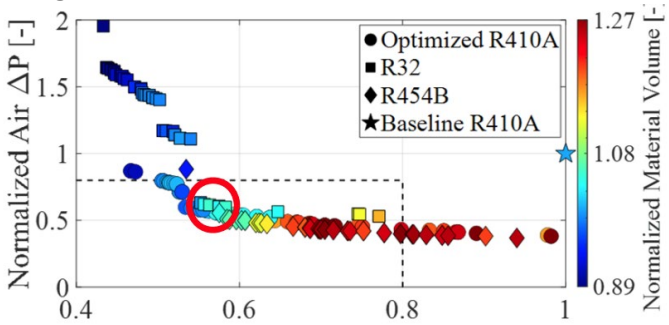


**Figure. 7 Optimization results (Colour: material volume).**

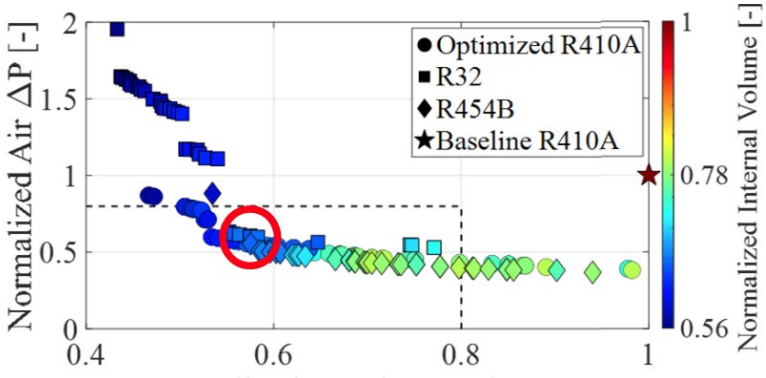


**Figure. 8 Optimization results (Colour: internal volume).**

1.1.1.3.3 Comparison of Optimal Designs for each Refrigerant

It is of interest to directly compare the optimal HX designs from each refrigerant case to one another to gain valuable insights into whether, and if so, to what extent, the refrigerant's unique thermophysical properties impact the final HX designs. First, we considered the entire set of optimal designs for each refrigerant as a whole. The similarities and differences across the optimal designs are listed below:

- All HXs have very similar tube pitches and numbers of tube banks, resulting in all HXs having similar airside pressure drops and HX core depths.
  - All R-410A and R-454B HXs have 4 tube banks.
  - Most R-32 HXs have 5 tube banks; the rest have 4 tube banks.
- On average, R-32 HXs have the fewest tubes per bank, while R-454B HXs have the most.
  - This could result from R-32 HXs having more tube banks, which then require fewer tubes per bank to achieve the desired capacity.
  - Fewer tubes per bank reduce the HX core height, resulting in the R-32 HXs having the smallest face areas. Because the air volume flow rate is fixed, the R-32 HXs have large inlet air velocities, which could lead to undesirable fan noise/tube aeroacoustics challenges.

Next, we considered three HX designs (one design per refrigerant), as highlighted with red circles in Figures 6 – 8. These HXs were chosen since they are all close together in the objective space (~40% reductions in both HX core envelope volume and airside pressure drop). The normalized values of different performance metrics for these HXs are highlighted in Table 5, and additional normalized values of HX geometry are listed in Table 6. As mentioned above, all HXs have the same tube shape and similar tube pitches; thus, these values are not listed.

**Table. 5 Comparison of normalized performance metrics for three optimal HX designs. All values are normalized with respect to the baseline R-410A HX.**

| Fluid | *VHX* | *ΔPair* | *Af* | *VMat* | *VInt* | Charge |
|---|---|---|---|---|---|---|
| R-410A | 0.58 | 0.56 | 0.81 | 1.04 | 0.65 | 0.63 |
| R-32 | 0.57 | 0.60 | 0.79 | 1.03 | 0.65 | 0.52 |
| R-454B | 0.58 | 0.56 | 0.81 | 1.04 | 0.65 | 0.55 |

**Table. 6 Comparison of normalized HX geometry values for three optimal HX designs. All values are normalized with respect to the optimal R-410A HX.**

| Fluid | *Number of tube bank* | *Number of tubes per bank* | *HHX* | *LHX* |
|---|---|---|---|---|
| R-410A | 1.0 | 1.0 | 1.0 | 1.0 |
| R-32 | 1.0 | 0.73 | 0.71 | 1.36 |
| R-454B | 1.0 | 0.97 | 0.97 | 1.04 |

It is clear from Tables 5 and 6 that the HXs themselves are quite different, while the HXs have very similar performance metrics. First and foremost, the R-32 and R-454B HXs have 15-20% lower refrigerant charges than the R-410A HX, which is especially advantageous given that R-32 and R-454B are mildly flammable refrigerants. Additionally, as noted above, the R-32 HX has much fewer tubes per bank, which is compensated by having ~36% longer tubes than the R-410A HX, while the R-454B HX is almost identical to the R-410A HX. Looking from a strictly HX standpoint, i.e., assuming that all other system components (e.g., compressor, flammability considerations, etc.) are changed to enable the use of R-32 and R-454B, the following conclusions can be drawn:

- R-32 should not be used as a direct drop-in replacement to R-410A HXs. Instead, HX optimization should be done specifically for R-32.
- R-454B could be a near drop-in replacement to R-410A in HXs designed initially for R-410A.
- Soft optimization methods (component selection, operating condition tuning, etc.) could be sufficient to transition R-410A HXs to R-454B efficiently.

#### 1.1.1.4 Conclusions

This report presents the application of a multi-scale, multi-physics analysis, and tube shape and topology optimization methodology, which is utilized to design residential A/C unit condensers for three different refrigerants: (i) R-410A and two lower-GWP alternatives (ii) R-32, and (iii) R-454B. This study's novel, non-round, shape-optimized tube geometry has been conventionally manufactured. The optimal HX designs deliver the same capacity as a state-of-the-art baseline tube-fin condenser while achieving at least 20% reductions in airside pressure drop and envelope volume, up to 11% reduction in tube material volume, and more than 40% reduction in tube internal volume, thus showcasing the viability of tube shape and topology optimization for the design of HXs using alternative refrigerants. Detailed comparisons of optimal HXs designs for each refrigerant were also presented. It was found that the R-32 HX geometries showed many differences compared to the R-410A HXs, while the R-454B and R-410A HX geometries were broadly similar. This suggests that when considering R-32 to replace R-410A, separate HX optimization studies may be required to ensure that the HXs deliver the desired performance. On the other hand, R-454B could serve as a near drop-in replacement in HXs originally designed for R-410A so long as appropriate soft-optimization techniques such as component selection and operating condition tuning are also considered. In summary, this study highlights how systematic optimization can result in highly compact and lighter HX designs for any of the new lower-GWP replacement refrigerants.

### 1.1.2 Thermodynamic analysis and carbon emission evaluation for saturation cycle heat pump

#### 1.1.2.1 Introduction

Low-temperature heat pumps face several challenges that can affect their performance and limit their potential applications. One of the main challenges is efficiency, as heat pumps typically become less efficient at lower temperatures, requiring more energy to extract heat from the environment. Additionally, low-temperature heat pumps have lower heat output capacity than high-temperature heat pumps, which can limit their ability to heat larger or colder spaces. Frost and ice buildup on the evaporator coils is another challenge that can reduce efficiency and potentially

cause damage to the system. Low-temperature heat pumps can also be more expensive to install than conventional heating systems, although they typically offer long-term energy savings.

Furthermore, low-temperature heat pumps may not be compatible with all heating systems or building designs, which can limit their potential applications. Lastly, low-temperature heat pumps may not produce enough heat in extremely cold temperatures, which can require backup heating systems or other heating sources. These challenges must be considered carefully when choosing and designing low-temperature heat pump systems to ensure optimal performance and efficiency.

The state-of-the-art (SOA) R-410A HP systems face severe capacity and efficiency degradation under extremely low temperatures due to inherent thermodynamic drawbacks. For instance, under -15°F (-26°C), the COP of the HP system decreases to 2.3 with a capacity degradation of more than 30% [45]. The resulting lower efficiency and high capacity degradation result from 1) compressor inefficiency under a high-pressure ratio, 2) condenser inefficiency with the higher superheated vapor phase ratio, and 3) selection of suitable low-GWP refrigerant and high enough critical temperature. Fig. 9a describes an HP system operated under -26°C evaporation and 35°C condensing conditions. The solid red line in Fig. 9a represents a conventional single-stage HP design. Typical compression ratios of single-stage mechanical gas compressors are around 2.5 to 4. However, the required total pressure ratio (PR) to achieve a high-temperature lift as high as 61K is 8.5. Multiple stage numbers (with a smaller PR) and different superheat degrees are used to illustrate the challenges of this specific high-temperature lift on the HP system performance.

We propose a set of technologies that aim to boost both COP and heating capacity for commercial rooftop heat pumps. The saturation cycle with two injections alone leads to a heating COP of 2.7 and capacity degradation of 20% under -15°F. With an additional novel implementation of safety control, the smart CCHP system will deliver a COP of 2.7 and capacity degradation of only 12% at -15°F while supplying an air discharge temperature higher than 95°F. The proposed technology leads to cost reduction compared to competing systems that need oversized and offers a payback period of 4.3 years for a system with 10 ton capacity of a standard RTU.

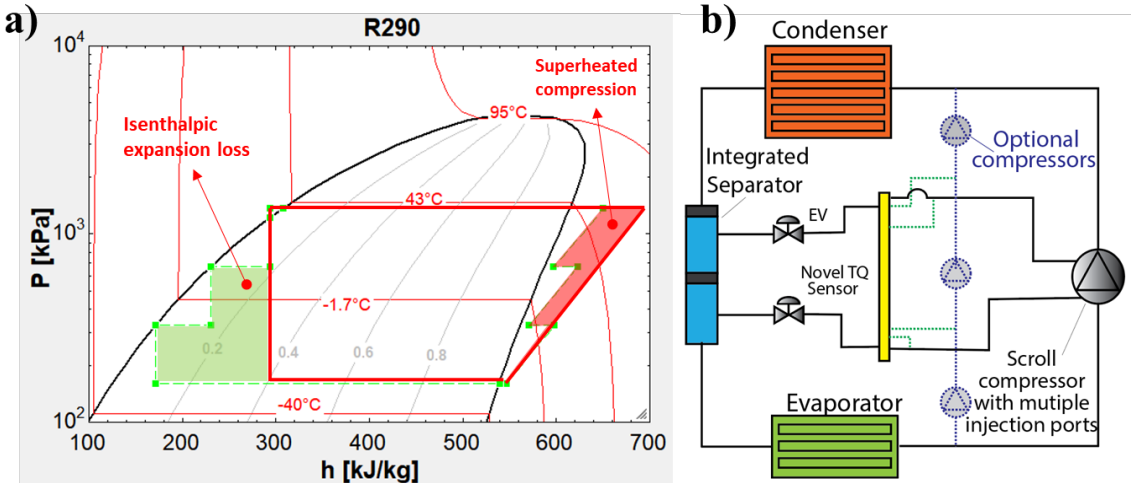


**Figure 9: Saturation heat pump cycle: a) P-h diagram and energy loss through expansion and superheated compression; b) realization of a saturation HP system via double injections**

### 1.1.2.2 Cycle description

Our previous studies have demonstrated the superior thermal performance of the saturation HP system with low-GWP working fluids for residential heat pumps [46, 47]. The COP and capacity improvement can reach 45% over non-saturation cycles. The recent development by Emerson on double injection (three stages) compressors makes the concept of saturation HPs ever closer to being commercially feasible. Fig. 10a-c succinctly shows the thermodynamic principles of saturation heat pumps. As the number of injections increases, the two significant irreversible losses, throttling loss and superheated compression (indicated in Fig. 16a), are reduced. Therefore, the cycle efficiency gradually approaches the theoretic Carnot limits. For example, under -26°C ambient temperature and 35°C air discharge temperature scenario, a two-stage cycle reaches COP of 2.5 and heating capacity degradation of 16%; a three-stage cycle reaches COP of 2.7 and heating degradation of 12%, and a four-stage cycle reaches COP of 2.8 and heating degradation of 10%.

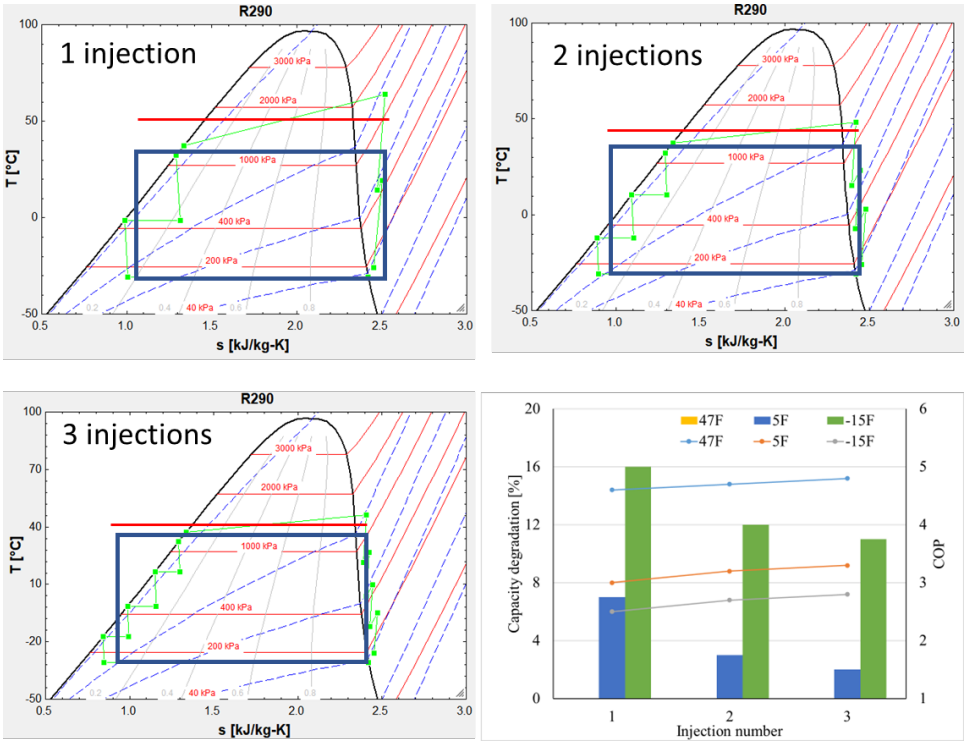


**Figure 10: a)-c) a higher equivalent condensing temperature achieved by higher injections; d) COP and capacity degradation on different injection numbers.**

Fig. 11a shows how the compressor work decreases along with stage number (PR decreases sharply). The energy saving from the compressor can be easily obtained from a smaller PR and staging multiple smaller PR compression processes to deliver a sufficient temperature lift. A 15% of energy saving can be achieved for a PR lower than 3. It should be noted that 5K superheat is assumed for the compression efficiency simulation. More energy-saving potential can be obtained by optimizing the compressor design. This process can be accomplished with CEEE's established compressor modeling tools. The degree of superheating at the compressor outlet is another critical factor that should be carefully designed when it comes to a high-pressure ratio HP, as it could

result in excessive compressor power and failure. The simple cycle simulation shows that the single-stage cycle's compressor outlet temperature can reach around 85°C. It is adopting a low-GWP refrigerant as a working fluid (eg. R-290) for a heat sink temperature of 35°C with an evaporating temperature of -26°C. Fig. 11b shows the amount of heat a superheated vapor delivers in terms of superheat increase. The mass flow rate of the refrigerant decreases with the increase in overall heating capacity due to higher superheating. However, the heat transfer area of the condenser increases almost linearly with a degree of superheating since the heat transfer coefficient of the two-phase region is one order higher than that of the superheated vapor.

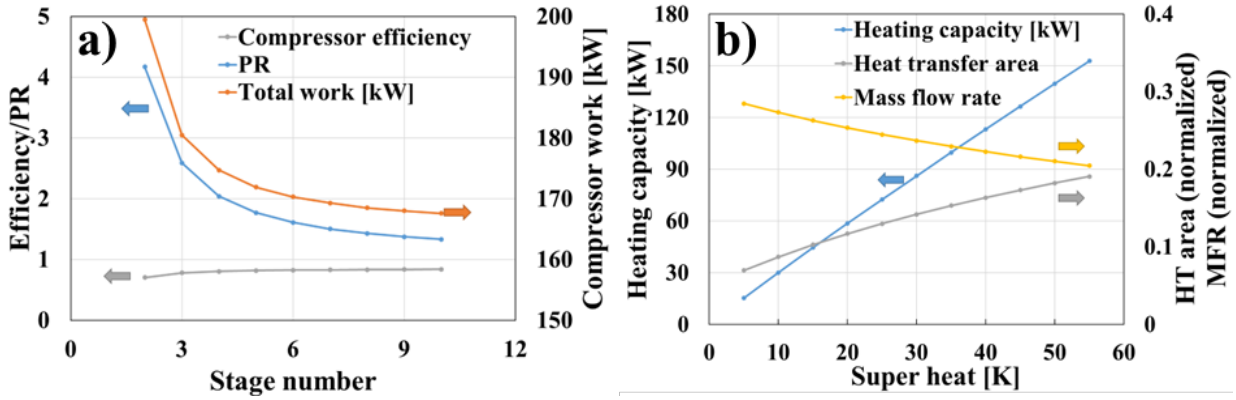


**Figure 11: Challenges for a conventional HP system a) stage number influence on compression efficiency; b) Superheat influence on HX performance**

One of the most critical design directions for the cold climate system is to reduce the excessive pressure ratio and the degree of superheating to their optimal values. To achieve this, the compression process can be divided into multiple stages with multiple refrigerant injections. Therefore, the design should incorporate multiple injection port locations to satisfy the requirements of the various compression stages. This approach can improve the system's overall efficiency and performance while reducing energy consumption and operating costs.

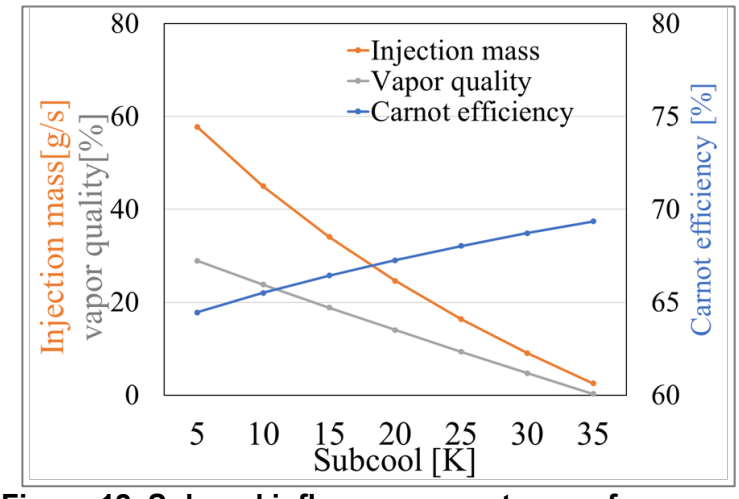


**Figure 12. Subcool influence on system performance**

To optimize the system efficiency, it is essential to consider the subcooling degree of the last compression stage, as indicated in Fig. 12. A lower subcooling degree leads to higher vapor quality after the last expansion, which in turn requires more two-phase refrigerant to satisfy the same superheat at the last compression inlet. While increasing the condensing capacity, this also results in higher power consumption for the last compression process. On the other hand, a higher subcooling degree is preferred to improve system efficiency, but excessive subcooling can have a negative impact on condenser performance. For the simulation work, a subcooling degree of 5 K was adopted, and further optimization is needed to determine the most suitable subcooling degree for optimal system performance.

#### 1.1.2.3 $CO_2$ emission analysis

Around one-third of global energy- and process-related $CO_2$ emissions are directly and indirectly attributed to the buildings sector. In 2021, approximately 8% of these emissions resulted from using fossil fuels in buildings, while 19% resulted from the generation of electricity and heat used in buildings. An additional 6% was related to manufacturing construction materials such as cement, steel, and aluminum. Therefore, addressing the impact of buildings and construction on $CO_2$ emissions is crucial by imposing emission restrictions throughout the entire value chain. These dedicated saturation HP systems can offer a total energy saving of 1.51 Quads, as the solid bar plot in Fig. 13, which is 85% and 21% more energy efficient than fossil fuel-based systems and SOA IHP systems. As a result, the saturation system can reduce 62.4 MMT of $CO_2$ (stripped bar plot in Fig. 13) if switching from the conventional system. The energy saving will defeat the SOA efficiency by 28% (black line chart). This carbon emission saving is equivalent to that of the energy consumption by 15.6 million U.S. homes. The payback period will decrease as the injection number increases at the beginning and slightly increases when too many injection ports are applied. This payback trend is caused by the requirement of multiple compressors and the challenge of manufacturing multi-port on a single compressor. Considering the on-shelf injection compressors and optimized low-cost heat exchangers, the proposed saturation system concept will still offer a payback period of 2.3 years (blue line chart in Fig. 13).

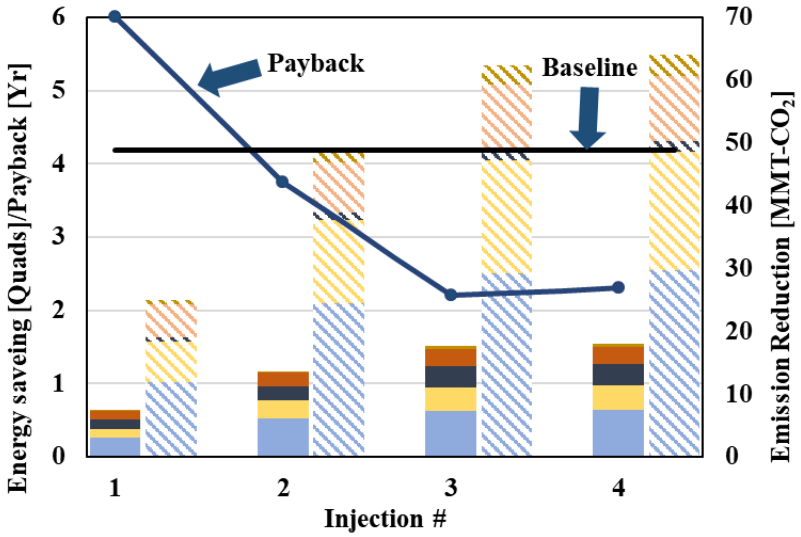


**Figure 13: Energy, emission, and payback performance**

## 1.2 Review of low GWP refrigerant for HP system

As highlighted by the speaker at the HFC lifecycle management workshop [48], reducing hydrofluorocarbons (HFCs), super-polluting greenhouse gases used in refrigeration, air-conditioning, insulating foams, and aerosol propellants, plays an important role for decarbonization. HFCs are hundreds to thousands of times more powerful than carbon dioxide and contribute to global warming. The global implementation of the Kigali Amendment to the Montreal Protocol requires a phase-down of HFCs by more than 80% over the next 30 years, which can prevent more than 70 billion metric tons of carbon dioxide equivalent emissions by the middle of the century, leading to a reduction in global warming by 0.1°C by 2050 and up to 0.5°C by the end of the century. It is crucial to emphasize the significance of replacing high-global-warming-potential HFCs with next-generation refrigerants and enhancing energy efficiency in order to decrease emissions. The speaker highlighted the benefits of increasing the capture and reuse of HFCs already inside refrigeration and air conditioning equipment. The United States has ratified the Kigali Amendment and is leading the way in reducing HFCs domestically through the 2020 American Innovation and Manufacturing Act. Collaboration with industry stakeholders and working together towards achieving a net-zero economy is essential for a successful transition.

Theresa [49] presents the results of a study on refrigerant use for air conditioning (AC) equipment maintenance in the United States. The study collected data from a survey of over 1,000 AC contractors and technicians, as well as an analysis of refrigerant sales data from a major supplier. The survey found that most technicians (68%) do not perform refrigerant recovery during AC maintenance and instead simply release the refrigerant into the atmosphere. The sales data analysis found that the most commonly sold refrigerants were R-22 and R-410A, both high global warming potential (GWP) refrigerants contributing to climate change. The study also estimated that the amount of refrigerant released into the atmosphere during AC maintenance is equivalent to the emissions from over 9 million cars each year. The authors argue that better training and education for technicians and stronger regulations and enforcement are needed to reduce refrigerant emissions from AC maintenance and address the climate impact of these emissions.

As discussed before [50], the harmonization of life cycle climate performance (LCCP) methodology is used to assess the greenhouse gas (GHG) emissions of products or systems throughout their life cycle. The authors highlight the importance of standardizing the methodology to ensure consistent and accurate GHG emissions calculations. They review different LCCP approaches and methods, such as the PAS 2050, the ISO 14044, and the Product Category Rules (PCR), and their strengths and limitations. The article emphasizes the need for a standardized, transparent, and flexible LCCP methodology that can be adapted to different sectors and product types. The authors also discuss the challenges of data collection and quality, the role of technology and innovation, and the importance of stakeholder engagement in developing and implementing LCCP methodologies. The article concludes that the harmonization of LCCP methodology can contribute to more informed decision-making and promote sustainable practices across different industries.

### 1.2.1 Refrigerants selection & evolution

Mark [51] discussed the evolution of refrigerant molecules, the constraints and regulations that have driven the need to consider new molecules, and the advancements in the tools and property models used to identify new molecules and design equipment using them. The authors highlight three comprehensive searches for new refrigerants in the 1920s, 1980s, and 2010s, which sometimes identified new molecules, but more often validated alternatives already under

consideration. The paper also notes that there is little that is genuinely new in the search for new refrigerants and that most of the "new" refrigerants were reported in the chemical literature decades before they were considered as refrigerants. The authors also review the NIST REFPROP database's evolution for the refrigerant properties calculation. Bell [52] surveyed existing data for refrigerant blends containing halogenated olefins and presented the data in graphical form. The data is primarily taken from the NIST SOURCE database. The conclusion is that there is a lack of experimental data for blends containing halogenated olefins, and some data classes are particularly sparse. The second part of the study compares the thermodynamic models in NIST REFPROP against the experimental data sets and identifies systems for which refitting of the thermodynamic model is required.

### 1.2.2 Alternative refrigerants

R-290 (propane) and R-1234yf (a low GWP refrigerant) are considered promising options as alternatives to traditional refrigerants due to their excellent thermodynamic properties, low environmental impact, and energy efficiency. These refrigerants have the potential to significantly reduce greenhouse gas emissions from the refrigeration and air conditioning industry. However, their flammability and toxicity properties should also be considered, and appropriate safety measures must be implemented during installation and maintenance. Additionally, further research is needed to fully understand the potential impact of these refrigerants on the environment and human health. Zhang compared the performance of R-290 and R-1234yf in heat pump water heaters with low charge [53]. The experimental results show that both refrigerants have comparable heating capacity and COP at low charge levels, with R-290 showing slightly better performance. However, R-1234yf has a lower flammability risk and a lower impact on the ozone layer, making it a safer and more environmentally friendly option. The study concluded that R-1234yf could be an excellent alternative to R-290 in heat pump water heaters with a low charge, especially in regions with stricter regulations on flammable refrigerants.

The Fraunhofer Institute for Solar Energy Systems is developing a low refrigerant charge refrigeration circuit with a propane heat pump as part of the "LC150" project funded by the German Federal Ministry of Economics and Climate Protection [54]. The research team has been building prototype brine heat pumps with reduced amounts of refrigerant by adjusting factors such as the internal volume of the heat exchangers, the amount of oil required, and reducing the number of components such as sensors. The final version of the refrigeration circuit is expected to achieve a maximum output of 8 to 10 kilowatts and a maximum charge of 150 grams of refrigerant, with a more balanced system using a fully hermetic compressor and slightly more refrigerant.

Alfares [55] provides a review of the experimental application of R-410A alternative refrigerants, with a focus on low-GWP refrigerants. The authors collected a wide range of experimental data from the literature and analyzed these refrigerants' performance and environmental impact. They found that DR-55 (R-452B) provides an overall performance closer to R-410A in existing refrigeration systems. Additionally, the authors conclude that DR-55 (R-452B) and DR-5A (R-454B) are the most suitable candidates for residential air conditioners and heat pumps. Overall, the paper provided valuable insights into using low-GWP refrigerants as alternatives to R-410A in refrigeration systems.

**Table 7. Alternative refrigerants normalized ranking parameters [55]**

| Refrigerant | Ranking parameters | | | | Total |
|---|---|---|---|---|---|
| | Heating ratio | Cooling ratio | COP ratio | Discharge temperature ratio | |
| DR-5A | -0.04 | -0.04 | 0.01 | 0.12 | 0.04 |
| DR-55 | -0.03 | 0.02 | 0.02 | -0.05 | -0.04 |
| R-32 | 0.02 | 0.05 | 0.02 | -0.19 | -0.11 |
| L41A | -0.09 | -0.07 | 0.00 | -0.06 | -0.22 |
| L41-2 | -0.13 | -0.11 | -0.01 | -0.09 | -0.34 |
| D2Y-60 | -0.30 | -0.19 | -0.03 | 0.07 | -0.45 |
| L41-1 | -0.50 | -0.46 | -0.05 | -0.06 | -1.08 |

Yasuharu [56] performed an in-silico screening of 10,163 molecules using quantum chemical calculations, machine learning, and database search to find suitable candidates. The author discussed the urgent need to develop new refrigerants with low GWP while meeting conventional requirements such as cooling performance, safety, and non-destructiveness to the ozone layer. It highlights the tradeoffs among various chemical properties and the need to control these properties to fulfill the requirements properly.

Rydkin [57] reviewed a novel refrigerant, HFO-1132E (GWP 1), and its binary mixture with R-1234yf. The author covered the binary blend's critical parameters, flammability classification, stability studies, initial materials, oil compatibility screening, and laboratory-validated refrigerant cycle performance properties. The binary blend is intended to replace R-134a and R-1234yf in heat pump applications as part of the phasedown of HFCs under the Kigali amendment and the US AIM Act.

## 1.3 Reference

[1] Kays, W. & London, A., Compact Heat Exchangers, 1984; McGraw-Hill, New York.

[2] Bacellar, D., Aute, V., Huang, Z., & Radermacher, R. Design optimization and validation of high- performance heat exchangers using approximation assisted optimization and additive manufacturing. Science & Technology for the Built Environment, 2017; 23(6): 896-911.

[3] Paitoonsurikarn, S., Kasagi, N., & Suzuki Y. Optimal design of micro bare-tube heat exchanger. Symposium on Energy Engineering, 2000; 972–979: Hong Kong, China.

[4] Saji, N., Nagai, S., Tsuchiya, K., Asakura, H., & Obata, M, Development of a compact laminar flow heat exchanger with stainless steel micro- tubes. Physica C, 2001; 354(1-4): 148-151.

[5] Kasagi, N., Suzuki, Y., Shikazono, N., & Oku, T. Optimal design and assessment of high performance micro bare-tube heat exchangers. 4th International Conference Compact Heat Exchangers and Enhancement Technologies for the Process Industries, 2003; 241-246: Crete, Greece.

[6] Chen, H.T., Lin, Y.S., Chen, P. C., & Chang, J.R. Numerical and experimental study of natural convection heat transfer characteristics for vertical plate fin and tube heat

exchangers with various tube diameters. International Journal of Heat & Mass Transfer, 2016; 100: 320-331.

[7] Bacellar, D., Huang, Z., Tancabel, J., Aute, V., & Radermacher, R. Multi-scale analysis, shape optimization and experimental validation of novel air-to-refrigerant heat exchangers, 9th World Conference on Experimental Heat Transfer, Fluid Mechanics, and Thermodynamics, 2017; Iguazu Falls, Brazil.

[8] Radermacher, R., Bacellar, D., Aute, V., Huang, Z., Hwang, Y., Ling, J., Muehlbauer, J., Tancabel, J., Abdelaziz, O., & Zhang, M. Miniaturized Air-to- Refrigerant Heat Exchangers, 2017; United States Department of Energy Report for Project Award DE-EE0006114.

[9] Tancabel, J., Aute, V., & Radermacher, R. Review of Shape and Topology Optimization for Design of Air-to- Refrigerant Heat Exchangers. 17th International Refrigeration and Air Conditioning Conference, Purdue University, 2018; Paper 1965: West Lafayette, Indiana, USA.

[10] Tancabel, J., Aute, V., Ling, J., & Radermacher, R. Multi-scale and multi-physics analysis of novel high performance, reduced charge evaporators with novel tube shapes. 9th International Conference on Compressor and Refrigeration, 2019; Xi'an, China.

[11] Tancabel, J., Aute, V., Ling, J., & Radermacher, R. Design optimization of high performance, reduced charge condensers with novel tube shapes. 25th International Congress of Refrigeration, 2019; Montreal, Quebec, Canada.

[12] Li, H. By, R. System Soft-Optimization Tests of Refrigerant R-32 in a 3-ton Split System Air- Conditioner. Air-Conditioning, Heating, and Refrigeration Institute (AHRI) Low-GWP Alternative Refrigerants Evaluation Program (Low-GWP AREP) Test Report #32; 2015.

[13] Alabdulkarem, A., Eldeeb, R., Hwang, Y., Aute, V., & Radermacher, R. Testing, simulation and soft- optimization of R-410A low-GWP alternatives in heat pump system. International Journal of Refrigeration, 2015; 60: 106-117.

[14] Mota-Babiloni, A., Navarro-Esbrí, J., Makhnatch, P., & Molés, F. Refrigerant R-32 as lower GWP working fluid in residential air conditioning systems in Europe and the USA. Renewable and Sustainable Energy Reviews, 2017; 80: 1031-1042.

[15] Heredia-Aricapa, Y., Belman-Flores, J.M., Mota- Babiloni, A., Serrano-Arellano, J., & García- Pabón, J.J. Overview of low GWP mixtures for the replacement of HFC refrigerants: R-134a, R404A and R-410A. International Journal of Refrigeration, 2020; 111: 113-123.

[16] Nair, V. HFO refrigerants: A review of present status and future prospects. International Journal of Refrigeration, 2021; 122: 156-170.

[17] Panato, V.H., Pico, D.F.M., & Bandarra Filho, E.P. Experimental evaluation of R-32, R452B and R-454B as alternative refrigerants for R-410A in a refrigeration system. International Journal of Refrigeration, 2021.

[18] Shen, B., Li, Z., & Gluesenkamp, K.R. Experimental study of R452B and R-454B as drop-in replacement for R-410A in split heat pumps having tube-fin and microchannel heat exchangers. Applied Thermal Engineering, 2021; 204: 117930.[19] Sieres, J., Ortega, I., Cerdeira, F., & Álvarez, E. Drop-in performance of the low-GWP alternative refrigerants R452B and R-454B in an R-410A liquid-to-water heat pump. Applied Thermal Engineering, 2021; 182: 116049.

[20] Simpson, T. W., Poplinski, J. D., Koch, P. N., & Allen, J. K. Metamodels for computer-based engineering design: survey and recommendations. Engineering with computers, 2001;17(2): 129-150.

[21] Abdelaziz, O., Aute, V., Azarm, S., & Radermacher, R., Approximation-assisted optimization for novel compact heat exchanger designs, HVAC&R Research 2010; 16(5): 707-728.
[22] Cressie, N., Statistics for Spatial Data, 1993; John Wiley & Sons, New York.
[23] Deb, K. Multi-objective Optimization using Evolutionary Algorithms, 2001; John Wiley & Sons, New York.
[24] Tancabel, J., Aute, V., & Ling, J. Optimization of R-290 Heat Exchangers using High-Performance, Non-round Tubes. 14th IIR-Gustav Lorentzen Conference on Natural Refrigerants; 2020.
[25] Private communications, 2019.
[26] Tiller, P.L., The NURBS Book. 1995; Springer, New York.
[27] Radermacher, R. Design and Manufacturing of High Performance, Reduced Charge Heat Exchangers (HPRC-HX), 2019; United States Department of Energy BTO Peer Review.
[28] ANSYS, Inc. Ansys® GAMBIT, Release 2.4.6, 2018.
[29] ANSYS, Inc. Ansys® Academic Research Fluent, Release 18.0, 2018.
[30] Shih, T.H., Zhu, J., & Lumley, J.L., A new Reynolds stress algebraic equation model, Computer Methods in Applied Mechanics and Engineering, 1995; 125(1-4): 287-302.
[31] Bergman, T.L., Incropera, F.P., DeWitt, D.P., & Lavine, A.S. Fundamentals of Heat and Mass Transfer – 7th Edition. 2011; John Wiley & Sons: Hoboken, NJ.
[32] Roache, P.J., Quantification of Uncertainty in Computational Fluid Dynamics, Annual Review of Fluid Mechanics, 1997; 29(1): 123-160.
[33] ASME, Standard for Verification and Validation in Computational Fluid Dynamics and Heat Transfer, ASME V&V 20-2009, 2009; American Society of Mechanical Engineers: New York, New York, USA.
[34] Oberkampf, W., Roy, C., Verification and Validation in Scientific Computing, 2010; Cambridge University Press, Cambridge, UK.
[35] Roy, C., Oberkampf, W., A Comprehensive Framework for Verification, Validation, and Uncertainty Quantification in Scientific Computing. Computer Methods in Applied Mechanics and Engineering. 2011; 200(25): 2131–2144.
[36] McKay, M.D., Beckman, R.J., & Conover, W.J., Comparison of Three Methods for Selecting Values of Input Variables in the Analysis of Output from a Computer Code, Technometrics, 1979; 21(2): 239-245.
[37] Hamad, H., A New Metric for Measuring Metamodels Quality-of-Fit for Deterministic Simulations. 38th conference on Winter Simulation, 2006; 882-888: Monterey, California, USA.
[38] Jiang, H., Aute, V., & Radermacher, R., CoilDesigner: A General Purpose Simulation and Design Tool for Air-to-Refrigerant Heat Exchangers, International Journal of Heat and Mass Transfer, 2006; 29(4): 601-610.
[39] Lemmon, E.W., Bell, I.H., Huber, M.L., & McLinden, M.O. NIST Standard Reference Database 23: Reference Fluid Thermodynamic and Transport Properties-REFPROP, Version 10.0, 2018; National Institute of Standards and Technology, Standard Reference Data Program, Gaithersburg, MD.
[40] Aute, V. and Radermacher, R. Standardized polynomials for fast evaluation of refrigerant thermophysical properties. 15th International Refrigeration and Air Conditioning Conference, Purdue University, 2014; Paper 1499: West Lafayette, Indiana, USA.
[41] Gnielinski, V. New equations for heat and mass transfer in turbulent pipe and channel flow. International Chemical Engineering, 1976;16(2): 359-368.

[42] Churchill, S.W. Friction-factor equation spans all fluid-flow regimes. Chemical Engineering, 1977: 91–92.
[43] Shah, M.M. Improved correlation for heat transfer during condensation in conventional and mini/micro channels. International Journal of Refrigeration, 2019; 98: 222-237.
[44] Xu, Y. and Fang, X. A new correlation of two- phase frictional pressure drop for condensing flow in pipes. Nuclear Engineering and Design, 2013; 263: 87-96.
[45] Hoseong Lee, Yunho Hwang, Reinhard Radermacher, Ho-Hwan, Chun, 2013, Investigation of potential benefits of saturation cycle, Applied Thermal Engineering. 56, 27–37.
[46] Hoseong Lee, Yunho Hwang, Reinhard Radermacher, Performance investigation of saturation cycle with natural working fluids, 11th IIR-Gustave Lorentzen conference, 2014.
[47] Hoseong Lee, Yunho Hwang, Reinhard Radermacher, Ho-Hwan, Chun, 2015, Performance investigation of multi-stage saturation cycle with natural working fluids and low GWP working fluid. IJR, 51, 103–111.
[48] Remarks for HFC Lifecycle Management Workshop Event. United States Department of State n.d. https://www.state.gov/remarks-for-hfc-lifecycle-management-workshop-event/ (accessed April 14, 2023).
[49] Theresa P. Analysis of Refrigerant Use for AC Equipment Maintenance 2022. https://www.ashrae.org/technical-resources/ashrae-journal/featured-articles/october-2022-analysis-of-refrigerant-use-for-ac-equipment-maintenance (accessed April 14, 2023).
[50] Huang, Y., & Benhelal, E. (2019). Harmonization of life cycle climate performance methodology. Building and Environment, 163, 106267.
[51] McLinden MO, Huber ML. (R)Evolution of Refrigerants. J Chem Eng Data. 2020;65(9):10.1021/acs.jced.0c00338. doi: 10.1021/acs.jced.0c00338. PMID: 35001966; PMCID: PMC8739722.
[52] Bell, Ian H., et al. "Survey of data and models for refrigerant mixtures containing halogenated olefins." Journal of Chemical & Engineering Data 66.6 (2021): 2335-2354.
[53] Zhang, J., Sun, X., Wang, C., Liu, C., & Wang, R. (2019). Performance comparison of R-290 and R-1234yf as low-GWP refrigerants for heat pump water heaters with low charge. Applied Thermal Engineering, 153, 1-11.
[54] Record: heat pump less than 10 g of propane per kW, 2022. https://iifiir.org/en/news/record-heat-pump-less-than-10-g-of-propane-per-kw (accessed April 18, 2023).
[55] Guilherme, Ítalo Franco, et al. "A review on the performance and environmental assessment of R-410A alternative refrigerants." Journal of Building Engineering 47 (2022): 103847.
[56] Okamoto, Yasuharu. "Tradeoffs and Compatibilities of Chemical Properties in CpHqFrOs System." Scientific Reports 9.1 (2019): 1-7.
[57] Rydkin, Ivan. "Overview of novel GWP 1 HFO Refrigerant 1132E and the Mixture of 1132E and R-1234yf." (2022).

# 2 Country Report: Sweden

**Prepared By:**

**Björn Palm**
**KTH Royal Institute of Technology,**
**Stockholm, Sweden**

**Metkel Yebio, Bassam Badran, Morgan Willis**
**RISE Research Institutes of Sweden,**
**Stockholm, Sweden**

## 2.1 Introduction

This year's national report from Sweden focuses mainly on Task 3 of Annex 54, i.e., a review of design optimization and advancement impacts on LCCP reduction. However, we also update Task 1, Review of State of the Art Technologies, and Task 2, Case studies and Design Guidelines.

The research cited and presented is mainly financed by the Swedish government and through the EU. The government finances research in this area through a few different funding agencies:

- **The Swedish Energy Agency** is a government agency to lead the energy system's transition towards sustainable solutions. The agency has sponsored research on heat pumps for many years through research programs. The most significant program is now called Termo, to " contribute to the development of heating and cooling solutions for the future energy system." Another program supporting heat pump research is E2B2, which focuses on energy-efficient building and living.
- **Formas** is the Swedish research council for sustainable development, supporting community building, forestry, and farming research.
- **Vinnova**, Sweden's innovation agency, supports innovation in selected areas through specific calls.
- **SSF,** the Swedish Foundation for Strategic Research, supports science, technology, and medicine research. The main focus is to promote the development of solid research environments of high international class.

Heat pump research in Sweden is also funded through the European Union, financing cooperation projects between industry, academia, and institutes. Swedish partners regularly participate in such projects, notably the projects SHERHPA, GREEN HP and NXTHPG specifically focused on heat pumps with natural refrigerants.

## 2.2 Review of state-of-the-art technologies

### 2.2.1 Introduction

The Swedish heat pump market is well developed, and more than 60% of all single-family houses are heated by heat pumps. A large share of these is extracting heat from the ground through geothermal wells in the bedrock. More than 500,000 such geothermal heat pumps are installed in a building stock of about 2 million houses.

The heat pump market is dominated by brands manufactured in Sweden: NIBE, Thermia, CTC, IVT/Bosch. During the last few years, a few foreign brands like Daikin and Mitsubishi have also become common. However, the market for small air-to-air heat pumps is entirely dominated by foreign brands. In the following, we provide examples of typical designs and common choices of refrigerants, focusing on units with low-GWP refrigerants.

### 2.2.2 Refrigerants used in heat pumps on the Swedish market

#### 2.2.2.1 Smaller residential units

*Air-to-air heat pumps*

There is currently no air-to-air heat pump production in Sweden in any relevant quantity. However, several manufacturers do import and sell air-to-air heat pumps. Considering the Swedish-based

manufacturers NIBE, Bosch Thermoteknik, Enertech, Electrolux, and Thermia, only Thermia, Electrolux, and Bosch officially sell air-to-air heat pumps. As is currently the case for almost all air-to- air heat pumps in Europe, these units all use R-32, which still can be considered low-GWP, although more stringent regulations may put this in question.

*Air-to-water heat pumps*

From a European manufacturer's perspective, the air-to-water product group can be considered the most important product group for smaller residential units. With approximately 984 thousand units produced in Europe during 2021, eighth times as many units compared to brine-to-water/water-to-water heat pumps switched to low-GWP for these units is most certainly a priority among manufacturers. Air-to-water heat pumps can be divided into split units and monoblock units which in turn is a factor that can influence the possibility of using certain types and amounts of low-GWP refrigerants. Looking at split-type air-to-water heat pumps, several European manufacturers have followed the same trend as air-to-air heat pumps by using R-32, which has the benefit of being a mildly flammable A2L refrigerant although with a substantially higher GWP than A3 refrigerants. Being a split-type unit means that refrigerant normally is passed through the walls of a house to an indoor unit, and as such, a possible leak occurring inside must be considered. Using $CO_2$ is also an option for split-type air-to-water heat pumps. It is commercially available from the manufacturer Mitsubishi Electric which has a strong presence in the Swedish market, although no manufacturing is done in Sweden.

Considering the major manufacturers, which can be considered Sweden-based, namely NIBE, Bosch Thermoteknik, Enertech, and Thermia, only Thermia offers a split-type air-to-water heat pump using low-GWP refrigerants. Thermias iTec Eco uses 1-2,2 kg of R-32 as a refrigerant (Thermia iTec Eco product brochure).

Monoblock-type air-to-water uses water (or brine) to transfer heat from the outside unit to an indoor unit. Considering flammable refrigerants, this offers the considerable advantage of placing the whole refrigerant circuit outside. This means the unit is not limited regarding refrigerant charge even when using an A3 refrigerant like R-290, even though safety-related issues, such as installer training, still exist. Therefore, we will likely see this product group convert to R-290, or other A3 refrigerants, in the coming years.

Looking again at NIBE, Bosch Thermoteknik, Enertech, and Thermia, only NIBE revealed a monoblock air-to-water heat pump using a low-GWP refrigerant. The S2125-series heat pump is offered in two different sizes, both using 800 g of R-290.

Regarding the status of refrigerant use in monoblock air-to-water units, one should be careful when making any conclusions regarding whether or not manufacturers have or have not currently released units with low-GWP refrigerants. Considering the necessity to phase down the use of HFCs combined with the benefits of using A3 refrigerants in monoblock units placed outdoors, it is hard to see any other outcome than that manufacturers will sooner or later release these products with R-290 or some other A3 refrigerant. As for split-type heat pumps, the future is not as clear, and several pathways are possible, including lowered refrigerant charges and use of HFOs and HFO blends. Compared to monoblock technology, the phase-out of the product itself is also a possible pathway.

*Brine/water-to-water heat pumps*

For several reasons, brine-water and water-water heat pumps can be considered one of the more challenging product groups when developing products with low-GWP refrigerants. This is mainly because most of these products must be constructed in such a way that it can be safely placed indoors at small family houses. In these circumstances, there must be absolutely no risk for leakages, even small, as even a small accident, on top of the actual risk for inhabitants, would have a huge negative impact on both the manufacturer of the products and the technology itself. In practice, this means that these products currently have limited options for using low-GWP refrigerants, which can be summed up as either using max 4xLFL for A3/A2 refrigerants (152 g for R-290, 520 g for R-152a) or using HFO-based A2L refrigerants. Even though larger refrigerant charges could be possible with current safety standards, it would require manufacturers to set minimum room areas for the products. Considering that these heat pumps are usually installed in small spaces such an option would only lead to small increases of reasonable refrigerant charge whilst at the same time space limits would reduce the attractiveness of the products as well as the practical issue of how manufacturer can ensure that installers and end users follow these limits. Future revisions of the safety standards open up other possibilities by using different technical safety functions and solutions, all with their own challenges, such as cost increases and installation complexity.

Looking at the Swedish-based manufacturers, as of yet, they have all focused on products using A2L refrigerants as a solution going over to low-GWP refrigerants for brine-water/water-water heat pumps targeted at small family house installations. The choice is perhaps unsurprising as, compared to reducing refrigerant charges to 150 g, it is by far the least technically challenging option.

Refrigerant charges can be held at similar levels as traditional HFCs, which means that the process of dimensioning and construction can remain basically the same and that manufacturers can use the same or similar components.

Looking at the current Swedish market development, we consider the Swedish-based manufacturers NIBE, Bosch Thermoteknik, Enertech, and Thermia. Other manufacturers do exist but are comparably smaller. One small company (0,5 MSEK turnover) worth mentioning, however, is the company Terrawatt Värmepumpar which has been producing brine-water/water-water heat pumps since at least 2003, with a small family house-sized unit containing 600-750 g of propane (Terrawatt Villa Komplett, 2015)

Considering the apparent will to phase down, and perhaps phase out, the use of HFC, it is clear that developing products with low-GWP refrigerants is a matter of survival for heat pump manufacturers and that it is only a question of when manufacturers will release low-GWP based products. At the time of writing, however, only two of the mentioned more prominent Sweden-based manufacturers have released brine-water/water-water heat pumps for the small family house market.

The manufacturer Thermia released its Calibra Eco series in December 2020 (Thermia lanserar Calibra Eco, Press Release, Thermia, 2020-12-11). The Calibra Eco series heat pumps offer three different sizes of inverter-driven heat pumps, 2-8 kW, 3-12 kW, and 4-16 kW, with built-in DHW storage. The heat pump uses R-452B as its refrigerant with charge levels of 900 g, 1350 g and 1850 g. It can be noted that the maximum charge for R-452B, according to EN60335-2-40, without any additional measures, is 1854 g. R-452B is a mixture of 67% R-32, 7% R125, and 26% R-1234yf and is marketed as Opteon ™ XL55 by Chemours™ as a low-GWP replacement for R-

410A. Thermia is transparent with its refrigerant choice and markets the Calibra Eco series heat pump as “The market's first geothermal heat pump with the future refrigerant R452B”.

The manufacturer NIBE revealed its S1256-series brine-water/water-water heat pump at the Swedish building and construction industry fair Nordbygg 25-29 of April 2022. The heat pump is, as of writing, not available for purchase, so publicly available information is scarce. However, there is a high probability that the S1256 will be inverter driven in three different sizes similar to the S1255 series sizes of 1,5-6 kW, 3-12 kW, and 4-16 kW. The refrigerant chosen by NIBE for these units is R-454B which is a blend of 68,9 % R-32 and 31,1 % R-1234yf. R-454B is marketed as Opteon ™ XL41 by Chemours™ as a low-GWP replacement for R-410A.

*Exhaust air heat pumps*

Exhaust air heat pumps have been an extremely popular choice for new build small family houses in Sweden since the beginning of the 1980s as it provides a cost-effective solution for well-insulated houses without the need for external units or drilling. Providing mostly DHW in the beginning, these exhaust air heat pumps have become more and more efficient to a level that, for well-insulated houses, is comparable to other types of heat pumps.

R-290 has been used in exhaust air heat pumps since at least the 1990s. The combination of low power and that smaller need for refrigerant charge, as well as the built-in ability for a possible leak to be mechanically ventilated with the exhaust air is without a doubt a good reason for enabling this.

Considering the Swedish-based manufacturers NIBE, Bosch Thermoteknik, Enertech, Thermia as well as the exhaust air-niched manufacturer ComfortZone, all but Thermia and Enertech currently provide exhaust air heat pumps.

All ComfortZone heat pumps use R-32 as refrigerant, which can be considered low-GWP. NIBE, which definitely can be considered a major player in exhaust air heat pumps, has had propane exhaust air heat pumps for decades. However, the well-known inverter-driven exhaust air heat pumps (F750 and F730 series) released in 2013 to comply with the new and stringent energy requirements for new buildings have been using the HFC R-407C (GWP 1,774). At the Swedish building and construction industry fair Nordbygg 25-29 of April 2022, however, NIBE revealed the new exhaust air heat pump S735 using R-290 as refrigerants, just as previous NIBE exhaust air heat pumps had used. S735 has a slightly larger capacity and efficiency than F750/730 with a modernized control. The charge size is 420 g.

#### 2.2.2.2 Larger residential and commercial units

*Site built units*

When considering low-GWP heat pumps for commercial use, the limiting factors are, in many cases, vastly different from those concerning units for smaller residential units. Whereas product standards for residential units tightly limit the use of, for instance, flammable refrigerants, commercial units have more cards to play.

When considering larger place-built units where the person and firm perhaps choose each component, the use of type and charge of the refrigerant is up to the customer. It is a question of cost optimizations many times. When no longer tied to the “natural incompetents” of a regular house owner, the need to foolproof safety and costs combined with mass production, several technical solutions can be used in order to use different amounts and types of low-GWP

refrigerants like propane, ammonia, and $CO_2$. These units can be built while safety is ensured by following standards like EN378 (among others), where options like alarms, detectors, ventilation, special rooms, etc., can increase the use of flammable or toxic refrigerants. However, considering the necessity for increased refrigerant charge with larger capacities, using A3 refrigerant is still complicated even with these technical measures, which means that $CO_2$ and ammonia are preferred for larger site-built heat pumps. One example is heat pump installations provided by Labkyl, a part of Nordic Climate Group, using the so-called DLE-technique. These installations use $CO_2$ and are offered in capacity ranges from 50-1,000 kW (DLE - Delta Lift Energy, Labkyl)

*Pre-manufactured units*

These units, especially in commercial applications, also benefit from being used in settings, which means that safety issues can be handled with external safety solutions, trained staff and adapted placement, etc. Capacity ranges can start around 20-30 kW for smaller multifamily houses to several hundreds of kW. Many of these units, however, can be combined to serve even larger heating capacities. Among the previously mentioned manufacturers of smaller heat pumps, NIBE, Bosch Thermoteknik, Enertech, and Thermia all offer larger heat pumps. However, none of these units currently use low- GWP refrigerants.

When looking, however, to the more professional market, a handful of manufacturers, with Swedish manufacturing appear. One example is the company Enrad started to develop and manufacture heat pumps and chillers using R-290 spurred by the lack of refrigeration and heat pumps using natural refrigerants. Today Enrad offers heat pumps with a capacity of 80 kW- 135 kW using a maximum of 4,3kg R-290 (Enrad modulserie, Enrad). These modular units can be connected in parallel and offer even higher capacities.

One other smaller heat pump manufacturer is the company Qvantum Energi AB. Qvantum is specialized in larger units in the range of 32 kW- 165 kW. Although most of their units use traditional HFC, their Qvantum RSe unit uses R-513A (GWP 573) as refrigerant, which can be classified as low- GWP. As a side note, it can be mentioned that Qvantum has big ambitions for growth with the aim to specialize in heat pumps for 5th generation district heating and cooling (5GDHC). They have acquired a new factory in Åstorp, Sweden, where they claim they will be able to produce 50 000 heat pumps annually beginning 2023 (Svensk tillverkare: Värmepumpar för…, VVSForum)

ComfortZone, which specializes in exhaust air heat pumps, offers two models for larger residential buildings using R-32. Relatively modest in capacity, the RXF120 and RXF180 offer capacities of around 12-18kW. However, by linking several units together, higher capacities can be achieved. Four linked units can, as an example, serve a 3000 square meter residential building with heating.

The very small manufacturer Terrawatt can be mentioned as they have been using propane for many years and offer brine/water-to-water heat pumps with capacities of up to 100 kW. With a turnover of 0,5M SEK the number of produced large heat pumps cannot be substantial.

## 2.3 Case studies and design guidelines for optimization of components and systems

### 2.3.1 Introduction

In this section, we report on a few interesting case studies with heat pumps with low-GWP refrigerants. We will also discuss some design guidelines for optimum performance of heat pump systems.

### 2.3.2 Case studies

*Case 1: EBox a propane heat pump for multifamily buildings*

EBox is a system for supplying factory-built complete heating systems consisting of one or several geothermal heat pumps using propane as a refrigerant. The systems are built into standard 20-foot containers at the factory and need a connection to the electricity grid, the geothermal loop, and the building's heating system. Typically, the container would be placed inside a small building for a better visual appearance (Megawattsolutions, 2022).

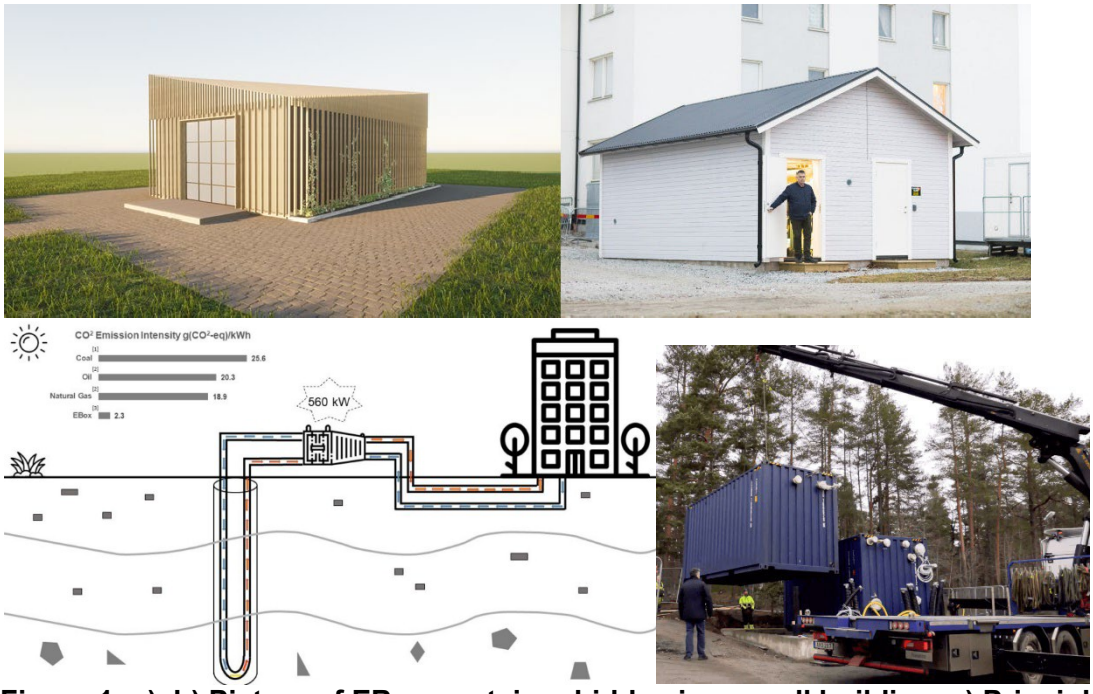


**Figure 1: a), b) Picture of EBox container hidden in a small building, c) Principle of EBox. d) Delivery of factory-built units. (Source: https://megawattsolutions.se)**

The capacity of the systems can be scaled to the needs by selecting the number of heat pump modules in each container (between 4 and 8 in a standard container) as well as the number of containers (see Fig. 1).

As the system is factory built and placed outside of the building itself, no additional safety precautions are necessary in the building or at the site, despite using propane as a refrigerant. The system can also be used for free cooling, using the boreholes as the cold source and, at the

same time, recharging the boreholes for the coming heating season. If necessary, the system can also be used for active cooling by reversing the heat pump cycle. Several such systems have been installed. Two installations have been made in the city of Södertälje, just south of Stockholm. The largest of these is in a residential block called Sjöboden, with a heating capacity of 864 kW. The heated floor area is close to 27000 square meters, and the heat pumps deliver heat both for domestic hot water and heating.

There are several advantages with this type of installations:

- Factory-built systems allow:
  - standardized designs, which decrease the cost
  - high quality as systems can be tested before delivery
  - high safety levels of the systems, even with flammable refrigerants
- The flexible capacity of the systems
- Simple installation, as no refurbishment of the building is necessary, except for the connection of the heating lines
- Short installation time

*Case 2: CO2-system for heating and cooling*

At a large block of stores in the city of Uppsala a complex system for heating, cooling, and energy storage has been installed, using $CO_2$ as the refrigerant. The prime purpose of the system is to supply cooling for the display cases in the large supermarket in the block. The hot side of this system is then used for heating not only the supermarket but also the neighboring building. When the heating capacity from the cabinet cooling is not sufficient, additional low-temperature heat from a borehole field is used as a heat source on the cold side. When there is no need for heating, the heat from the hot side of the cooling system can be dumped into the outdoor air or fed into the same ground source loop through a subcooler. By subcooling, the capacity and efficiency of the cooling of the cabinets are increased. The supermarket is large, with about 11000 $m^2$ floor area, while the neighboring building, which is heated by the system, has an area of 5000 $m^2$. The system can be seen as a cooling system with heat recovery or a geothermal heat pump with cooling. Figure 2 shows a sketch of the system. As shown, there are two de-superheaters connected to the heating system. A gas cooler is provided for the case there is no heating needed. The sub-cooler is connected to the geothermal loop. This loop has 20 boreholes, each 225 m long.

The system can also deliver air conditioning to the buildings. This can be done passively by using the cold brine from the boreholes or actively running the compressor marked PC in the diagram.

$CO_2$ is becoming the standard choice of refrigerant for refrigeration systems in supermarkets in northern Europe. Utilizing the hot side of these systems for heating is quite common. The system described above, however, is one of few which are also connected to a borehole field and allows delivering higher heating capacities than would be possible using only the cooling cabinets and display cases as the heat source. A theoretical comparison of the energy- and cost-efficiency of the described system compared to other solutions is underway. Preliminary results indicate that the solution is economically feasible under the local technical and economic conditions. More about this and other similar systems can be found in the M.Sc. thesis of Almebäck and Magnius (2022).

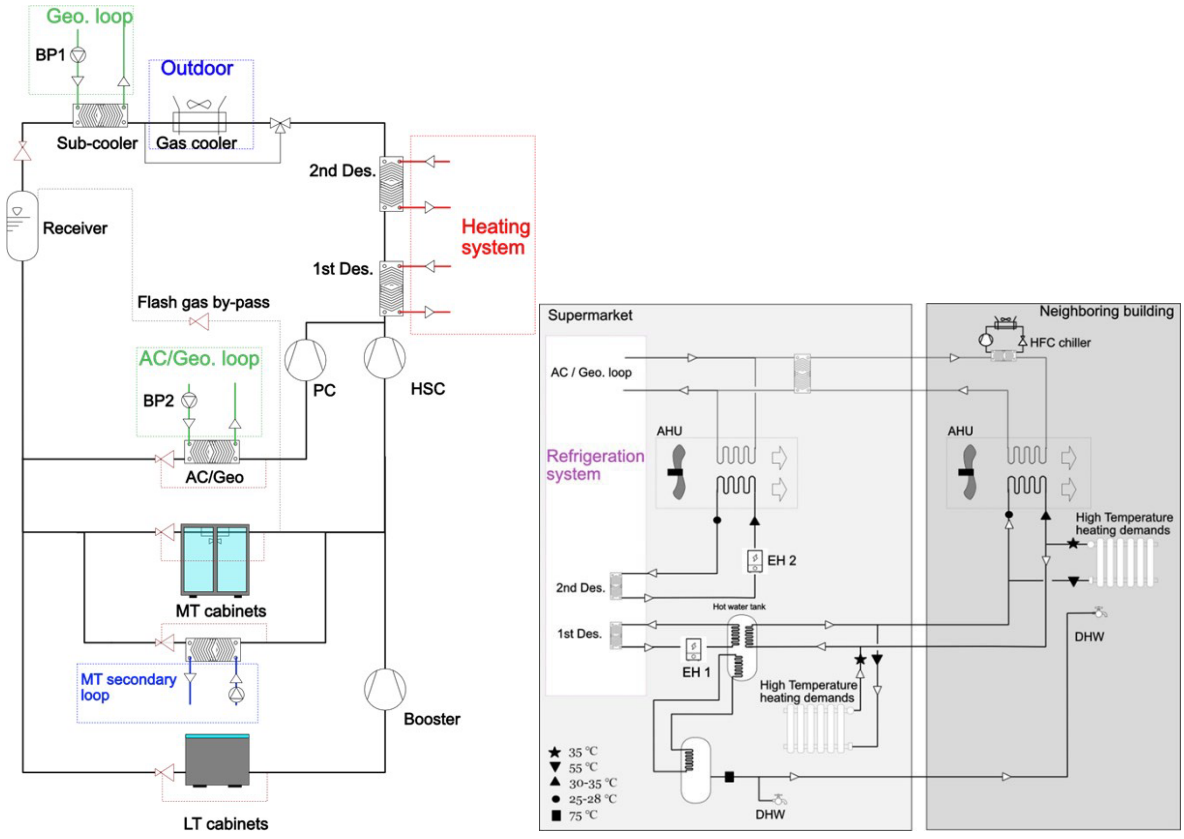


**Figure 2: Drawing of $CO_2$ system for heating and cooling, connected to supermarket cabinets, to the heating system and to geothermal loops. (Used with permission of Sotirios Thanasoulas, KTH)**

*Case 3: R-290 Heat pumps and chillers that produce both process cooling and heating*

The heat pump manufacturer Enrad AB was a Decarbindustry winner in 2022. Their project involved the world's most environmentally friendly furniture factory called the Plus factory building, which was a great example of the use of heat pumps in an industrial process; it combines energy-efficient Passivhaus strategies with a streamlined, robot-assisted production line, which according to Vestre, reduces its energy consumption by 90 percent compared to a conventional factory.

Its energy and heating demands are partly met with the help of 900 rooftop solar panels, 17 geothermal wells, and heat pumps hidden behind the walls to capture excess heat from the process of drying the components and convert it into heat that is then fed back into the production line and used to warm the building. The Heat pumps and chillers use R-290 refrigerant that produces both process cooling and heating for the production line, also comfort cooling and heat to the building by using waste heat, generating 55 percent lower emissions from energy and materials than a comparable building. Details of the heating and cooling capacities of the system are provided in the schematics see Figure 3.

The company claims this also makes the project "Paris-proof", bringing it in line with global targets set out in the Paris Agreement to halve emissions by 2030. the project is reportedly on track to become the first industrial building in the Nordic countries to reach the highest rating in the BREEAM environmental certification scheme, which is only awarded to the top one percent of projects.

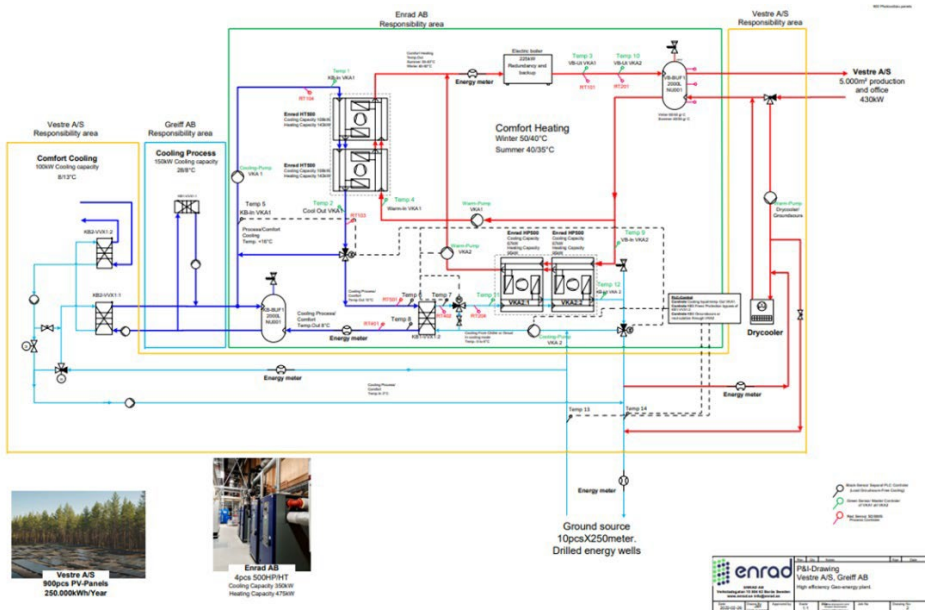


**Figure 3: Drawing of R-290 system for heating and cooling (Used with permission of Enrad AB)**

*Design guidelines for optimization of components and systems*

During the design of a heat pump, there are several choices to be made related to the size and design of the components as well as the size of the heat pump in relation to the energy demand of the building. The optimum is in a first approximation, independent of the refrigerant used in the system, but in some cases, the optimum may shift somewhat.

Many of the choices can be considered as searching for an economic optimum rather than a technical one. For example, increasing the size of evaporators and condensers will decrease the temperature differences and thereby increase the COP of the system, which in turn will decrease the running costs. On the other hand, larger heat exchangers are more costly and therefore increase the first cost. An optimum size can only be found by taking into account factors such as the cost of electricity, the marginal cost of heat exchanger surface, interest rate, number of running hours per year, and the effect of increased surface area on the COP of the system. Likewise, the capacity of the heat pump in relation to the need of the building is an economic optimum: A larger heat pump may cover the heating requirements on the coldest day of the year but will be more costly than a smaller heat pump. First, costs will be higher, but the running costs will be lower. On the other hand, the volume flow/velocity of the heat source and heat sink fluids can be considered as a technical optimum: Higher flow rates require higher pumping power which tends to decrease the COP of the system, but will also decrease temperature differences which tend to increase the COP. Similarly, the choice of the number of parallel sections in an evaporator or condenser is a technical optimization. Assuming a constant total tube length, the cost of the unit is more or less

the same, but with fewer parallel channels, the pressure drop and the heat transfer coefficients will be higher than with a larger number of parallel tubes. A certain number of parallel channels will give the highest evaporation temperature (lowest condensing temperature) and, thereby, the highest COP.

The above examples are generally independent of whether the refrigerant has a high or low GWP. However, there are other factors that should be taken into account, specifically when designing for low GWP refrigerants. Low GWP refrigerants are flammable except for carbon dioxide (and water, which is rarely used as a refrigerant). For this reason, standards stipulate the maximum allowable charge of refrigerant if the system is to be placed inside a building. This maximum charge is related to the floor area and/or volume of the room where the heat pump is located. To reduce risks related to flammability, or in general related to the release of refrigerant, it is advisable to try to decrease the refrigerant charge per unit heating capacity. Apart from reducing risks, the small charge could also allow the installation of a higher-capacity heat pump in a given machine room.

To reduce the charge, it is important to understand the following:

- A large share of the charge is located in the heat exchangers.
- Depending on the type of heat exchanger, the amount of refrigerant in the condenser may be larger or smaller than in the evaporator.
- Standard hermetic or compressors have an oil sump with considerable amounts of oil. With oils miscible with the refrigerant, the amount of refrigerant in the oil may be substantial.
- The density of the liquid phase is much higher than that of the vapor phase.
- A small receiver may be necessary if the heat pump is operating under varying conditions, but the system should be designed so that the receiver is empty of liquid at the most extreme conditions (typically high heat source temperatures). Alternatively, the system should be designed to allow some liquid to rise into the condenser under certain running conditions.
- It is often the case that the highest COP is reached with several degrees of refrigerant subcooling (if no receiver is used). However, the optimum is usually relatively flat, so the effect on COP of decreasing the subcooling by reducing the charge is relatively small.

Based on the above, the following recommendations can be given for designing systems with flammable refrigerants if the systems are to be located inside where the charge may be limited due to flammability-related risks:

- Flat channels, e.g., extruded aluminum multichannel tubes or plate heat exchangers with small pressing depths, should be used to reduce the charge in the heat exchangers. Such tubes /channels have much less volume per heat transfer area than circular tubes.
- It is important to note that smaller channels do not necessarily mean a higher pressure drop. The tube length should be decreased for small channels, and the number of parallel channels should increase.
- Special care should be taken when designing the headers, as these may otherwise contain more refrigerant than the tubes.

- Charge reduction should not be achieved by decreasing the heat transfer areas in the evaporator and condenser, as this would lead to a lower COP of the system. Instead, use heat exchangers with flat channels.
- All lines should be as short as possible, but in particular, it is important to have a short liquid line. The length of the suction line and the high-pressure line is less crucial.
- The charge of oil in the compressor should be selected based on the volume of the system. Compressor suppliers usually assume that the compressor will be part of a large-volume system and therefore adds extra oil to the sump as part of the oil will be distributed to the rest of the system during operation. If the system volume is kept low, the necessary charge of oil is usually lower than the original charge from the factory.

## 2.4 Review of design optimization and advancement impacts on LCCP reduction

### 2.4.1 Introduction

In this section, we describe some ongoing research on using low-GWP refrigerants. Three topics are treated in some detail: First, some projects related to charge reduction are presented. Charge reduction can be seen as a means to increase safety, but it may also be considered a means to decrease the environmental impact, particularly the LCCP. Second, a detailed analysis of different oils and their properties is presented. The study is quite general, but at the end, recommendations for selecting oil for low-GWP refrigerants are presented. Third, we present some ongoing research on high-temperature heat pumps with low-GWP refrigerants. But we start with a short update on the legislation related to the use of F-gases in Europe, including Sweden,

### 2.4.2 Legislation in Europe, including Sweden

Ever since the implementation of the so-called F-gas directive (EU/517/2014) back in 2015, it has been clear that the legislator intends to gradually phase out the use of high-GWP refrigerants on the European market. The F-gas directive has used a number of tools in order to limit both the amount of F-gases on the market as well as the subsequent release them to the atmosphere. These have included limiting the amount of substances put on the market through quota systems as well as other direct bans and requirements of leakage checks and training of installers. One can, of course, have different opinions about the effectiveness of these legislative tools. However, the general aim has always been clear. The phase down and eventually phase out of high-GWP substances. It should therefore be clear to any manufacturer that, at least in the long run, high-GWP refrigerants will not be an option, whether because of availability and cost issues or outright ban on products. Although it is currently not clear at the moment exactly how it will affect the heat pumps and refrigerants, there is also an ongoing process considering including all so-called PFAS substances in the REACH regulation. This could limit, or even make it practically impossible, to use so-called HFO as a replacement for HFC refrigerants. Whatever the outcome of this process, it is clear that there is an inherent financial risk when designing products for use with HFO or HFO/HFC blends.

The F-gas directive is currently under revision, and the final outcome is unclear at of time of writing. One important proposal in the commission proposal 2022/0099 (COD), published on the 5 of April 2022, which can affect how fast the market changes to low-GWP refrigerants for small residential heat pumps is the proposed ban on use of refrigerants with GWP above 150 for brine/water-to-water heat pumps and monoblock air-to-water heat pumps by 2025. This will mean a rapid phase-

out of the use of pure HFC for these products in favor of HFO, HFC/HFO-blends, and natural refrigerants and has most certainly increased the stress levels among manufacturers considering that many current products, especially brine/water-to-water heat pumps, will not be possible to sell. Regarding air-to-water monoblock units, using flammable natural refrigerants, the switch is relatively easy as limiting refrigerant charge is not as critical as the units placed inside. The possible ban for brine/water-to-water heat pumps is more alarming as there is not easily interchangeable HFO or HFO/HFC- blend available under GWP 150, as well as the drawbacks mentioned above. This is a possible option for using flammable natural refrigerants, and there are commercially available units (Ecoforest). However, it will mean an entirely new redesign of the product.

Considering split-type air-to-water and air-to-air heat pumps, the proposal for a GWP threshold is set at 150 in the commission proposal for units with capacities below 12 kW by 2027. This requirement is also challenging for the manufacturers as limiting refrigerant charges for split units is perhaps even more challenging considering the need for refrigerant piping. However, the newly released standard IEC60335-2-40:2022, opens up the possibility to use of even A3 refrigerants in these systems if safety issues can be addressed. As an example, the manufacturer Midea released an R-290 air-to-air heat pump on the European market in 2021 (Midea launches R-290 split, IIFIIR) with a capacity of 3,53 kW and a refrigerant charge (5 m piping) of 380g (KlimaWorld).

It must be mentioned that the F-gas revision is not processing without the heat pump and refrigerant business standing idly by. There is a high chance that these specific bans will be relaxed when the legislation is finally decided upon. Prolonging the time frame and increasing the threshold to allow HFO/HFC-blend is possible.

### 2.4.3 Research on charge reduction

#### 2.4.3.1 EcoPac

EcoPac is a research project with the goal of investigating the feasibility of using a small heat pump to boost the performance of a larger heat pump by using the subcooling of the liquid after the condenser of the larger heat pump as a heat source for the smaller heat pump. The cycle has been analyzed theoretically (Granryd et al. 2022) and tested in a prototype propane heat pump at the laboratory of KTH, Royal Institute of Technology using propane, R-290, in the primary circuit (Forsgren, 2020, Kronström 2021, Ölén et al. 2022). A drawing of the installation is shown in Figure 4.

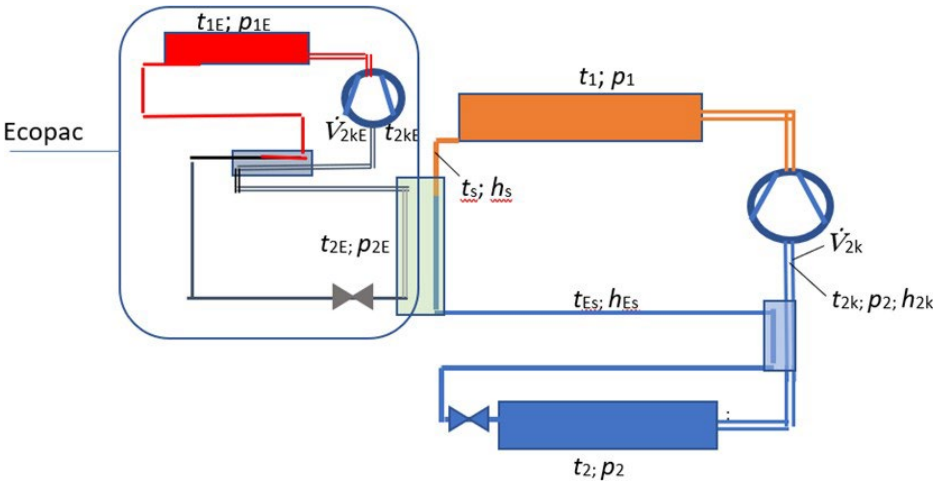


**Figure 4: Drawing of the EcoPac heat pump unit connected to a larger heat pump.**

**(From Granryd et al., 2022)**

As the evaporation temperature of the EcoPac unit is higher than for the larger heat pump, isobutane R-600a was selected as the refrigerant. This would allow reaching high condensing temperatures without excessive pressure levels. The investigation showed, both theoretically and experimentally, that a combined system of this type can reach higher COPs and higher capacities compared to the larger heat pump alone. The total performance depends on the selected condensing temperature levels in the two cycles. One possible solution would be to use a large heat pump to heat the building and pre-heat domestic hot water. In contrast, the EcoPac unit could be used to increase the temperature of the preheated domestic hot water to the 60°C required in order to avoid legionella. In this way, the condensing temperature in the main loop could be decreased, which will increase the COP of this system.

During tests, the EcoPac unit was operated with the evaporation temperature of 15 - 35°C, while the condensing temperature was 50 - 70°C. Two different versions of the EcoPac unit were built. The first standard components (semi-hermetic compressor, standard plate heat exchangers) were used. In the second version, measures were taken to reduce the refrigerant charge to a minimum. To this end, prototype plate heat exchangers with small pressing depths and a DC compressor of the type normally used in AC-systems of electric cars, SHS33 from Sanden were used. This type of compressor has a very small internal volume and requires very small amounts of oil. It also has a very broad speed range. In the tests, the compressor was run at 2000, 4000, and 6000 rpm, giving a heating capacity at 25°C evaporation temperature from about 3 to 9 kW. However, the allowable speed of the compressor is up to 8000 rpm, according to the manufacturer, thus allowing even higher capacities. More importantly, it was demonstrated that this system could be run with a charge of about 120 g of isobutane only. A special challenge to reach this low charge was the design of the internal heat exchanger. As no commercial heat exchanger with a low enough charge was found, a prototype was designed based on multichannel aluminum tubes (see Fig. 5). The EcoPac project continues, and new designs of the internal heat exchanger have been developed and will be tested in a coming prototype system.

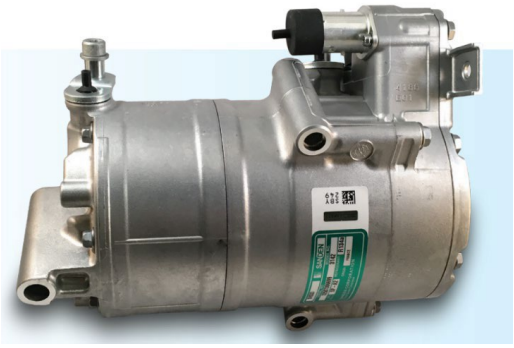

**Figure 5: Scroll compressor, Sanden SHS33, used in the EcoPac system (from https://sanden.wpengine.com/).**

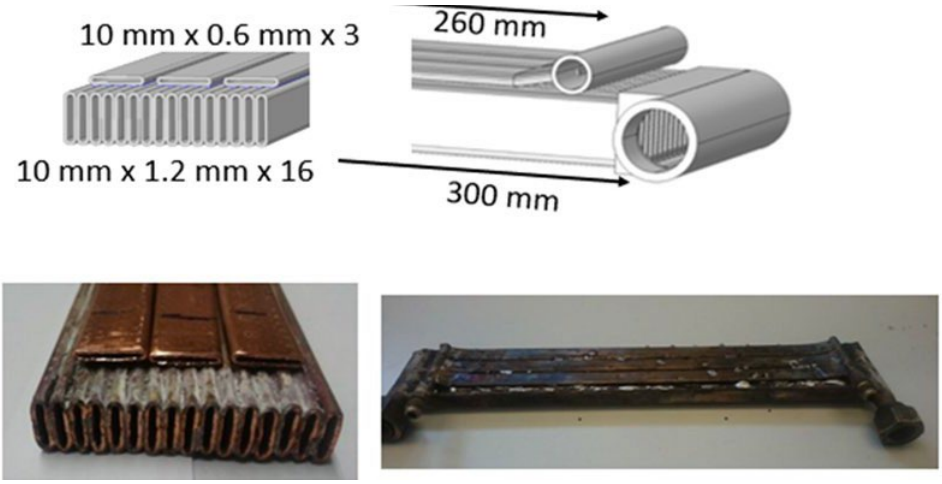


**Figure 6: Drawing and photo of prototype internal heat exchanger of the EcoPac unit. (From Ölén, V., et al. 2022)**

#### 2.4.3.2 ProPac

In the ProPac project, a prototype split AC-system was designed, using propane as a refrigerant. The project's goal was to use less than 150 g of propane for a system with a capacity of 3,5 kW. The system is described in some detail in a report to the Swedish Energy Agency (Andersson K., 2022). Some of the solutions are similar to those in the EcoPac project.

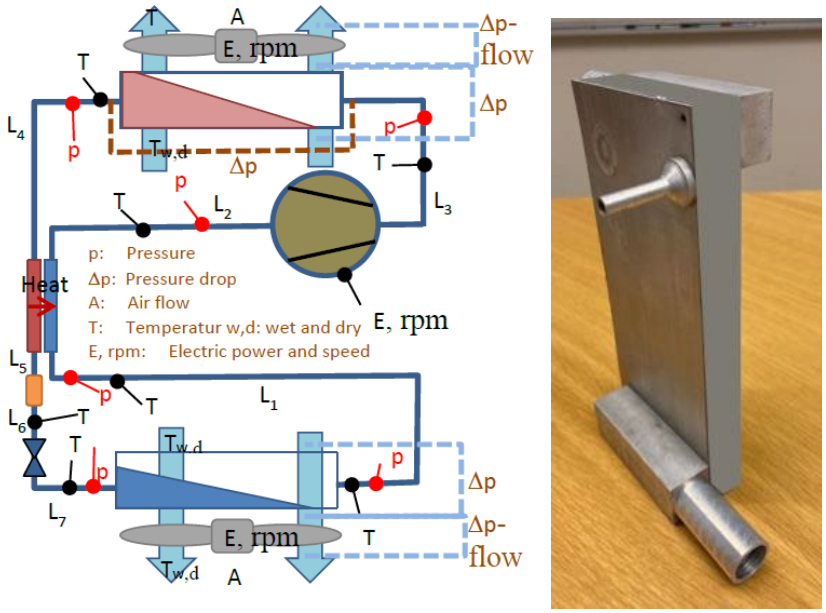


**Figure 7: a) Sketch of the ProPac system. b) internal heat exchanger (From Andersson, K., 2022)**

To reach the low charge, several uncommon design options were used for the components: The condenser was made from extruded flat microchannel tubes with small rectangular channels and fins on the outside. This was perhaps the most standard component of the system. However, special measures were taken to reduce the accumulation of liquid refrigerant in the headers. In spite of this, the charge in the headers was estimated to be almost three times the charge in the tubes (35,6 g as compared to 13,6 g). For the evaporator, different versions of microchannel heat exchangers were tested. It was concluded that even the distribution of refrigerant to the 1000 parallel channels in the evaporator is a key factor in achieving low charge while maintaining low-pressure drop and high heat transfer. Tests were done with the horizontal flow as well as with vertical upflow and vertical downflow. In the end, a solution with vertical downflow was found to give the best results, with low charge and reasonable performance. In order to avoid liquid pools in the top header, part of the tubes inserted into the headers were removed, see Figure 9. The baffle plate originally installed in the evaporator was also removed. Finally, spray nozzles were used to distribute the refrigerant evenly along the top header.

For the internal heat exchanger, a new type was designed together with the participating industrial partners, see Figure 7b.

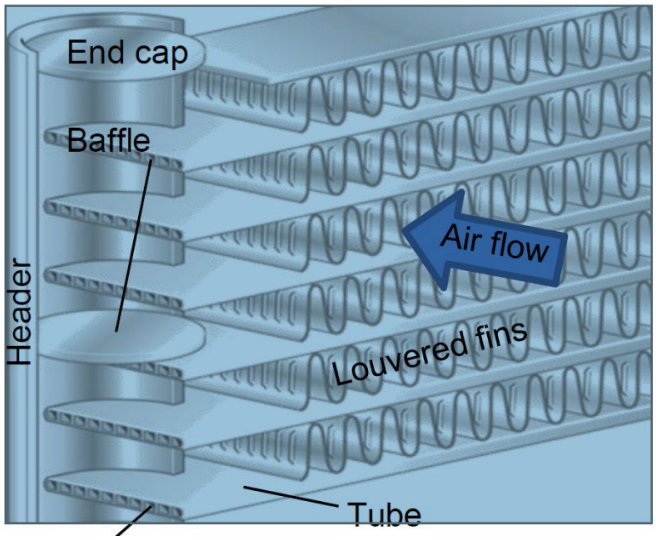


**Figure 8: Design of condenser (From Andersson, K., 2022)**

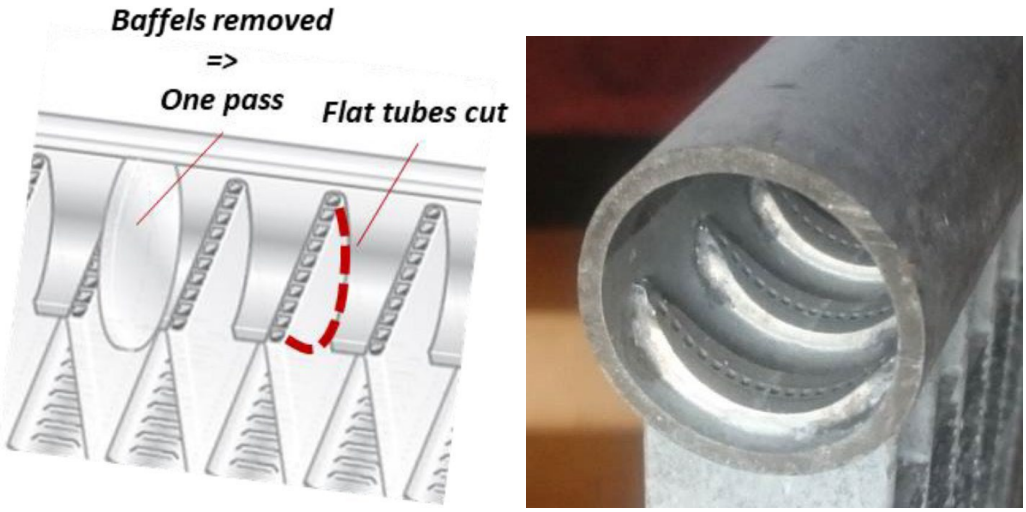


**Figure 9: Original top header and modified header (From Andersson, K., 2022)**

The system used a DC compressor developed for AC systems in electric vehicles and originally designed for R°1234yf (Sanden SHS33, same as for the EcoPac project). According to the report, this compressor has a speed range from 800 to 8500 rpm. The expansion device was a standard electronic valve from Sanhua.

The project goal was reached, with a final charge of 147 g of propane when the connecting lines between the indoor and outdoor units were 6 m long. It should be noted that the expansion device is located close to the condenser (in the outdoor unit) and that the connecting line to the indoor unit is a two-phase line. The charge in this two-phase line (6 m) was about 10 g, and 7 - 8 g in the suction line. The COP (cooling), including the fan power, was 3.5.

### 2.4.4 Selection of oil

#### 2.4.4.1 Lubricant/oil refrigerant mixtures.

In this report, the relationship between lubricant/oil as a substance and refrigerants should be cleared and defined. The term Lubricant-Refrigerant Mixture (LRM) states the effect of the refrigerant on the lubricant in the compressor sump only, while Refrigerant-Oil Mixture (ROM) investigates the effect of the dissolved oil within a circulating refrigerant on the refrigeration system and its effect on the refrigerant thermophysical properties.

Lubricants, in general, have many roles to play in many machines that have moving parts. It acts as a coolant transferring the heat from bearings and mechanical elements to a heat sink, which, in turn, dissipates this heat to the biggest sink reservoir, the environment. It also helps reduce noise generated by moving parts. Compressors, for example, used in HVAC and refrigeration systems require a lubricant to separate the gas on the discharge side from the gas on the suction side. Hermetic compressors, in which the electric motor is always exposed to the lubricant, also require a lubricant with electrical insulating properties. As the lubricant is charged only once in the hermetic system, the chemical stability required of the lubricant is the most important characteristic in the presence of refrigerants. Lubricants used in refrigeration compressors are primarily selected based on their viscosity and miscibility/solubility with refrigerants. Figure 10 shows the relationship between the total efficiency of a compressor and the lubricant's viscosity. It is clear from the figure that low viscosity values lead to poor lubricant film and low volumetric efficiency. In contrast, high viscosity values lead to good film thickness but high frictional losses or low mechanical efficiency within the compressor.

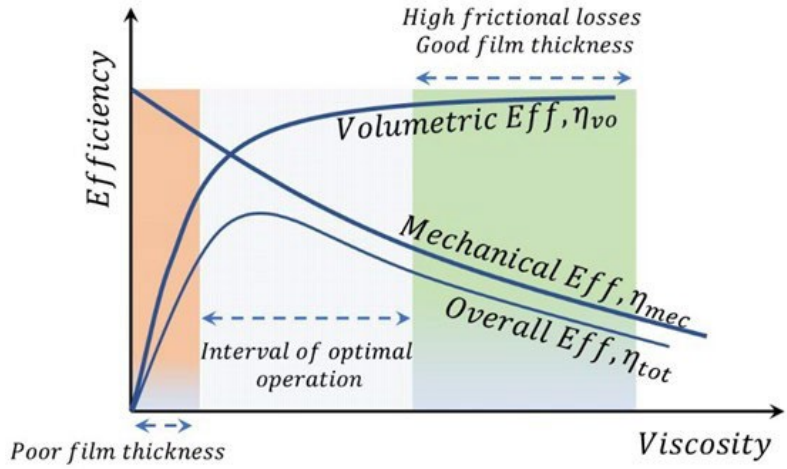


**Figure 10. Relationship between compressor's efficiency and viscosity.**

Other relevant properties are lubricity; chemical and thermal stability; low hygroscopicity; low temperature properties (low pour point, low wax); thermal conductivity; electrical resistivity; non-deposit forming; and environmentally acceptable. Generally, the higher the lubricant's viscosity, the better the sealing and noise reduction capabilities.

The behavior of the oil in the refrigeration systems and its physical interaction with refrigerants are of great importance to the design of the whole system parts. The viscosity of the ROM solution, for example, is crucial for the flow of the mixture within the components of the refrigeration system

and their lifetime. Oil can be soluble in refrigerant, and the refrigerant gas phase carries some oil to different parts of the refrigeration cycle. It flows through the condenser, expansion valve or control devices, and evaporator and returns to the compressor in a reasonable time and must have adequate fluidity at low temperatures. It must be free from suspended matter or components such as wax that might clog equipment in the refrigeration system or deposit it on the evaporator or condenser surfaces, adversely affecting the heat transfer coefficient and the heat transfer process.

#### 2.4.4.2 Lubricant/Oil Types

Lubricants/oils that are frequently used with low -GWP) refrigerants, whether they are synthetic or natural, are mineral oils (MOs); alkyl-benzenes (ABs); Poly-alpha- olefins (PAOs); poly-alkylene-glycols (PAGs); poly-vinyl-ethers (PVEs); and poly-ol-esters (POEs). Rudnick (Rudnick 2013) put together an excellent introduction to all types of synthetic lubricants, including polyglycols and esters.

*Mineral Oils (MOs)*

Mineral oils, also called petroleum oils, were the lubricant of choice for the vast majority of refrigerants before 1990, and they remain the least expensive oils in the market up to date. They are used with CFCs and some of the HCFCs as well as HCs. They are not miscible with most HFC or HFO refrigerants due to their high polarity, which was the primary reason for the major shift to oxygenated synthetic lubricants. HFC refrigerants are forbidden from using mineral oil because of their poor miscibility in lower temperature conditions. The primary limiting property for this oil is its “pour point,” which can vary greatly depending on the exact hydrocarbon mix of the lubricant. Inadequate pour point properties make mineral oils unacceptable for applications requiring very low evaporator temperatures (less than –40°C); this problem led to the first use of synthetic lubricants in refrigeration systems (Rudnick 2013). Mineral oils’ properties vary depending on their molecular weight and the process by which they are refined. They are supplied in a liquid form and made from carbon and hydrogen molecules only. They are light yellow in color and slightly hygroscopic. MOs are blends of linear and branched alkanes, cyclic alkanes (naphthene), and aromatic compounds.

*Alkyl-benzenes (ABs)*

The chemical structure of ABs of unsaturated double-bond carbon ring results in a stable molecule. Made to replace MOs. The viscosity of ABs is controlled by the size of the hydrocarbon chain, the degree of branching of the chains, and the number of chains attached to the aromatic ring. ABs have improved solubility and miscibility in HCFCs (Takigawa 2002), better oxidation stability with respect to MOs, and lower Pour Point, which makes them suitable for very low-temperature applications (less than –50°C) using CFC and HCFC refrigerants compared to MOs.

*Poly-alpha-olefins (PAOs)*

PAOs are derived by controlled oligomerization of linear alpha-olefins derived from ethylene, and they are 100% synthetic hydrocarbons. PAOs are classified according to their approximate kinematic viscosity (KV) at 40°C. Kinematic viscosity is controlled by the degree of polymerization of the olefin and by the amount of rearrangement of the reactants and products to produce branched isomers. The commercial name of PAO comes with a number; the higher the number, the higher the viscosity of the lubricant/oil. For example, PAO-10 has 9.87 cSt, 64.50 cSt, and 34600 cSt values based on ASTM D 445 test at 100°C, 40°C, and -40°C, respectively, while PAO-40 has 41 cSt, 410 cSt, 40000 cSt, for the same temperatures.

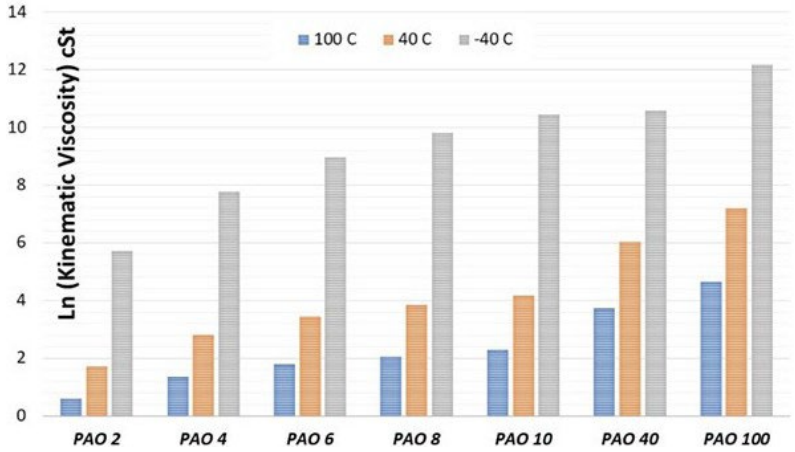


**Figure 11: KV values of PAOs for different test temperatures.**

Figure 11 indicates the increasing trend of kinematic viscosity values of PAOs. PAOs have improved properties compared to mineral oils with higher viscosity index (VI), decreasing the pour point to -75°C suitable for cold weather, improved thermal stability, and increasing the flash point to the range of 290°C. Table 1 compares POA-4 synthetic oil with several mineral oils: 100 Neutral (100N), 100 Neutral with low pour point (100NLP), and hydrotreated high viscosity index (VHVI). It shows the improved properties of PAOs over several mineral lubricants. PAOs have also been used in ammonia and fluorocarbon refrigeration compressors because of their low-pour points.

*Poly-alkylene-glycols (PAGs)*

PAGs derive from the controlled polymerization of propylene oxide (PO), or a mixture of PO and ethylene oxide (EO). The average molecular weight of the polymer chain determines the viscosity of PAGs. The properties can be easily tailored to control viscosity while also optimizing compatibility (miscibility/solubility) with a particular refrigerant, as seen in Figure 12. Polymerization is usually initiated either with alcohol or by water. Initiation by mono-alcohol results in a “monol” (mono-end-capped); initiation by water or a di-alcohol results in a “diol” (uncapped). Another type is the double-end-capped PAG, a mono-capped PAG that is further reacted with alkylating agents.

Double-end-capped PAGs are common lubricants in automotive air-conditioning systems using R-134a because of their benefits in boundary lubrication and refrigerant miscibility. PAGs have a very high viscosity index, excellent lubricity, low pour point, and good compatibility with most elastomers. However, they are susceptible to depolymerization in the presence of trace amounts of strong acids, bases, and free radicals. Developed for R-134a, color light blue, viscosity has three types 46 cSt, 100 cSt, 150 cSt, highly hygroscopic, mixed well with HFC, could not be used in hermetic compressors for its low electrical resistivity.

**Table 1: PAOs compared to Mineral Oils (Rudnick, 2013).**

| Oil/Properties | PAO-4 | 100N | 100NLP | VHVI |
|---|---|---|---|---|
| KV @ 100°C | 3.84 | 3.81 | 4.02 | 3.75 |
| KV @ 40°C | 16.7 | 18.6 | 20.1 | 16.2 |
| KV @ -40°C | 2390 | Solid | Solid | Solid |
| Viscosity Index | 124 | 89 | 94 | 121 |
| Pour Point | -72 | -15 | -15 | -27 |
| Flash Point | 213 | 200 | 197 | 206 |

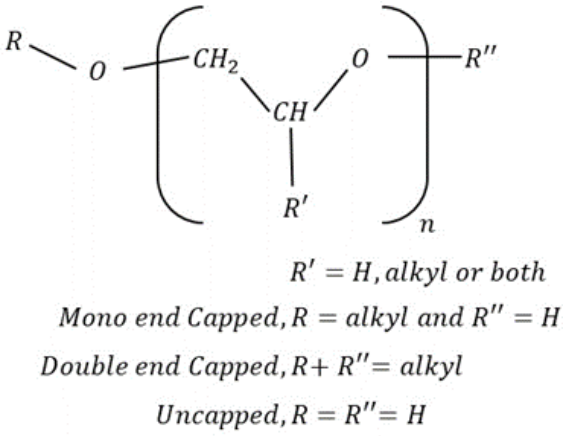


**Figure 12: PAGs chemical formulation**

*Poly-vinyl-ethers (PVEs)*

PVEs belong to a special class of PAOs where the side chains contain oxygen atoms and make it more miscible with HFC refrigerants than traditional PAOs. Similar characteristics to MOs. The chemical structure's side chain has characteristics of PAG oils with good solubility and no hydrolysis.

*Esters or poly-ol-esters (POEs)*

The POEs have four general structures, neo-pentyl glycol (NPG), tri-methylol-propane (TMP), penta-erythritol (PE), and Di-penta-erythritol (DiPE) (NIH 2022). They are manufactured by the reaction of a carboxylic acid with an alcohol, as per Figure 13.

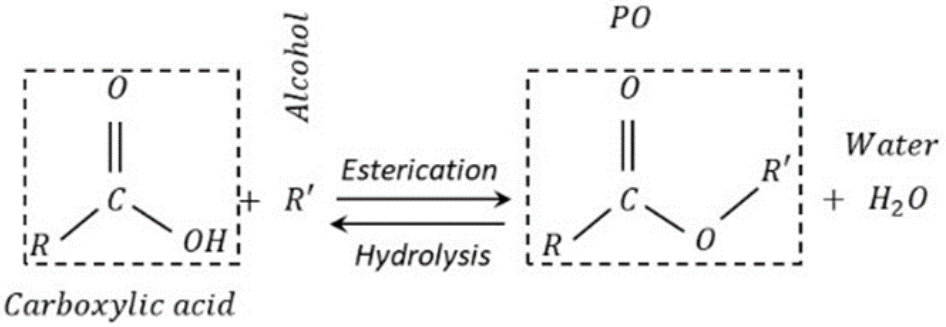


**Figure 13: POEs chemical process.**

POEs are used in HFC refrigerants where their cohesive properties (miscibility and solubility) can be designed to optimize their compatibility with a given working fluid. The oil-refrigerant mixture should remain a single phase within the temperature and pressure operating envelope. Too much compatibility between the two could lead to undesirable viscosity dilution of the lubricant by the refrigerant, leading to poor lubrication of the moving parts within the compressor. The objective is to be sufficiently miscible to ensure proper oil return to the compressor while limiting solubility to avoid excessive viscosity reduction in the compressor. In general, the miscibility decreases with increasing molecular weight and linear acid content because more refrigerant molecules must organize around each ester molecule to achieve solubility. POEs lose miscibility with HFC when linear carbon chain lengths exceed six carbons, so using branched-chain acids will improve the miscibility. They are universal oil, clear color, not used for R-134a, slightly hygroscopic, polar mix better with HFCs, biodegradable, and miscible with MOs.

Pentaerythritol esters (PECs), which are linear, branched, and/or cyclic-chained esters, are the main precursors and components of POEs lubricants is an excellent solvent for impurities such as moisture, compressor wax, and mineral oils (Herbe and Lundqvist, 1997). It also prevents clogging in the fluid line components such as filters, vanes, and valves. Many experimental studies regarding PECs with R-1234yf and R-134a, as well as other fluorinated refrigerants including R-1234ze(E), R-32, R- 152a, R-143a and R-125 have been recently published (Sun et al., 2017, Sun et al., 2020, Wahlström and Vamling 1999, Wahlström and Vamling 2000, and Wang et al., 2016).

The Polyethylene Glycol Dimethyl Ethers (PEGDMEs) family has also been promoted as alternative lubricants to be an excellent solvent for HFC and HFO. There is numerous vapor-liquid equilibrium (VLE) data available for mixtures of PEGDMEs with R-134a (Chaudhari et al., 2008, Coronas et al., 2002, López et al., 2009, López et al., 2004, Marchi et al., 2006, Tseregounis and Riley, 1994, and Zehioua et al., 2010), while data for R-1234yf is not enough (Fang et al., 2018).

#### 2.4.4.3 Lubricant/Oil Classifications

According to DIN 51503 Part 1, refrigeration oils are classified alphabetically into the following groups:

*Class KAA*

Refrigeration oils immiscible with ammonia are mineral oils and/or synthetic oils based on poly-alpha- olefin (PAO), alkyl-benzene (AB) or hydrogenated mineral oils. Highly refined, naphthenic refrigeration oils are mostly used as KAA oils. Hydrogenated refrigeration oils and PAOs are becoming increasingly popular in practice.

*Class KAB*

Refrigeration oils miscible with ammonia are Poly-alkylene-glycol (PAG). The PAG lubricants normally used should not exceed a maximum water content of 350 ppm (fresh oil).

*Class KB*

Refrigeration oils for carbon dioxide ($CO_2$) – synthetic polyol esters (POE), poly-alkylene-glycols (PAG) or poly-alpha-olefins (PAO). POE oils generally have good $CO_2$ miscibility. PAG oils are significantly less miscible with $CO_2$ (larger miscibility gap with $CO_2$). Synthetic refrigeration oils based on poly-alpha-olefins are referred to as refrigeration oils that are immiscible with $CO_2$.

Class KC

Refrigeration oils for fully and partially halogenated chlorofluorocarbons (CFC, HCFC) are usually mineral oils and alkyl benzenes (ester oils are also possible in individual cases). Mostly highly refined, naphthenic mineral oils and specially treated alkyl benzenes (alkylates) are used. The water content of the KC oils (fresh oils) should be less than 30 ppm. If the water content is higher, it can be assumed that undesirable reactions with the refrigerant will occur, leading to the decomposition of the oil- refrigerant mixture.

*Class KD*

Refrigeration oils for fully and partially fluorinated Fluorocarbons (FC, HFC) are polyol ester oils (POE) or poly-alkylene-glycols (PAG). The refrigeration machine oils described in group KD are polar products with highly hygroscopic properties. A maximum permissible water content of 100 ppm in fresh oil applies to polyol esters (POE). Poly-alkylene-glycols are preferably used in A/C systems. They should not exceed a maximum water content of 350 ppm (fresh oil).

*Class KE*

Refrigeration oils for hydrocarbons (e.g., propane, isobutane) are mineral or synthetic oils based on alkylbenzenes, PAO, POE or PAG. Depending on the substance group, the maximum permissible water content is 30 ppm for mineral oils/ Alkylbenzenes, 50 ppm for PAO, 100 ppm for POE, and 350 ppm for PAG (new oil parameters).

#### 2.4.4.4 Mixtures' Properties.

To understand the core relationship between oil and refrigerant in any refrigeration or heat pump system, we should though focus and differentiate between the relationship of ORMs, which represent the effect of the presence of the oil within the refrigerant charge in the refrigeration cycle components, and RLMs, which shows the effect of refrigerant within lubricant in the compressor sump on the other hand. ORMs have many important properties for which boiling point of the mixture, heat load for vaporization and condensation, densities of the liquid and gas phases, blockage, and materials compatibility are the most crucial properties that we should investigate. In contrast, RLMs have different properties for which viscosity, solubility, viscosity index (VI), lubricity, and hydrolytic stability are the most important properties that we need to understand to prevent the compressor from failure.

Several factors should be investigated when using ORMs in a refrigeration system. The amount of the oil dissolved should also be known where increasing the mass fraction of the oil within the refrigerant can affect the thermos-physical properties of the mixture, such as mixture viscosity, vapor pressure, vapor density, and the performance of the system. The compatibility issues

between the oil and the refrigerant's chemical structure are also important, where the new low GWP refrigerants use only certain types of oils.

Figure 14 illustrates the ORM factors that should be addressed and solved. In the condenser, hydrolytic stability, as well as thermal properties, should be examined. In the evaporator, miscibility and thermal properties should be understood carefully where the boiling point could be altered if the amount of the oil varies, oil holdup within the evaporator and the condenser can decrease the heat transfer coefficient, reduce the design cooling capacity, and decrease the COP of the system. Chen (2019) studied the distribution of R-134a with different pressure ratios, compressor strokes, and refrigerant charges, indicating that the condenser holds the maximum charge.

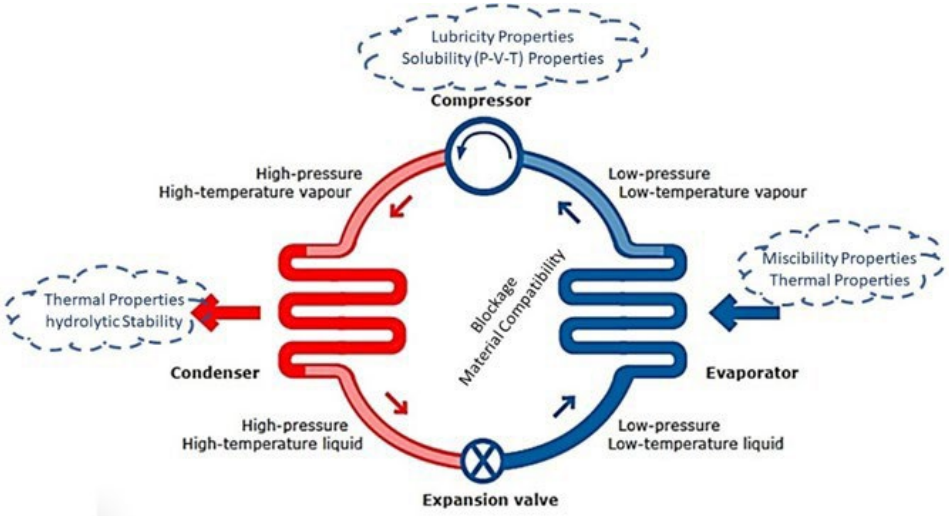


**Figure 14: Oil/Refrigerant issues in heat pump equipment.**

Figure 15 shows the refrigerant mass ratio holdup within different parts of one specific system. In this case, 70% of the total charge is within the condenser, 10% within the evaporator, 15% within the liquid line, and 5% within other components. The distribution trend can be seen with different strokes and pressure ratios.

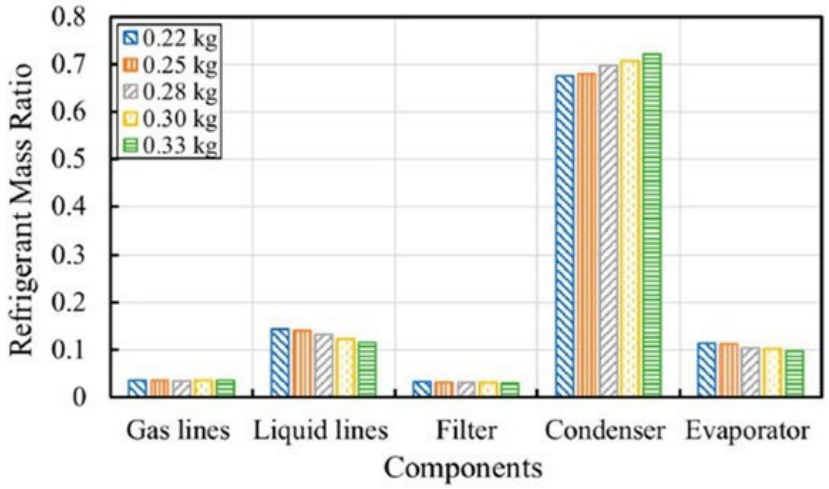


**Figure 15: Refrigerant R-134a distribution in a refrigeration system.**

#### 2.4.4.5 Refrigerant-lubricant mixture (RLM) Properties

The effect of the vapor or liquid refrigerant within the lubrication fluid in the compressor sump will be highlighted and studied. Lubricant properties vary with its chemical family. These properties are viscosity, solubility, viscosity index (VI), lubricity, pour point, thermal and hydrolytic properties, and oxidation stabilities.

*Viscosity*

Dynamic viscosity selection depends upon the minimum film thickness required to avoid wear surfaces, maximum allowable viscous drag, minimum sealing, minimum flow rate, and minimum variation within the operating envelope (temperature, pressure, and refrigerant flood back). The viscosity of the lubricant in the presence of any refrigerant may decrease as much as an order of magnitude since the refrigerant viscosity is typically 2 to 3 orders of magnitude smaller than that of oil (A. M. Yokozeki 1994). Figure 16 shows the viscosity variation for POE with R-32, R-134a, R-410A, and R-22 at 40°C. The curvature of the lines depends on the molecular weight of the refrigerant. The lighter values, the faster the decrease in the viscosity (Toumas and Jonsson 1999).

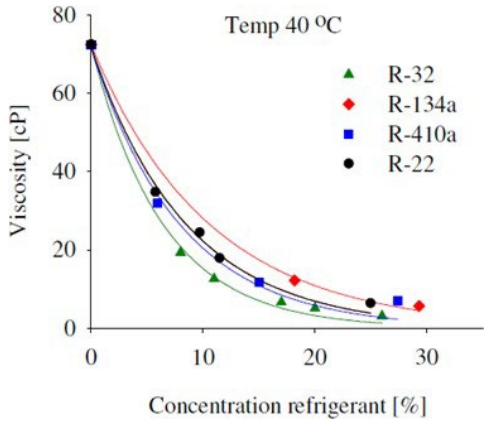


**Figure 16: Viscosity vs. concentration.**

The viscosity of RLMs can be given analytically by relating the viscosity of the lubricant and the refrigerant as in equation (1) (Schroeder, 1986). The density of the mixture also can be given as in equation (2):

$$ln\,\vartheta_{RLM} = (1-\gamma_{ref}) * ln\,\vartheta_{lubricant} + \gamma_{ref} * ln\,\vartheta_{ref} \quad (1)$$

$$\rho_{RLM} = \frac{1}{1-k} * \frac{\rho_{lubricant}}{1+\gamma_{ref}\left(\frac{\rho_{lubricant}}{\rho_{ref}}-1\right)} \quad (2)$$

where $\gamma_{ref}$ is a refrigerant mass fraction and (k) can be computed by interpolation from the data published by Jaeger (Jaeger 1972).

Figure 17 shows how the viscosity and density of the sample lubricants vary with temperature. The sample of three lubricants (SL-22, SL-68, SL-220) have different viscosities and are used in an open drive reciprocating compressor, Coldex-Frigor type. The figure shows that the viscosity and the density decrease with the increase in the temperature of the mixture for all lubricants. It also indicated that SL-220 sample with the highest viscosity demonstrates maximum power

consumption (Afsharia et al., 2017). Viscosity can also be obtained from PVxT chart. The parameters used to construct the chart are pressure, temperature, solubility, and kinematic viscosity. The combined PVxT data that includes isobaric curves is called Daniel Plot. The Plot of any mixture is derived from refrigerant solubility data (x), density data ($\rho$), and viscosity data versus temperatures ($\mu$). To get the dynamic viscosity of a specific RLM:

- pressure and temperature are selected first.
- pressure versus temperature is used to measure solubility parameters.
- solubility versus temperature is used to measure kinematic viscosity (KV or$\vartheta\vartheta$ = $\mu\mu/\rho\rho$, cSt) and density parameters.
- dynamic viscosity ($\mu\mu$, cP) is obtained by the product of KV and density.

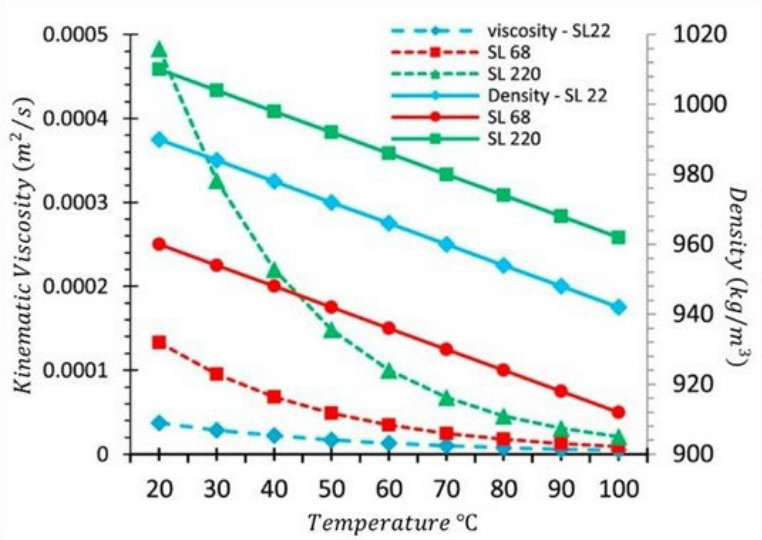


**Figure 17: Viscosity and density of RLM with respect to temperature .**

Figure 18 gives the kinematic viscosity parameter from Daniel Chart for Fuchs' SEZ 32 lubricants with R-1234yf, a low GWP refrigerant (FUCHS 2014). In Daniel Chart, constant pressure (isobaric) curves are incorporated to show the effect of pressure on viscosity. The pressure curves are typically 10, 15, 25, and 35 bar.

Figure 19 and Figure 20 give the relationship between kinematic viscosity (cSt), pressure (MPa), and temperature (C) for refrigerants R-1234yf and R-1234ze(E) as refrigerants with International ISO VG 32 lubricant (Morais 2020). ISO VG stands for "International Standards Organization Viscosity Grade" and is reported in numbers ranging from 2 all the way up to 1500. The ISO VG 32 gives the flow speed of this lubricant in milli-meter per second under the effect of gravity forces inside a Capillary U-Tube Viscometer Test controlled at (40C or 104F). In industry practice, the liquid composition often only ranges from pure lubricant 100% down to about 70% as seen in the figures. To find the viscosity range of the lubricant containing the refrigerant in ($mm^2/s$=1 centistokes or cSt) and the concentration of the refrigerant within the lubricant, we need to specify the range of the operating temperatures (horizontal axis) plus the superheated temperatures values and the corresponding evaporation pressures in (MPa).

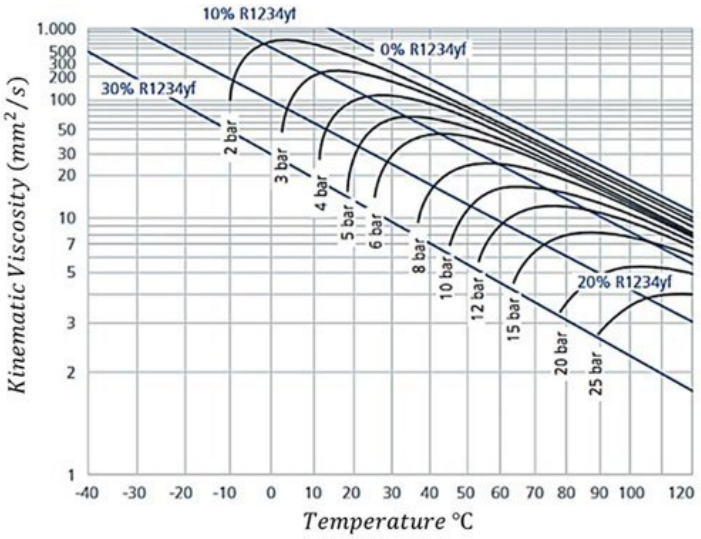


**Figure 18: Daniel Chart for R-1234yf and Fuchs' SEZ 32 lubricant mixtures.**

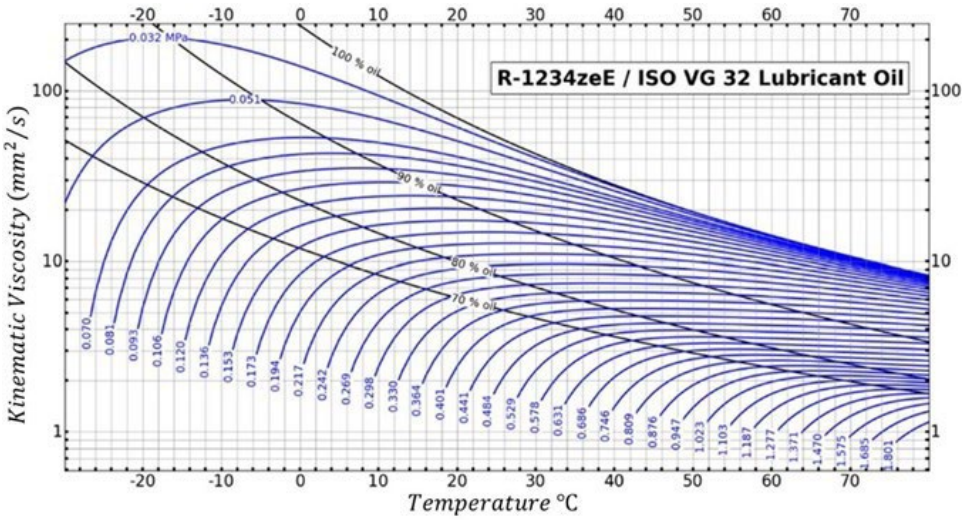


**Figure 19: Daniel Chart for R-1234ze (E) with ISO VG 32 lubricant.**

The curved blue lines toward the horizontal axis are the pressure lines of the mixture. It is obvious from the figure that the increase in the compressor suction temperature and the evaporation pressure for a specific concentration will ultimately lead to a decrease in the lubricant viscosity of the compressor. An analytical model was developed to predict the PVxT parameters for any nonconventional mixing rules between RLM using cubic equations of state (EOS), namely the modified Soave-Redlich-Kwong (SRK) equation. The matching between the model and experimental vapor-liquid-liquid equilibrium (VLLE) or vapor-liquid equilibrium (VLE) data for several mixtures was validated. Figure 21 shows the pressure in MPa versus refrigerant molar concentration in a specific lubricant. The solid lines represent the model fitting the experimental vapor-liquid-liquid equilibrium (VLLE) data for certain RLM.

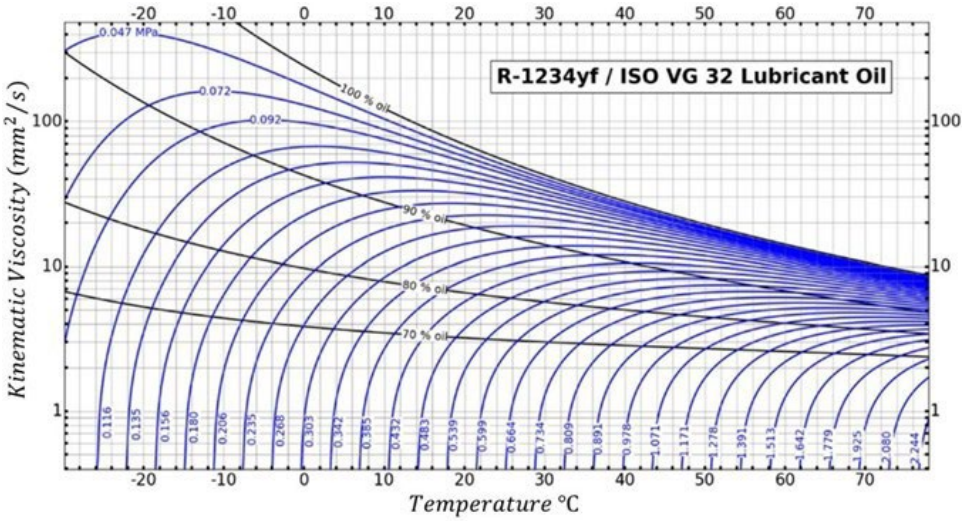


**Figure 20: Daniel Chart for R-1234yf with ISO VG 32 lubricant.**

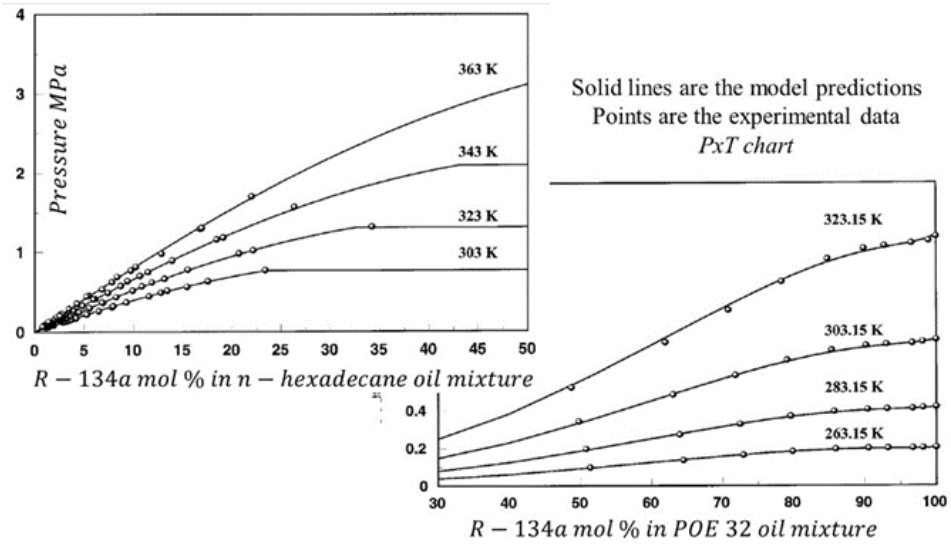


**Figure 21: SRK analytical model results for an RLM solution.**

Another analytical model used to define the correlation between RLM concentration and pressure is the soft-SAFT equation of state (Albà, Llovell, and Vega 2021). They have obtained the PVxT chart for R-134a in POE lubricant, PEC5 type lubricant (Wahlström et al. 1999), and R-1234yf in POE lubricant, TrEGDME type lubricant (Fang et al., 2018) at different temperatures as seen in Figure 22. Both models need to be verified for new low GWP refrigerants.

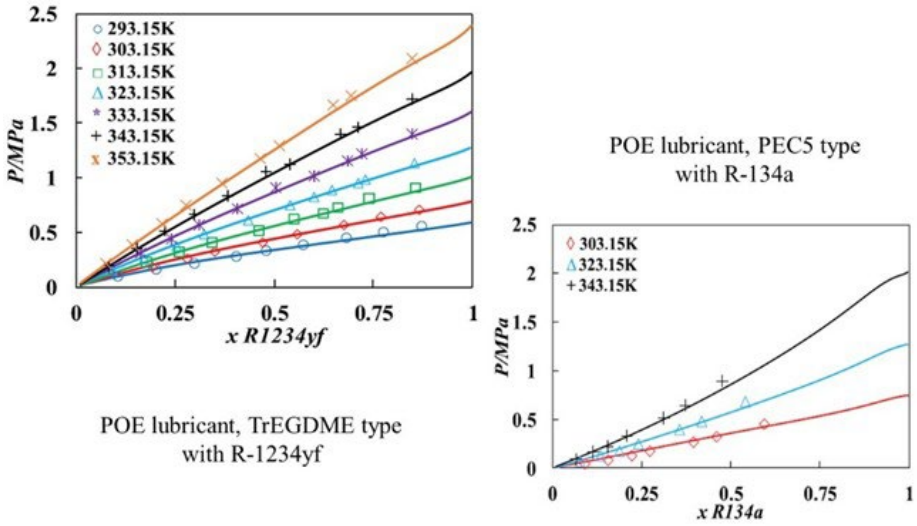


**Figure 22: Soft-SAFT analytical model results for an oil refrigerant mixture.**

*Viscosity Index (VI)*

The viscosity index is used to measure a fluid's change of viscosity in relation to temperature. This index is used to characterize the viscosity-temperature behavior of lubricants. The higher the VI, the smaller the relative change in viscosity with temperature, and the lower the VI, the more viscosity is affected by changes in temperature. VI improvers, also known as viscosity modifiers, are additives that increase the fluid's viscosity throughout its useful temperature range. These modifiers are polymeric molecules that are sensitive to temperature. At low temperatures, the molecule chain contracts and does not impact the fluid viscosity; at high temperatures, the chain relaxes and increases viscosity.

*Hydrolytic Stability*

Lubricant’s ability to resist chemical decomposition in the presence of water is known as the lubricant’s hydrolytic stability (DIN 51777). Some lubricants are, by nature, hygroscopic fluids, which absorb vapor water from the air. Polyol esters (POEs) and phosphate esters fluid are an example of such lubricants. The existence of water in the POEs lubricant can change the structure of the lubricant when metal catalysis exists. Over time, these impurities break down the chemical structure of the lubricant and produce carboxylic acids. By measuring the acid number (AN), we can determine the by-product of oxidation or lubricant depletion rate. Acids can erode the copper piping and heat exchanger plates and can lead to component damage. The interaction between HFO refrigerants, pure or blend, with PVEs has been studied. Figure 23 indicates that the AN value increases in the presence of metal catalysis and when the water content increase. Figure 24 shows the moisture absorption (hygroscopicity) of different lubricants. Nonpolar lubricants such as MOs and PAOs, which normally have water contents of less than 30 ppm show no significant increase in water content. POEs which are described as polar, hygroscopic lubricants, display a marked increase in water content. The diagram also shows the increase in water content in relation to viscosity. Low-viscosity ester oils absorb moisture more rapidly than high-viscosity ester oils. PAGs, which are mostly used in aircon systems with R-134a, are even more hygroscopic. PAGs absorb large quantities of moisture in relatively little time and thus rapidly exceed permissible thresholds of about 800 ppm.

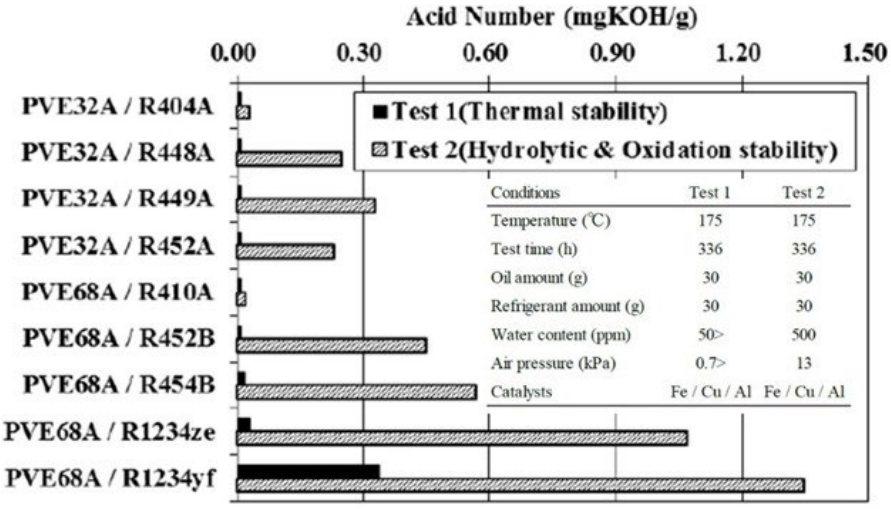


**Figure 23: Hydrolysis test for several HFO refrigerants.**

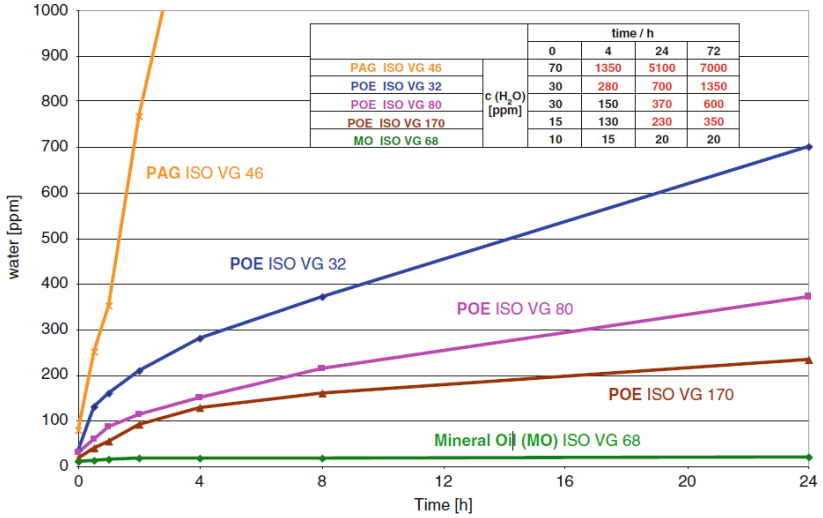


**Figure 24: Water absorption (hygroscopicity) of lubricants.**

*Pour Point*

The pour point is defined as the lowest temperature at which a lubricant is observed to flow by gravity in a specified lab test (ASTM D97-17b). Specifically, the pour point is 3 degrees C (5 degrees F) above the temperature at which the lubricant shows no movement when a lab sample container is held horizontally for 5 seconds. Pour point depressants are polymers that allow lubricants to flow at low temperatures. They are typically used in paraffinic base oils.

*Oxidation Stability*

Oxidation stability is a chemical reaction that occurs with a combination of lubricant and oxygen. The rate of oxidation is a time function, and it will be accelerated by high temperatures, water content, acids, and catalysts such as copper and other materials. Oxidation will lead to an increase in the oil's viscosity and deposits of varnish and sludge that could harm the compressor on start-up.

*Lubricity*

Lubricity is the ability of a fluid to minimize the degree of friction between surfaces in relative motion under load conditions. When the lubricity is unsatisfactory, excessive wear and metal damage can occur, leading to inefficient performance, shortened service life, and high replacement costs. The refrigerant introduction into the lubricant would decrease its viscosity, leading to better lubricity. Inserting additives to the oil, such as phosphate-based additives, improve the lubricity with refrigerant R-134a (Tuomas 2006). The chlorine in HCFC refrigerants acts as an additive and delays early compressor failure. Refrigerants with two or more chlorine atoms in the chemical structure of the refrigerant showed improved lubrication properties (Murray, S. F.; Johnson, R. L.; Swikert, M. A.1956). It is reported that the wear rate of the bearing surfaces typically requires 50% higher viscosity when lubricated with a POE/R-134a mixture than for a bearing lubricated with MO/R-22 (Jacobson 1994). Refrigerant HFC, HFO, and HC with no chlorine particles mixed with POEs have shown poor lubricating properties. There are different additives based on their functionality: Anti Wear (AW), Extreme Pressure (EP), and Friction Modifier (FM) (Urrego 2012).

#### 2.4.4.6 Oil-refrigerant mixture (ORM) Properties

The ORM properties do not differ from RLM properties, but miscibility-solubility properties and the thermo-physical properties are the most insisting issues that need to be evaluated to understand the effect of the mixture on the energy efficiency of the systems and their performance.

*Miscibility - Solubility*

Miscibility is the property of two substances that mix entirely in all proportions or concentrations to form a clear homogeneous solution, whereas solubility is the ability of one component (the solute) to dissolve in the other component (the solvent) till saturation point or phase separation occurs. An example of miscible solutions is water and alcohol. The chemical miscibility of the oil-refrigerant mixture is a good indicator of how well the refrigerant will help move the oil around the system. We must indicate that the amount of oil circulated with the refrigerant is small, but its effect is crucial.

Miscibility is typically studied by mixing known concentrations of refrigerant and lubricant and lowering the temperature until a phase separation is observed (DIN 51514). The results are used to plot a curve of concentration versus temperature which indicates the miscibility boundaries before causing the separation of an oil-rich phase. The curve shows the amount of refrigerant mixed with the oil-rich phase (solubility of refrigerant in oil). Knowing where the separation phase will form and how much refrigerant is needed to dilute an oil-rich phase will help us determine which types of lubricants are acceptable for use with a given refrigerant.

Figure 25 states all the possibilities of miscibility gaps between refrigerants and oils. The miscibility curves of Fuchs' POE SEZ 32 oil with refrigerant R-134a and low GWP refrigerant R-1234yf are seen in Figure. The horizontal axis represents the concentration of the oil mass in a corresponding refrigerant. For R-134a, the target area of full miscibility is between -15°C and 90°C for all oil concentrations, and the area(s) of phase separation is located at the bottom and the top of the figure. In the case of refrigerant R-1234yf and Fuchs' SEZ 170 oil mixture, the whole miscibility area has completely changed where the phase separation is between oil concentration of 5% till 48% for all temperatures range -60°C and 120°C. The amount of oil in R-1234yf is less than 5% which will not affect the thermal properties of the heat pump cycle, or more between 48% and 57%, as seen in the figure. Increasing the oil concentration within the refrigerant is not recommended due to its effects on the thermal properties of the refrigeration cycle and performance.

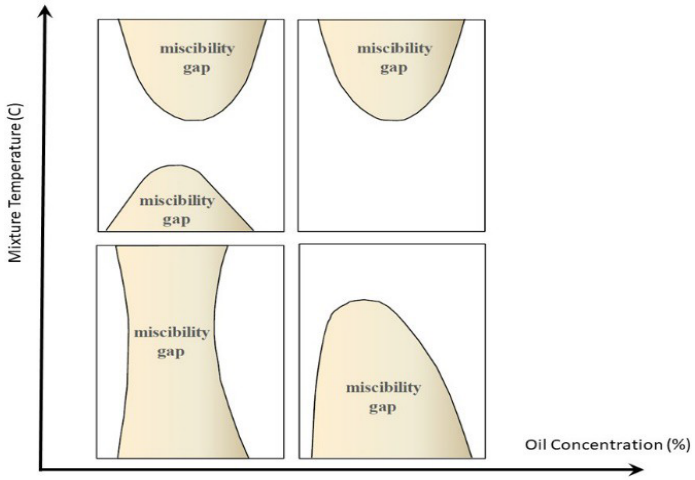


**Figure 25: Possible miscibility gaps.**

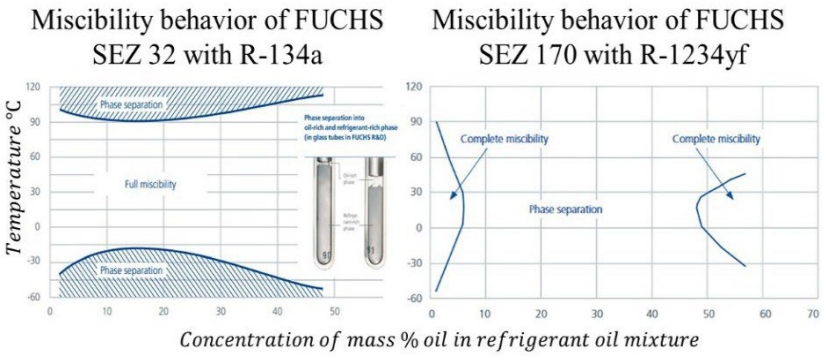


**Figure 26: Fuchs' miscibility charts with R-134a & R-1234yf.**

The miscibility property is crucial to prevent phase separation between the lubricant and refrigerant mixture, especially in the evaporator. When the refrigerant vapor migrates from the evaporator to the compressor's crankcase, it is absorbed, condensed, and precipitated as a refrigerant liquid at the bottom of the crankcase because it is heavier than the oil. The refrigerant, either in the form of liquid or vapor, travels to places where pressure is the lowest. These places are the compressor's suction line or the compressor's crankcase. Manufacturers will incorporate a crankcase heater on the compressor to prevent this phenomenon. The resulting vapor will be forced back into the suction line and may condense, causing slugging in the compressor's cylinders on the next start-up; blockage thus happens during the compressor's long shutdown period.

Experimental results on the miscibility of POE and PVE oils with the low GWP refrigerant R-1234ze(E) showed that the non-miscible area of R-1234ze(E) and PVE 68 oil mixture is 13% larger than that of R-1234ze(E) / POE 68 mixture (Lee et al., 2016). Other experiments have been performed on R152a (HFC) / OMO (mineral oil) mixture with different concentrations indicating that oil cannot be dissolved completely, but refrigerant R-161 (HFC) was totally miscible with the same oil, as seen in Figure 27.

The figure also shows the relationship between miscibility and solubility of the same mixture, where solubility is another indicator of the mixtures' compatibility (Zhai et al., 2019).

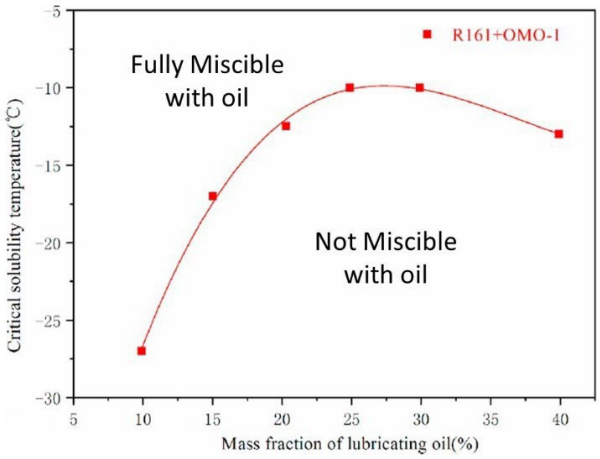


**Figure 27: Miscibility and Solubility of HFC R161 with mineral oil.**

#### 2.4.4.7 Thermophysical properties

The existence of the oil dissolved in the refrigerant has some effects on the energy efficiency of the system. The changes in the working fluid from a pure refrigerant with well-known properties to a poorly understood mixture, with properties that depend on the oil type and concentration, can affect the heat transfer processes in the evaporator and condenser. This effect can improve or impair heat transfer depending on oil concentration. The boiling point of the mixture is elevated above that of the pure refrigerant, according to Raoult's Law, and the heat-carrying capacity of the mixture is reduced during evaporation because the oil holds a proportion of the refrigerant in the liquid phase, thereby reducing the latent heat pick-up. As will be shown later, this effect implies a reduction in the COP. Heat pumps using reciprocating compressors usually have very low oil circulation (typically less than 5%), so the effects on COP are not severe (Huges et al., 1980). However, if a higher oil circulation ratio, possibly more than 10%, the effect on COP can become quite significant with a 30% reduction, and some thoughts need to be given on reducing the problem. Figure 28 illustrates the deviation between ORM and pure refrigerant in a heat pump system.

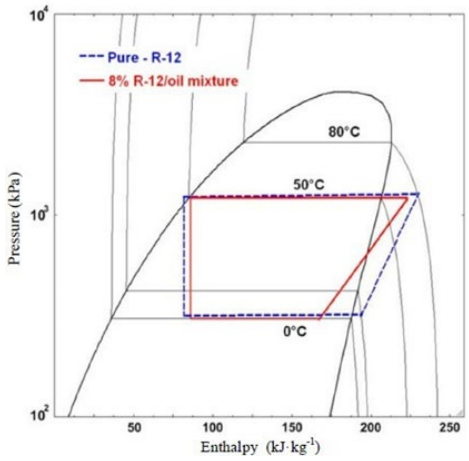


**Figure 28: Pressure-enthalpy chart deviation of pure and ORM.**

We can see that an oil concentration of 8% in the refrigerant R-12 could reduce the COP by as much as 30% due to the change in vapor mass velocity and its effect on the flow in heat exchangers, boiling point of ORM, and saturation pressures and temperatures.

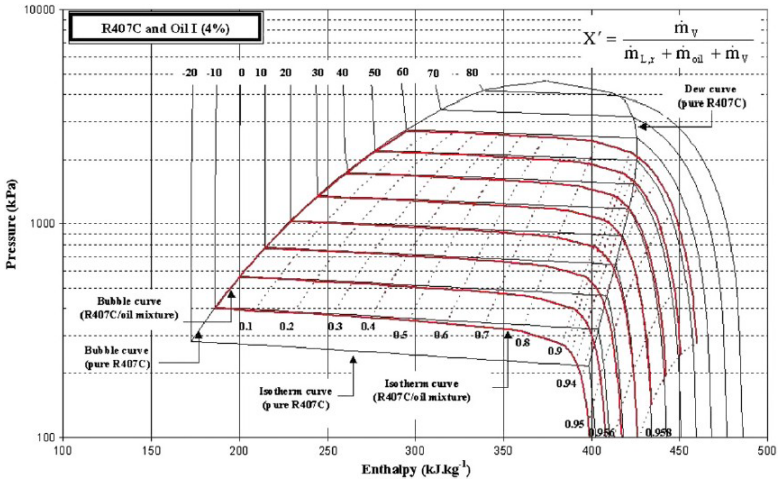


**Figure 29: Log(P)-h diagram of R-407C and 4% of POE oil.**

Figure 29 shows the log(P)-h diagram for R-407C with 4% of POE oil in a refrigeration cycle, and Figure 30 shows the same diagram for R-290 and 5% of POE 68. It proves that the vapor line in the vapor-liquid mixture zone is not as obvious as in pure refrigerant, as the oil remains in the liquid state. Two regions during evaporation appear to take place. ORM behaves as the pure refrigerant in the beginning and part of the evaporator (isothermal lines) and sensible heat region closer to the vapor line of pure refrigerant where the amount of the oil within the refrigerant increases.

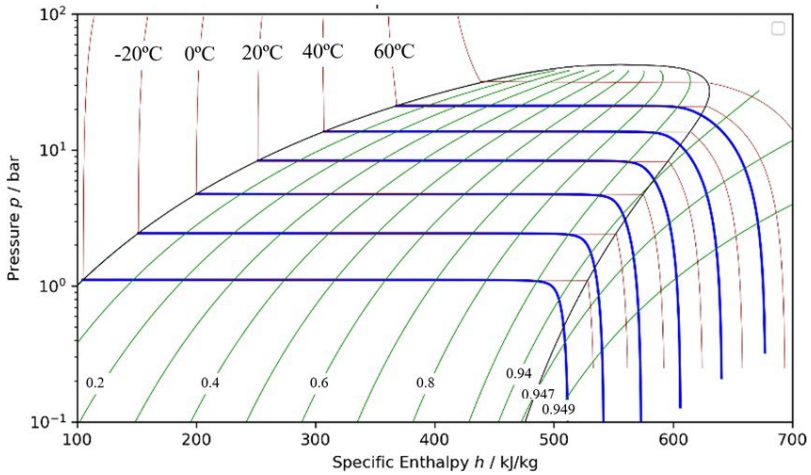


**Figure 30: Log(P)-h diagram of R-290 and 5% of POE 68.**

### 2.4.4.8 Suitability of oils and refrigerants

The suitability of oils and refrigerants is a grey area that we still have much to learn about. Table (2) summarizes the possibilities of using lubricant/oil with refrigerants in general. The (√√) sign means that there are supported facts to possibly use the refrigerant category with the mentioned oil. The (NR) sign means “Not Recommended” which states that no facts to account for the

suitability of the oils and refrigerants. The (Res) indicates that there is still ongoing research on compatibility in ORM. R-717 (Ammonia), R-718 (Water), and R-744 (Carbon Dioxide) are not included here in this report.

**Table 1: Summary of oil/lubricant refrigerant compatibilities issues.**

| Refrigerant/Oil | MO | AB | PAO | PAG | PVE | POE |
|---|---|---|---|---|---|---|
| HCFC | √√ | √√ | √√ | NR | NR | Res. |
| HFC | NR | √√ | NR | √√ | Res. | √√ |
| HFO | NR | NR | NR | √√ | Res. | Res. |
| HC | √√ | Res. | Res. | Res. | NR | Res. |

#### 2.4.4.9 Conclusions

In refrigeration or heat pump systems, many variables and factors must be considered before choosing the proper refrigerant. Data from compressor manufacturers are always taken as given, and we never question or even ask if the lubricant they supply is appropriate because we lack knowledge or expertise on these matters. Several of these factors can be related to compressor performance or refrigerants. Several studies focus on RLM issues and how to calculate the necessary dynamic viscosity of the oil in the compressor but neglect the importance of the oil concentration within the ORM. When oil is present in the refrigerant, refrigeration, and heat pump systems can suffer performance losses of 25% in COP values.

There has been extensive research on the compatibility issues of RLM and concrete methods of choosing the right lubricant for the compressor. For several lubricants, the effect of the refrigerant on the dynamic viscosity has been studied and measured. Not all low GWP refrigerants were researched. Only R-1234yf and R-1234ze(E) were investigated thoroughly to replace R-134a. Other potential synthetic refrigerants such as R-1336mzz (Z), R-1233zd (E), and natural ones such as R-601 with high critical temperatures are in need to be evaluated. On the side of ORM, scarce research has been done to study the oil concentration´s effect on the performance of the system and its energy efficiency with low GWP refrigerants.

### 2.4.5 High temperature heat pumps

The definition for a high-temperature heat pump is when the temperature of the sink reservoir can reach above 100°C, and the source temperature for the heat pump should be above 40°C. Synthetic Refrigerants with good thermo-physical properties to cover these ranges are scarce in the market, and if they are found, they might have some environmental issues such as the formation of TFA upon decomposition. Natural refrigerants such as R-600 or R-601 are more appealing but dangerous with their flammability issues. The transition to the new refrigerant must be smooth and without any drawbacks. We should not fall into the same problems that we have faced during the move from CFC to HCFC and HFC refrigerants, where the market was stormed with the news of banning the use of CFC. The industry at that time was not ready for that transition. This move led to many compressor failures due to many factors, such as unsuitable lubricants, undersized and oversized heat exchangers, and problems such as higher power consumption and

lower values of coefficient of performance (COP). The new move against PFAS that cover several F-gases in the EU countries, including certain HFCs and HFOs and the hidden danger of TFA, which is an atmospheric degradation product of R-1234yf and R-134a should help us out in stirring our research in developing better and safe machines using better synthetic, safe HC, and natural refrigerants in the coming years.

Various criteria should be considered to identify the right refrigerant with the best thermophysical and thermodynamic properties, which maximizes the system's performance and minimizes the environmental impact. Figure 31 shows the families of synthetic refrigerants obtained from natural ones and how the chemical processes would be done to obtain the required synthetic refrigerant.

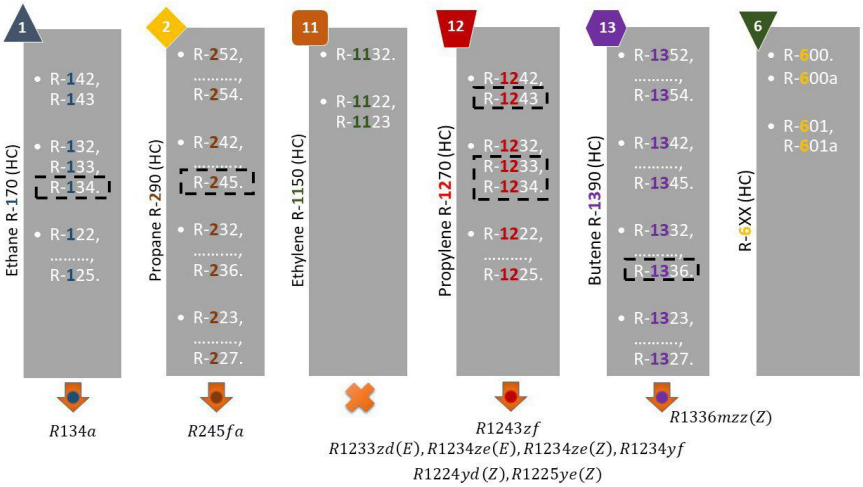


**Figure 31: Synthetic refrigerants' families.**

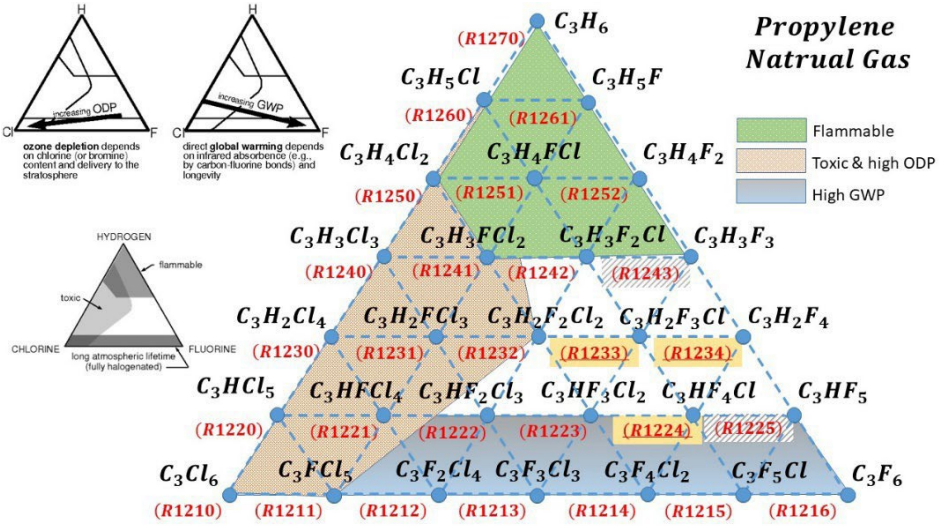


**Figure 32: Synthetic refrigerants from natural ones.**

Figure 32 represents the triangle of elements, Hydrogen on the top, Chlorine on the bottom left, and Fluorine on the bottom right, where we can locate flammable, toxic, and long atmospheric lifetime (fully halogenated) areas. We can also find areas where refrigerants have high GWP

values and high ozone depletion potential (ODP) rates. Figure 31 indicates how we can make R-1234, not its isomers, from Propylene gas R-1270. Many advertised refrigerants such as R-1243zf, R-1233zd (E), R- 1234ze(E), R-1234ze(Z), R-1234yf, R-1224yd(Z), and R-1225e(Z) can be obtained from Propylene.Most of these gases are in the safe area of low flammability, no toxicity, and low GWP values. It is worth mentioning here that the isomers of R-1336, which are R-1336mzz(Z) and R-1336mzz(E), are produced from Butene gas R-1390.

Royal Institute of Technology (KTH) / Energy Technology lab (EGI) has developed a high-temperature heat pump to test several available refrigerants in the market. Figure 33 shows the schematic of the test rig already built in the EGI lab and an actual setup at KTH lab. This project will help to support the Swedish industry in its endeavor to save energy and reduce GHGs emissions. It will also strengthen KTH, a well-known research place, and maintain an advanced position among prestigious international universities and institutes.

The Research Institute of Sweden (RISE) has been granted a project from the Swedish Energy Agency (SWEA) to work on heat pumps for drying processes. The project aims to build international knowledge on resource-efficient drying with heat-pumping technology. The proposed project will be used as a Swedish national project to contribute to the overall aim of the new IEA HPT Annex 59 in the form of a joint project with RISE, CIT, and KTH as the executive team. The project will collect Swedish case studies focused on industrial drying, mainly in forests, pulp/paper, and agriculture/food. Both state-of-the-art and innovative solutions will be investigated and described, including needs surveys, analyses, and in-depth case studies will be analyzed from a technical, practical, and financial perspective to achieve a shift towards electrified resource-efficient drying. The successful implementation of these drying processes will address complex multidimensional challenges. This proposed project will explore opportunities to significantly increase the efficiency, flexibility, and cost-effectiveness of heat pump drying applications. The IEA Heat Pumping Technologies (HPT) Technology Collaboration Platform (TCP) has initiated a new Annex 59 focusing on structure and describing the numerous possibilities and advantages of heat pump integration in dryers. The Annex is led by Austria and is believed to attract many countries. Sweden has long experience and extensive expertise in heat pump technology. It has the potential to contribute to Annex 59 fruitfully and to learn from the other participating countries and their experience of drying with heat pumps.

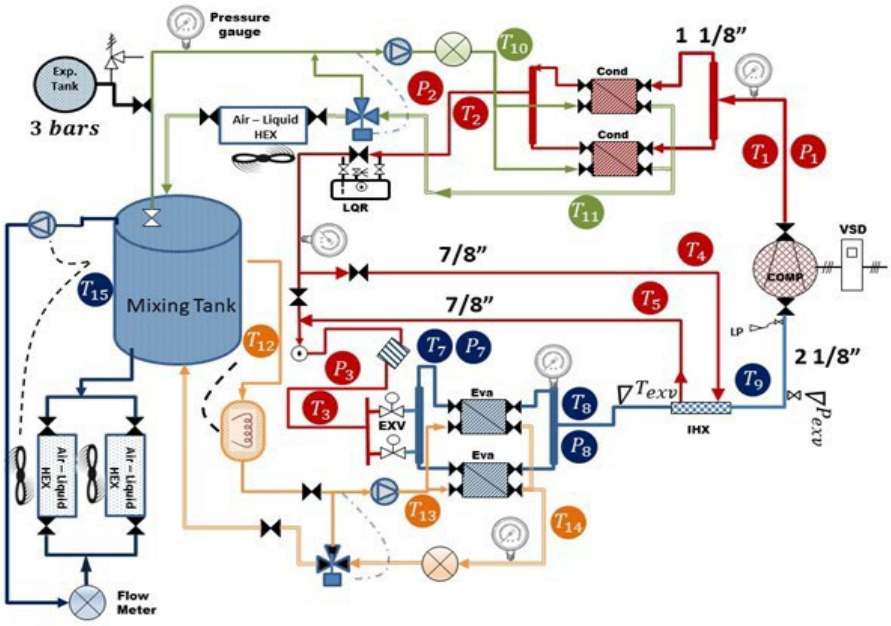


**Figure 33: HTHP test rig schematic layout.**

## 2.5 References

Afsharia, F., O. Comakli, A. Lesani, and S. Karagoz. 2017. "Characterization of lubricating oil effects on the performance of reciprocating compressors in air–water heat pumps." *International Journal of Refrigeration* 505-516.

Albà, Carlos G., Fèlix Llovell, and Lourdes F. Vega. 2021. "Searching for suitable lubricants for low global warming potential refrigerant R513A using molecular-based models: Solubility and performance in refrigeration cycles." *International Journal of Refrigeration* 252–263.

Almebäck, J and Magnius, R., 2022, Heat export from Supermarkets: Refrigeration Systems Field Measurements and a Techno-economic analysis, M. Sc. Thesis, KTH Royal Institute of Technology, Department of Energy Technology. Available at http://www.diva-portal.se/smash/get/diva2:1682964/FULLTEXT01.pdf.

Andersson, K., 2022, PROPAC – Air conditioner with less than 150g propane, Report for the Swedish Energy Agency program Termo. 48254-1-miljovanlig-saker-luftkonditionering--propac-pdf.pdf (termoinnovation.se)

Bock, Wolfgang. 2014. "Refrigeration Oils." In *Encyclopedia of Lubricants and Lubrication*, by Theo Mang, 54-77. SpringerLink.

Boyde, S. 2000. "Hydrolytic stability of synthetic ester lubricants." *Journal of Synthetic Lubrication* 297

- 312.

Chen, Xinwen, et al. 2019. "Modelling of Refrigerant Distribution in an Oil-Free Refrigeration System using R-134a." *Energies.*

Chu, Wenxiao. 2021. "A review on experimental investigations of refrigerant/oil mixture flow boiling in horizontal channels." *Applied Thermal Engineering* Vol. 196 (117-270).

*DLE - Delta Lift Energy*, viewed 28 November 2022, https://www.nordicclimategroup.se/labkyl/dle/

*Enrads modulserie,* viewed 28 November 2022, https://enrad.se/produkter/enrad-modulserie/

Fang, Y., W. Guan, K. Bao, X. Han, and G. Chen. 2018. "Isothermal vapor–liquid equilibria of the absorption working pairs (R-1234yf + NMP, R-1234yf + DME- TrEG) at temperatures from

293.15K to 353.15K." *Journal of Chemical & Engineering Data* 1212-1219.

Forsgren, E., 2020, Evaluation of an economizer solution for a heat pump, Master's thesis, School of Industrial Engineering and Management, Royal Institute of Technology KTH.

FUCHS, Industrieschmierstoffe. 2014. "Kältemaschinenöle."

Granryd, et al. 2022, Ecopac – isobutane heat pump acting as economizer, 15th Gustav Lorentzen Conference on natural refrigerants. Trondheim, Norway

Heide, R. et al.,. 2001. "Mischbarkeit von Schmierölen mit Kohlendioxid." *KI Luft- und Kältetechnik*

466-470.

Herbe, L., and P. Lundqvist. 1997. "CFC and HCFC refrigerants retrofit —experiences and results."

*International Journal of refrigeration* 49–54.

Huges, D. W. 1982. "Determination of the Thermodynamic Properties of Refrigerant-Oil

Mixtures."

*International Compressor Engineering Conference.* Purdue e-Pubs.

Huges D. W., 1980. "Lubricant Related Problems with Heat-Pumps." *International Compressor Engineering Conference.* Purdue e-Pubs.

Jacobson, B. 1994. "Lubrication of screw compressor bearings in presence of Refrigerants."

*International Compressor Engineering Conference.* Purdue. vol. 1, pages 115-120.

Jaeger, H. P. 1972. *Empirische methoden zur Vorausberechnung thermodynamischer Eigenschaftern yon Ol-Kiiltemittel-Gemischen.* Dissertation, T. U. Braunschweig.

Kronström, C., 2021. Performance comparison between reciprocating and scroll compressor heat pump with R600a refrigerant. Master's thesis. School of Industrial Engineering and Management, Royal Institute of Technology, Stockholm.

Lee, Byung-Moo Lee, et al. 2016. "Miscibility of POE and PVE oils with low-GWP refrigerant R-1234ze(E)." *Science and Technology for the Built Environment* 1263-1269.

Liu, Y. L. 2013. "Efficiency model of pumping low viscosity fluids." *6th International Conference on Pumps and Fans with Compressors and Wind Turbines.* IOP Publishing. Vol 52. doi:10.1088/1757-899X/52/7/072002.

Mang, T. 2014. "*Encyclopedia of Lubricants and Lubrication."* Springer-Verlag Berlin Heidelberg. DOI 10.1007/978-3-642-22647-2.

Matsumoto, Tomoya. 2017. "Evaluations of PVE Lubricants for Refrigeration and Air Conditioning system with the Low GWP Refrigerants." *10th International Conference on Compressors and their Systems.*

Megawattsolutions, 2022, *https://megawattsolutions.se as accessed Nov. 2022.*

Midea launches R-290 split ACs on the European market, viewed 29 November 2022, https://iifiir.org/en/news/midea-launches-R-290-split-acs-on-the-european-market

Midea Klimaanlage All Easy Blue 12, viewed 29 November 2022, https://www.klimaworld.com/midea- klimaanlage-all-easy-blue-12-inverter-mit-3-52-kw.html

Morais, et al. 2020. "Viscosity and Density of a PolyolEster Lubricating Oil Saturated with Compressed Hydrofluoroolefin Refrigerants." *Journal of Chemical & Engineering Data* 4335-4346.

Murray, S. F.; Johnson, R. L.; Swikert, M. A. 1956. "Difluorodichloromethane as a Boundary Lubricant for Steel and Other Metals." *Mechanical Engineers,* Vol. 78, pages 233-236.

NIH, National Center for Biotechnology. 2022. *Pub Chem.* Accessed 2022. Pubchem.ncbi.nlm.nih.gov.

Ossorio, R. 2022. "Impact of Lubricant in the Evaporator as a function of Oil Circulation Rate in Variable Speed Heat Pumps working with R-290." *26th International Compressor Engineering Conference at Purdue.*

Rita, A. 2020. "Viscosity and Density of a Polyol Ester Lubricating Oil Saturated with Compressed Hydrofluoroolefin Refrigerants." *J. Chem. Eng. Data* Vol. 65 (4335−4346).

Rudnick, Leslie R. 2013. *SYNTHETICS, MINERAL OILS, and BIO-BASED LUBRICANTS, Chemistry and Technology, Second Edition.* Taylor & Francis Group, LLC, ISBN 978-1-4398-5538-6.

Schroeder, M. 1986. *Beitrag zur Bestimmung thermophysikalischer Eigenschaften von Mischungen synthetischer Kaltemaschinenrle mit Ein-und Zweistoffkaltemitteln.* Dissertation, Universitat Hannover.

*Svensk tillverkare: Värmepumpar för enskilda lägenheter är nästa grej*, viewed 28 November 2022, https://www.vvsforum.se/2022/11/svensk-tillverkare-varmepumpar-for-enskilda-lagenheter- ar-nasta-grej/

Takigawa, Katsuya. 2002. "Solubility and viscosity of refrigerant/lubricant mixtures: hydrofluorocarbon/alkylbenzene systems." *International Journal of Refrigeration* 25 (8): 1014-1024.

*Terrawatt Villa Komplett,* viewed 28 November 2022, https://www.terrawatt.nu/files/pdf/terrawatt- villa-komplett-5-10kw-2015-01-29.pdf

*Thermia lanserar Calibra Eco,* viewed 28 November 2022, https://www.thermia.se/nyheter/pressmeddelande-thermia-lanserar-calibra-eco-bergvaermepump-med-nytt-miljoevaenligare-koeldmedium/

Thermia iTec Eco product broschure, viewed 28 November 2022, https://tcmadmin.thermia.se/docroot/dokumentbank/iTec%20Eco%20produktdatablad_2022 00611.pdf

Tomczyk, John. 2017. "Inside Refrigerant and Oil Relationships." *The News*, October 2. 2017. "Inside Refrigerant and Oil Relationships." *The News*, October 2.

Tuomas, R., and U. Jonsson. 1999. "Influence of refrigerant on viscosity and pressure-viscosity coefficient of refrigeration compressor lubricants." *Proceedings of the 25th Leeds-Lyon Symposium.* Elsevier Science B.V.

Tuomas, R. 2006. *Properties of Oil and Refrigerant Mixtures.* Dissertation, Luleå, Sweden: Luleå University of Technology.

Urrego, Hessel, et al. 2012. *PVXT data, on R-410A and 22 ISO grade POE.* New Jersey: Chemtura corporation.

Wahlström, A., and L. Vamling. 1999. "Solubility of HFC32, HFC125, HFC134a, HFC143a, and HFC152a in a pentaerythritol tetrapentanoate ester." *Journal of Chemical & Engineering Data* 823–828.

Wahlström, A., and L. Vamling. 2000. Solubility of HFCs in pentaerythritol tetraalkyl esters. *Journal of Chemical & Engineering Data* 97–103.

Yokozeki, A Michi. 1994. "Solubility and viscosity of refrigerant oil mixtures." *International Compressor Engineering Conference.*

Yokozeki, A. 2001. Solubility of Refrigerants in Various Lubricants. *International Journal of Thermophysics* 1057 - 1071.

Youbi-Idrissi, M. 2008. "The effect of oil in refrigeration: Current research issues and critical review of thermodynamic aspects." International Journal of Refrigeration, Vol. 3, pp. 1 6 5 – 1 7 9.

Zhai, Rui, et al. 2019. "Research on miscibility performances of refrigerants with mineral." *Applied Thermal Engineering* 1359-4311.

Ölén et al., 2022. EcoPack – High temperature low charge Isobutane heat pump, 15th Gustav Lorentzen Conference on natural refrigerants. Trondheim, Norway.

# 3 Country Report: Austria

**Prepared by:**

AIT AUSTRIAN INSTITUTE OF TECHNOLOGY T. Natiesta, C. Köfinger

AUSTRIAN ENERGY AGENCY F. Zach

TU Graz Graz University of Technology M. Verdnik, R. Rieberer

Contact: christian.koefinger@ait.ac.at

## 3.1 Executive Summary

National and international regulations aim to reduce the greenhouse gas emissions caused by the release of refrigerants into the atmosphere by defining restrictions for refrigerants with high GWP values in specific applications and limiting the total $CO_2$ equivalent of refrigerants on the market through a phase-down concept. However, currently, most used refrigerants have GWPs of a magnitude of 1000 or even more. While in other sectors like refrigerators or freezers, natural refrigerants such as R-290 and R-600a can easily be used for heat pumps. However, the situation is different due to higher capacities and refrigerant charges. In IEA HPT Annex 54, the potential replacement of conventional (high GWP) refrigerants by so-called Low GWP refrigerants (e.g. R-290) and its implications are investigated.

Task 3 work is based on the investigations regarding the technical implications of changing a heat pump system from an R-410A baseline system to a charge-optimized R-290 system using Modelica simulations in Task 2. This third Task focuses on the impact of these system adaptation on the Life Cycle Climate Performance (LCCP) of a heat pump system.

In order to achieve comparability, unified calculations were performed to determine the LCCP of both the R-410A baseline system and the charge-optimized R-290 system. The LCCP was calculated using the software *Pack Calculation Pro*. As this calculation tool excludes indirect emissions from equipment manufacturing, equipment recycling, and refrigerant manufacturing, this missing emission share was calculated with the Excel-based tool *IIR-LCCP-Calculation-Tool* (IIR, 2018).

The investigations show that the charge-optimized R-290 system does not only perform better regarding direct carbon dioxide equivalent ($CO_{2e}$) emissions (refrigerant leakages) due to its very Low GWP but also due to a better energy efficiency performance due to better thermodynamic properties:

Based on the leakage rates proposed by IIR (2016), the direct $CO_{2e}$ emissions due to refrigerant leakage and end-of-life refrigerant losses of the R-410A baseline system would account for approx. 38.3 tons $CO_{2e}$, those of the charge optimized R-290 system to only 8 kg.

The (electrical) energy consumption of the R-410A baseline system during its lifetime leads to indirect CO2e emissions of approx. 20.3 tons CO2e. Due to better thermodynamic properties, the respective value of the charge-optimized R-290 system is significantly lower (16.6 tons CO2e).

The direct $CO_{2e}$ emissions from refrigerant leakage and the indirect $CO_{2e}$ emissions due to the (electrical) energy consumption sum up to a Total Equivalent Warming Impact (TEWI) of approx. 58.5 tons $CO_{2e}$ (R-410A baseline system) and 16.6 tons $CO_{2e}$ (charge optimized R-290 system).

Adding indirect $CO_{2e}$ emissions from manufacturing and recycling the LCCP of the R-410A baseline system and the charge-optimized R-290 system is calculated to approx. 59.6 tons and 17.4 tons $CO_{2e}$, respectively.

To better understand the significance of these values, the TEWI values were compared with the lifetime $CO_{2e}$ emissions of a comparable natural gas-fired heating system: the latter would account to $CO_{2e}$ emissions of approx. 128 tons $CO_{2e}$. In relation to this value, the TEWI values of the R-410A baseline system and the charge-optimized R-290 system are 46% and 13% of this value, respectively. The deviation in performance between the R-410A baseline system and the charge-optimized R-290 system supports the call for replacing conventional refrigerants with Low GWP

refrigerants. Reducing the refrigerant charge and improving refrigerant leakage rates are further valid approaches for improving the LCCP of heat pump systems.

Furthermore, it should be mentioned that for Austria's domestic heat pump market, the actual refrigerant leakage rate and end-of-life refrigerant leakage might be lower than assumed in this investigation. As in Austria, the exact situation regarding refrigerant leakages is not known, the assumptions in this investigation were made as recommended by the IIR. In the future, comprehensive investigations regarding the actual refrigerant leakage situation in Austria's domestic heat pump market are highly recommended.

## 3.2 Introduction

Task 3 focuses on the impact of changing a heat pump system from a R-410A baseline system to a charge-optimized R-290 system on global warming. To determine the Life Cycle Climate Performance (LCCP) of both systems, unified calculations are performed with specialized tools.

The LCCP is expressed as the amount of carbon dioxide equivalent ($CO_{2e}$) emissions emitted during a technical system's whole life cycle. The latter is a metric measure used to compare the emissions from various greenhouse gases based on their GWP by converting amounts of other gases to the equivalent amount of carbon dioxide with the same global warming potential (Eurostat, 2017).

Within this task, a concurrent bachelor thesis (Gattermeyer, 2022) was written by a Renewable Energy Technologies Program student at the University of Applied Sciences FH Technikum Wien. This thesis is the foundation of this chapter, and the information was taken from IIR (2016).

### 3.2.1 Definition of "LCCP"

The LCCP analysis is a method to evaluate the amount of greenhouse gas generated and released over the lifetime of a system. It takes all emissions into account from the manufacturing, the operation, and the final disposal. The occurring emissions are split into direct and indirect emissions. In LCCP analyses, those emissions are both treated separately and linked together in the result. Besides the investigated system configuration, the outcome of an LCCP analysis depends on several parameters, e.g. climate data, electricity mix, etc. The also often used calculation method "Total Equivalent Warming Impact" ("TEWI") also takes into consideration the above mentioned direct and indirect CO2e emissions but in contrast to the LCCP does not include indirect $CO_{2e}$ emissions from manufacturing and recycling.

#### 3.2.1.1 Calculation of direct emissions

Direct emissions comprise the effects of refrigerant released into the atmosphere over the lifetime of the unit and at its disposal. This includes:

- Refrigerant loss from annual leakage (during the lifetime of the unit)
- Losses at the end-of-life disposal of the unit
- Atmospheric reaction products from the decomposition of the refrigerant in the atmosphere

Each group is calculated using the rate of refrigerant leakage multiplied by the refrigerant charge and the GWP of the refrigerant.

#### 3.2.1.2 Calculation of indirect emissions

Indirect emissions result from the use of the unit over its lifetime and include $CO_{2e}$ emissions from:

- Electricity generation
- Manufacturing of materials
- Manufacturing of refrigerants
- Disposal of the unit (except for end-of-life refrigerant losses)

Each $CO_{2e}$ emission share is calculated separately and then summed up. The main contributor to the indirect emissions is the $CO_{2e}$ emissions from the (electrical) energy consumption of the unit.

### 3.2.2 Calculation Method

The calculation result is the amount of kg $CO_{2e}$ or of kg $CO_{2e}$/kWh for the "specific" LCCP. The assumption-based input values shall be the same for every simulated system to get comparable results. As stated previously, there are two general emission categories: direct (Formula 1) and indirect emissions (Formula 2). Those two are treated individually and summed together (Formula 3).

$$Direct\ Emissions = C * (L * ALR + EOL) * (GWP + Adp.GWP) \quad (1)$$

$$Indirect\ Emissions = L * AEC * EM + \sum(m * MM) + \sum(mr * RM) + C + (1 + L * ALR) * RFM + C * (1 - EOL) * RFD \quad (2)$$

$$LCCP = Direct\ Emissions + Indirect\ Emissions \quad (3)$$

The meaning of the abbreviations used in the formulas above is as follows (IIR, 2016):

- *"C = Refrigerant Charge (kg)*
- *L=Average Lifetime of Equipment (yr)*
- *ALR = Annual Leakage Rate (% of Refrigerant Charge)*
- *EOL = End of Life Refrigerant Leakage(% of Refrigerant Charge)*
- *GWP = Global Warming Potential (kg $CO_{2e}$/kg)*
- *Adp. GWP = GWP of Atmospheric Degradation Product of the Refrigerant (kg $CO_{2e}$/kg)*
- *AEC = Annual Energy Consumption (kWh)*
- *EM = $CO_2$ Produced/kWh (kg $CO_{2e}$/kWh)*
- *m = Mass of Unit (kg)*
- *MM = $CO_{2e}$ Produced/Material (kg $CO_{2e}$/kg)*
- *mr = Mass of Recycled Material (kg)*
- *RM = $CO_{2e}$ Produced/Recycled Material (kg $CO_{2e}$/kg)*
- *RFM = Refrigerant Manufacturing Emissions (kg $CO_{2e}$/kg)*
- *RFD = Refrigerant Disposal Emissions (kg $CO_{2e}$/kg)"*

### 3.2.3 Tools to perform LCCP-Analyses

To perform LCCP analysises, there are different tools and methods available. The following sections briefly discuss and explain the tools used in Task 3.

#### 3.2.3.1 Pack Calculation Pro

*Pack Calculation Pro* (IPU, 2022) is an application for comparing the yearly energy consumption of refrigeration systems and heat pumps. The application compares different systems taking into account their geographical location. *Pack Calculation Pro* provides a detailed simulation of the yearly energy consumption and a TEWI calculation. Pack Calculation Pro can simulate a real system in several different locations at different loads. (IPU, 2021)

As the calculation of the indirect $CO_{2e}$ emissions caused by manufacturing and recycling are not included in this tool, the calculation of these shares of $CO_{2e}$ emissions is performed separately with the tool described in 1.3.2.

#### 3.2.3.2 IIR-LCCP-Calculation-Tool

With the *LCCP-Calculation-Tool* (IIR, 2018) provided by the International Institute of Refrigeration (IIR), running a LCCP-analysis in an MS Excel-environment is possible. The needed inputs are described on the tools main page and have to be entered there. The following inputs are necessary:

- Refrigerant (LCCP calculation available for HFC-32, HFO-1234yf, HFC-134a, R-290, HFC-404A, HFC-410A, L-41b and DR-5)
- Refrigerant charge in kg
- Unit weight in kg
- Annual refrigerant leakage rate in %/year
- End-of-life Leakage in %
- Lifetime in years
- Type of manufacturing emissions (virgin manufacturing or mixed manufacturing with shares of virgin materials and of recycled materials)
- AHRI Standard 210/240 test bench performance data at operating points A, B, H1, H2, H3
- Carbon Intensity per Electricity Generation Region

The results are then presented in tables for the climates in Miami (Florida), Phoenix (Arizona), Atlanta (Georgia), Chicago (Illinois), and Seattle (Washington State). The climate data required for these calculations is included in the tool. The separate $CO_{2e}$ emission shares and the total $CO_{2e}$ emissions (LCCP) are listed individually. For a visual illustration, graphs show the total $CO_{2e}$ emissions and the percentage of the total $CO_{2e}$ emissions (IIR, 2018).

This report uses the IIR-LCCP-Calculation-Tool to calculate some of the indirect $CO_{2e}$ emissions (e.g. those emitted by equipment manufacturing). Since the *IIR-LCCP-Calculation-Tool* includes climate data for regions in the USA only, the calculation of the main part of the $CO_{2e}$ emissions was carried out using *Pack Calculation Pro,* which does include climate data for Austria (see 1.3.1).

### 3.2.4 Limitations of LCCP analyses

The calculations are impacted by several assumptions regarding the input parameters. The empirically determined values that are used to perform LCCP analyses are all subject to a certain amount of uncertainty. Therefore, the calculated results are not meant to be taken as an exact prediction of lifetime $CO_{2e}$ emissions but more as a comparable “value” between different settings and systems. Due to the uncertainty of the input values, small differences between systems may not have significance. Comparing different refrigerants regarding their LCCP only makes sense under certain circumstances. When comparing different systems, similar capacities are necessary for the results to be comparable.

## 3.3 LCCP Calculation – Comparison R-290 vs. R-410A

The approach of the Austrian IEA HPT Annex 54 Team focused on the present national situation regarding the refrigerants used in heat pumps installed in Austria: as in Task 1 and 2, R-290 was identified as the sole refrigerant that corresponds to a low-GWP refrigerant in the narrower sense and has a broad potential area of application due to its thermodynamic properties, among other

things, the LCCP analyses in Task 3 were only carried out for this refrigerant and for the synthetic refrigerant R-410A, which is the most frequently used refrigerant in Austria's domestic heat pumps (KPC, 2021).

The heat pump system optimized to R-290 (see Task 2) was compared with an R-410A baseline system using the LCCP analysis software *Pack Calculation Pro* (see 1.3.1), and for some part, the Excel-based tool *IIR-LCCP-Calculation-Tool* (see 1.3.2).

### 3.3.1 TEWI calculation

As explained in 1.3, with the calculation tool *Pack Calculation Pro* the TEWI of the investigated system(s) can be calculated, but the tool does not provide the calculation of $CO_{2e}$ emissions caused during equipment manufacturing and recycling as well as refrigerant manufacturing. This section describes the TEWI calculation with *Pack Calculation Pro* only. The calculation of the $CO_{2e}$ emissions caused by equipment manufacturing and recycling as well as refrigerant manufacturing, is described in 0.

#### 3.3.1.1 $CO_{2e}$ emission intensity of electricity provision in Austria

The main share of indirect $CO_{2e}$ emissions from heat pump systems is currently accounted for by electricity consumption during the system's lifetime. Since all electricity in Austria is to come from 100% renewable sources by 2030 (BMK, 2021), the $CO_{2e}$ emission intensity of electricity provision in Austria decreases each year. Due to a lack of information on the exact annual development of the electricity $CO_{2e}$ emission intensity of electricity provision, a linear reduction to the target value of 0 kg $CO_{2e}$/kWh in 2030 was assumed.

For the calculation, a product lifetime of 15 years, from 2022 to 2036, was assumed. In 2022 the $CO_{2e}$ emission intensity of electricity provision in Austria was approximately 0.2 kg $CO_{2e}$/kWh (Umweltbundesamt, 2022). This results in an annual reduction of this value by 0.025 kg $CO_{2e}$/kWh until 2030, when 0 kg $CO_{2e}$/kWh is assumed. This linear reduction is shown in Figure 1. The $CO_{2e}$ emission intensity values of the individual years and their average value are listed in Table 1. The average value that accounts for 0.06 kg $CO_{2e}$/kWh is used to calculate the indirect $CO_{2e}$ emissions due to the systems' lifetime consumption of (electrical) energy using *Pack Calculation Pro*.

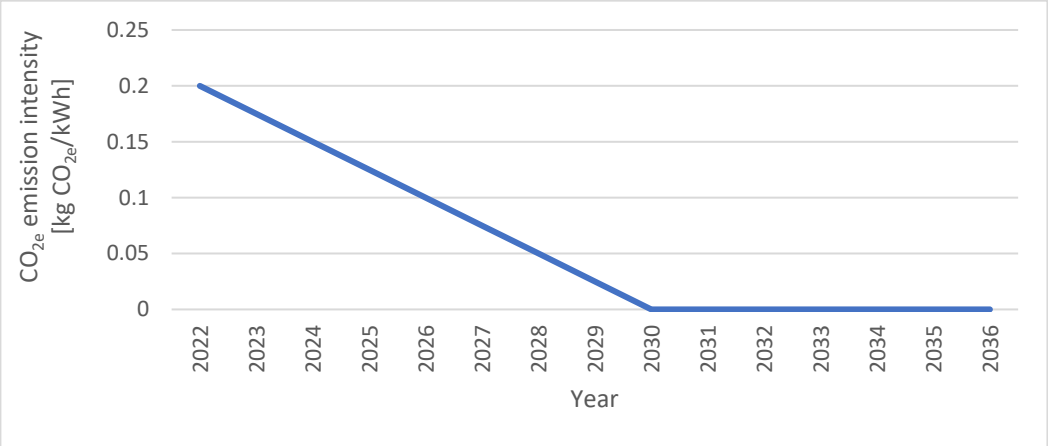


**Figure 1: Assumed development of the $CO_{2e}$ emission intensity of electricity provision in Austria in kg $CO_{2e}$/kWh**

**Table 1: $CO_{2e}$ emission intensity of electricity provision in Austria**

| Year | $CO_{2e}$ emission intensity [kg $CO_{2e}$/kWh] |
|---|---|
| 2022 | 0.2 |
| 2023 | 0.175 |
| 2024 | 0.15 |
| 2025 | 0.125 |
| 2026 | 0.1 |
| 2027 | 0.075 |
| 2028 | 0.05 |
| 2029 | 0.025 |
| 2030 – 2036 | 0 |
| **2022 – 2036 Average** | **0.06** |

#### 3.3.1.2 Calculation with Pack Calculation Pro

The R-410A baseline system and the charge-optimized R-290 system were defined in *Pack Calculation Pro* in relation to the models used for the system simulations in Task 2. In the model library used for the system simulations in Task 2, a specific R-290 compressor model comparable to the compressor model used for the R-410A baseline system was unavailable. Therefore, a compressor model not yet certified for R-290 was used. Pack Calculation Pro only allows the combination of refrigerants with certified compressors for that particular refrigerant; a similar but slightly different compressor (Bitzer 4PESP-12P) to the one used for the system simulations in Task 2 was defined. The compressor defined in *Pack Calculation Pro* for the R-410A baseline system is the same compressor as the one used in the system simulations in Task 2. Due to the simplicity of the modeling approach in *Pack Calculation Pro*, the refrigerant cycle adaptions defined in Task 2 are not represented accordingly: Besides the compressors, the R-410A baseline system and the charge-optimized R-290 system are modeled with the same components. The refrigerant cycle components of the *Pack Calculation Pro* models are default standard components. The tool's standard refrigerant cycle includes an internal heat exchanger, while the investigated refrigerant cycles in Task 2 were modeled without internal heat exchangers. Table 2 lists the main properties of both systems. Nevertheless, the resulting inaccuracy of the calculations was considered insignificant enough.

**Table 2: Main properties of the R-410A baseline system and the charge-optimized R-290 system**

| Configuration | R-410A baseline system | Charge-optimized R-290 system |
|---|---|---|
| Heat pump type | Air source heat pump | Air source heat pump |
| Refrigerant | R-410A | R-290 |
| Compressor | Bitzer GSD60154VA, 50Hz | Bitzer 4PESP-12P, 50Hz |
| Design capacity (A-15/W55) | 30 kW | |
| Supply temperature | 55°C | |
| Total superheat | 5.0 K | |
| Non-useful superheat | 0.0 K | |

***Annual (electrical) energy consumption***

For the R-410A baseline system and the charge-optimized R-290 system, one year of operation was simulated, and the hourly load profile was calculated based on climate data for Vienna/Austria (weather station *Hohe Warte*). The simulations were performed hourly by performing one steady-state simulation for each hour in the year.

The diagram in Figure 2 shows the (electrical) energy consumption per month of the simulated systems. Each bar equals the sum of the compressor energy consumption and the energy consumption of additional equipment (condenser and evaporator fans and pumps used in the system). The detailed results of this calculation are shown in Table 3. The charge-optimized R-290 system achieves a 4% lower (electrical) energy consumption than the R-410A baseline system.

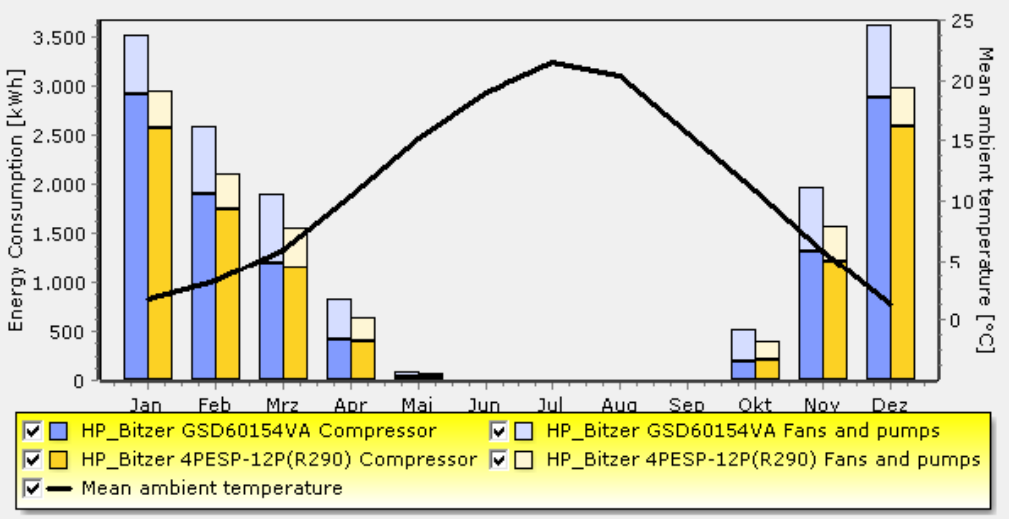


**Figure 2: (Electrical) energy consumption of compressor as well as of fans and pumps - monthly values**

**Table 3: Results regarding the annual energy consumption of both investigated systems**

| | R-410A baseline system | Charge optimized R-290 system |
|---|---|---|
| Refrigerant | R-410A | R-290 |
| Average COP [-] | 2.01 | 2.48 |
| **Energy consumption** | | |
| Pumps and fans [kWh] | 4,173 | 2,401 |
| Compressor [kWh] | 10,851 | 9,875 |
| **Total [kWh]** | **15,024** | **12,276** |
| **Savings** | | |
| Yearly energy savings [kWh] | - | 2,748 |
| Yearly energy savings [%] | - | 18.3% |

***TEWI***

For the calculation of the TEWI in *Pack Calculation Pro*, essential input parameters must be assumed and entered into the program:

In Task 2, the refrigerant charge of the R-410A baseline system and the charge-optimized R-290 system were calculated for the components evaporator, condenser and liquid line. The design capacity of both systems is 30 kW (A-15/W55). As the refrigerant charge in the compressor and the refrigerant mass dissolved in the lubricant were not included in this calculation, a different approach to estimate the total refrigerant charge was applied:

The refrigerant charge of the R-410A baseline system was estimated based on empirical values. For the refrigerant charge value of the charge-optimized R-290 system, the refrigerant charge of the GreenHP prototype (Zottl, 2016) was used. The empirical value regarding the refrigerant charge of the R-410A baseline system was estimated as the mean specific refrigerant charge of 18 air/water heat pumps with the refrigerant R-410A, of which the relevant manufacturers' data were available (from other projects). The estimated average value is 440 g R-410A/kW design capacity resulting in an absolute refrigerant charge for a 30 kW design capacity of 13.2 kg. The refrigerant charge of the GreenHP prototype (30 kW design capacity) is 1.9 kg resp. 63 g R-290/kW design capacity.

The average lifetime of the two systems is assumed to be 15 years, with an annual refrigerant leakage rate of 4% and the end-of-life refrigerant leakage rate of 15% (IIR, 2016). These values are considered to be typical "standard values." As no exact data is available for Austria, these values were adopted, but it can be assumed that the refrigerant leakages, in particular the annual refrigerant leakage rate, would be lower. The above-mentioned assumptions are summarized in Table 4.

**Table 4: Assumed input parameters for the TEWI calculations for the R-410A baseline system and the charge-optimized R-290 system**

| | R-410A baseline system | Charge-optimized R-290 system |
|---|---|---|
| System lifetime [years] | 15 | 15 |
| Estimated specific refrigerant charge [g/kW] | 440 | 63 |
| Design capacity (A-15/W55) [kW] | 30 | 30 |
| Refrigerant charge [kg] | 13.2 | 1.9 |
| End-of-life refrigerant leakage rate [%] | 15.0 | 15.0 |
| Annual refrigerant leakage rate [%/year] | 4.0 | 4.0 |

The $CO_{2e}$ emissions of the R-410A baseline system due to refrigerant leakage accounts for approx. 15.8 tons $CO_{2e}$, which is approx. 27% of the R-410A baseline system's TEWI. The corresponding value of the charge-optimized R-290 system is only about 3 kg $CO_{2e}$, which is a neglectable share of its TEWI.

While the end-of-life refrigerant losses of the R-410A baseline system cause approx. 22.4 tons $CO_{2e}$ emissions (corresponding to approx. 38.3% of the TEWI), the end-of-life refrigerant losses of the charge optimized R-290 system lead to $CO_{2e}$ emissions of only about 5 kg $CO_{2e}$, also a neglectable share of the TEWI. The reason for the low values regarding the charge-optimized R-290 system is clearly the very Low GWP of its refrigerant R-290 (GWP = 3).

The $CO_{2e}$ emissions of the R-410A baseline system due to its (electrical) energy consumption during its lifetime accounts to approx. 20.3 tons $CO_{2e}$, which is approx. 34.7% of the R-410A baseline system's TEWI. The corresponding value of the charge-optimized R-290 system is approx. 16.6 tons $CO_{2e}$, which is almost 100% of its TEWI.

In total, the TEWI of the R-410A baseline system accounts for approx. 58.6 tons $CO_{2e}$, compared to approx. 16.6 tons $CO_{2e}$ of the charge optimized R-290 system. This means a reduction in $CO_{2e}$ emissions of approx. 72%. The values mentioned are summarized in Table 5.

**Table 5: Direct $CO_{2e}$ emissions caused by refrigerant leakage and end-of-life refrigerant losses as well as indirect $CO_{2e}$ emissions from (electrical) energy consumption during the systems' lifespan and TEWI**

| | Refrigerant leakage [kg $CO_{2e}$] | End-of-life refrigerant losses [kg $CO_{2e}$] | Indirect $CO_{2e}$ emissions (energy consumption) [kg $CO_{2e}$] | TEWI [kg $CO_{2e}$] |
|---|---|---|---|---|
| R-410A baseline system | 15,828 (27.0%) | 22,423 (38.3%) | 20,282 (34.7%) | 58,533 |
| Charge-optimized R-290 system | 3 (0.0%) | 5 (0.0%) | 16,572 (100.0%) | 16,581 |

#### 3.3.1.3 $CO_{2e}$ emissions from manufacturing and recycling

As shown in 1.3, the share of indirect $CO_{2e}$ emissions attributable to the manufacturing and recycling of the examined heat pump systems had to be determined separately, as these are not considered in the calculation tool used (*Pack Calculation Pro*). For the calculation of this share, assumptions were made regarding the material composition of the two heat pump systems based on the data in the *IIR-LCP calculation tool. T*he LCCP values were determined using known material-specific $CO_{2e}$ emission intensity values to manufacture and recycle the used materials.

As the $CO_{2e}$ emissions from manufacturing and recycling correspond to a small share of the LCCP, no detailed investigation was performed on the exact mass and material distribution of the units. Although there are differences in the system design defined in Task 2, the same unit mass and material distribution were assumed for the R-410A baseline system and the charge-optimized R-290 system. Therefore, the results regarding the $CO_{2e}$ emissions from manufacturing and recycling are the same for both systems. The results of the two systems thus only differ with regard to the $CO_{2e}$ emissions caused by the manufacturing of their refrigerants.

A mass of 230 kg was assumed for both heat pump systems. The assumed individual shares of the materials and their $CO_{2e}$ emissions in the *IIR-LCP calculation tool* correspond to the information in the IIR's LCCP Guideline (IIR, 2016). In this, the share of steel is 46%, the share of aluminum is 12%, the share of copper is 19%, and the share of plastics is 23%. Manufacturing emission values are calculated using 1.43 kg $CO_{2e}$/kg for steel, 4.5 kg $CO_{2e}$/kg for aluminum, 2.78 kg $CO_{2e}$/kg for copper, and 2.61 kg $CO_{2e}$/kg for plastics. The $CO_{2e}$ emission values of the production of the materials refer to virgin material not mixed with any recycled material. $CO_{2e}$ emission values of 0.07 kg $CO_{2e}$/kg are used for the recycling of metals. Recycling emissions from plastics are 0.01 kg $CO_{2e}$/kg.

For the $CO_{2e}$ emissions from the manufacturing of R-410A, a value of 17.12 kg $CO_{2e}$/kg, and for those from the manufacturing of the R-290, a value of 0.08 kg $CO_{2e}$/kg was assumed. Due to a lack of data regarding indirect $CO_{2e}$ emissions from refrigerant recycling, this share is neglected. The values just mentioned are summarized in Table 6.

**Table 6: Materials, shares regarding material use in heat pump systems, $CO_{2e}$ emission intensity values for manufacturing and recycling of units and their refrigerants**

| Material | Share | $CO_{2e}$ emission value [kg $CO_{2e}$/ kg] |
|---|---|---|
| **Manufacturing** | | |
| Steel | 46% | 1.43 |
| Aluminum | 12% | 4.50 |
| Copper | 19% | 2.78 |
| Plastics | 23% | 2.61 |
| **Refrigerant manufacturing** | | |
| R-410A | N/A | 17.12 |
| R-290 | N/A | 0.08 |
| **Recycling** | | |
| Metals | N/A | 0.07 |
| Plastics | N/A | 0.01 |

Compared to the systems' indirect $CO_{2e}$ emissions caused by the (electrical) energy consumption during the heat pump systems' lifetime, the indirect $CO_{2e}$ emissions from manufacturing and recycling are low: the $CO_{2e}$ emissions of both systems due to equipment manufacturing account for approx. 817 kg $CO_{2e}$, the value regarding equipment recycling accounts for approx. 13 kg $CO_{2e}$.

While manufacturing the refrigerant for the R-410A baseline system causes $CO_{2e}$ emissions of approx. 86 kg $CO_{2e}$, the manufacturing of the refrigerant for the charge optimized R-290 system causes $CO_{2e}$ emissions of only 0.15 kg $CO_{2e}$. This very low value is plausible, as R-290 (propane) is produced as a by-product of natural gas processing and petroleum refining.

In total, the $CO_{2e}$ emissions from equipment manufacturing and recycling as well as refrigerant manufacturing, the R-410A baseline system accounts for approx. 1056 kg $CO_{2e}$, compared to approx. 831 kg $CO_{2e}$ of the charge-optimized R-290 system, which is 21% less than the baseline value. The values just mentioned are summarized in Table 7.

**Table 7: Indirect $CO_{2e}$ emissions from equipment manufacturing, equipment recycling, and refrigerant manufacturing**

| | Equipment manufacturing [kg $CO_{2e}$] | Equipment recycling [kg $CO_{2e}$] | Refrigerant manufacturing [kg $CO_{2e}$] | Indirect $CO_{2e}$ emissions from manufacturing/recycling and ref. manuf. [kg $CO_{2e}$] |
|---|---|---|---|---|
| R-410A baseline system | 817.4 | 12.9 | 226.0 | 1056.4 |
| Charge-optimized R-290 system | 817.4 | 12.9 | 0.15 | 830.5 |

### 3.3.2 LCCP

To calculate the LCCP, including both the TEWI and the indirect $CO_{2e}$ emissions from manufacturing and recycling, the results of both separate calculations are summed up as follows:

The TEWI of the R-410A baseline system of approx. 58.5 tons $CO_{2e}$ (see 2.1.2) and the indirect $CO_{2e}$ emissions regarding manufacturing and recycling of approx. 1.1 tons $CO_{2e}$ (see 0) sum up to an LCCP of approx. 59.6 tons $CO_{2e}$.

The TEWI of the charge optimized R-290 calculated with *Pack Calculation Pro* of approx. 16.6 tons $CO_{2e}$ and the $CO_{2e}$ emissions regarding manufacturing and recycling of approx. 0.8 tons $CO_{2e}$ sum up to an LCCP of approx. 17.4 tons $CO_{2e}$. This value is approx. 42.2 tons $CO_{2e}$ resp. 71% less than the baseline value. The direct and indirect $CO_{2e}$ emissions, the TEWI and the LCCP are summarized in Table 8.

**Table 8: Direct and indirect $CO_{2e}$ emissions, TEWI and LCCP**

| **$CO_{2e}$ emission source (calculation method)** | **Unit** | **R-410A baseline system** | **Charge-optimized R-290 system** |
|---|---|---|---|
| Refrigerant leakage (*Pack Calculation Pro*) | [kg $CO_{2e}$] | 15,828.0 | 3.0 |
| End-of-life refrigerant losses (*Pack Calculation Pro*) | [kg $CO_{2e}$] | 22,423.0 | 5.0 |
| Indirect $CO_{2e}$ emissions from (electrical) energy consumption ( *Pack Calculation Pro*) | [kg $CO_{2e}$] | 20,282.0 | 16,572.0 |
| TEWI (Pack Calculation Pro) | [kg CO2e] | 58,533.0 | 16,580.0 |
| Indirect $CO_{2e}$ emissions from equipment manufacturing (IIR-LCCP-Calculation-Tool) | [kg CO2e] | 817.4 | 817.4 |
| Indirect $CO_{2e}$ emissions from equipment recycling (IIR-LCCP-Calculation-Tool) | [kg CO2e] | 12.9 | 12.9 |
| Indirect $CO_{2e}$ emissions from refrigerant manufacturing (IIR-LCCP-Calculation-Tool) | [kg CO2e] | 226.0 | 0.15 |
| Indirect $CO_{2e}$ emissions regarding manufacturing and recycling (IIR-LCCP-Calculation-Tool) | [kg CO2e] | 1056.3 | 830.45 |
| LCCP | [kg CO2e] | 59,589.3 | 17,410.5 |

## 3.4 Conclusions

Due to the very Low GWP of R-290 (GWP = 3) the direct $CO_{2e}$ emissions (refrigerant leakage and end-of-life refrigerant losses) of the charge-optimized R-290 system are neglectable. In contrast, the direct $CO_{2e}$ emissions of the R-410A baseline system accounts to approx. 38 tons $CO_{2e}$. Furthermore, the charge-optimized R-290 system achieves an approx. 18.3% lower (electrical) energy consumption than the R-410A baseline system, which reduces the indirect $CO_{2e}$ emissions by approx. 3.7 tons $CO_{2e}$.

The $CO_{2e}$ emissions of the R-410A baseline system sum up to an LCCP of approx. 59.6 tons $CO_{2e}$, while those regarding the charge optimized R-290 sum up to an LCCP of approx. 17.4 tons $CO_{2e}$, which is approx. 42.2 tons $CO_{2e}$ resp. 71% less than the baseline value.

These values show that the charge-optimized R-290 system does not only perform better regarding direct $CO_{2e}$ emissions (refrigerant leakages) due to its very Low GWP of 3 but also due to a better energy efficiency performance due to better thermodynamic properties.

To understand better the significance of the calculated LCCP, a comparison with a natural gas-fired heating system may be helpful. The $CO_{2e}$ emissions of a comparable natural gas-fired heating system are roughly estimated as follows: the amount of thermal energy delivered in 15 years by the R-410A baseline system resp. The charge-optimized R-290 system is roughly 453 $MWh_{th}$. An assumed energy efficiency of 95% for a modern natural gas heating system would lead to a natural gas consumption of approx. 477 MWh. Applying the $CO_{2e}$ emission intensity for natural gas of 0.268 kg $CO_{2e}$/kWh (Umweltbundesamt, 2022), the $CO_{2e}$ emissions during a 15 years-lifetime would account for approx. 128 tons. As shown in Table 9, the TEWI of the R-410A baseline system and the charge-optimized R-290 system is 46% and 13%, respectively, of the $CO_{2e}$ emissions emitted by the above-defined natural gas heating system in 15 years.

**Table 9: TEWI values of the R-410A baseline system and the charge optimized R-290 system and $CO_{2e}$ emissions in 15 years of a natural gas heating system.**

| System | TEWI (heat pump systems) resp. $CO_{2e}$ emissions in 15 years (gas system) [tons $CO_{2e}$] | Relative values |
|---|---|---|
| R-410A baseline system | 58.5 | 46% |
| Charge-optimized R-290 system | 16.6 | 13% |
| LCCP reduction by R-410A → R-290 | 41.9 | 33% |
| Natural gas heating system (simplified calculation) | 127.8 | 100% |

In other words, replacing a natural gas heating system with the R-410A baseline system would lead to a reduction in $CO_{2e}$ emissions of 54%. In comparison, the replacement by a charge-optimized R-290 system would achieve a reduction in $CO_{2e}$ emissions of 87%. The deviation in performance between the R-410A baseline system and the charge-optimized R-290 system supports the call for replacing conventional refrigerants with Low GWP refrigerants. Reducing the refrigerant charge and improving refrigerant leakage rates are further valid approaches for improving the LCCP of heat pump systems.

Furthermore, it should be mentioned that for Austria's domestic heat pump market, the actual refrigerant leakage rate and end-of-life refrigerant losses might be lower than assumed in this investigation. As in Austria, the exact situation regarding refrigerant leakages is not known, the assumptions were based on IIR recommendations (IIR, 2016). In the future, comprehensive investigations regarding the actual refrigerant leakage situation in Austria's domestic heat pump market are highly recommended.

## 3.5 References


[1] Beshr, M., Aute, V. C., 2014, LCCP Desktop Application v1.0 Engineering Reference. Oak Ridge National Laboratoryhttps://info.ornl.gov/sites/publications/files/pub49128.pdf (Accessed 28.12.2021)

[2] BMK (2021): Energiewende für Österreich eingeleitet: Bundesregierung präsentiert Erneuerbaren-Ausbau-Gesetz. https://www.bmk.gv.at/service/presse/gewessler/20210311_eag.html#:~:text=%C3%96sterreich%20wird%20im%20Jahr%202030,den%20Ausbau%20der%20Erneuerbaren%20investiert (Accessed 08.12.2022)

[3] EPA, 2014a, Municipal Solid Waste Generation, Recycling, and Disposal in the United States, Tables and Figures for 2012. https://www.epa.gov/sites/default/files/201509/documents/2012_msw_dat_tbls.pdf (Accessed 28.12.2021)

[4] EPA, 2014b, WARM Version 13. https://www.epa.gov/warm/versions-waste-reduction-modelwarm#13 (Accessed 17.12.2021)

[5] European Copper Institute Copper Alliance, 2012, The Environmental Profile of Copper Products: A Cradle to Gate Life-Cycle Assessment for Copper Tube, Sheet and Wire Produced in Europe.

[6] Eurostat, 2017, Glossary: Carbon dioxide equivalent. https://ec.europa.eu/eurostat/statistics-explained/index.php?title=Glossary:Carbon_dioxide_equivalent#:~:text=A%20carbon%20dioxide%20equivalent%20or,with%20the%20same%20global%20warming (Accessed 10.12.2022)

[7] Franklin Associates, 2014, Cradle-To-Gate Life Cycle Inventory of Nine Plastic Resins and Four Polyurethane Precursors. Fronius, 2021, FRONIUS Symo. https://www.fronius.com/~/downloads/Solar%20Energy/Datasheets/SE_DS_Symo_Advanced_EN.pdf (Accessed 17.12.2021)

[8] Gattermeyer M., 2022, Einfluss einer Photovoltaikanlage auf die Ergebnisse einer LCCP Analyse einer Wärmepumpenanlage in einem Einfamilienhaus, Bachelorarbeit, Fachhochschule Technikum Wien

[9] International Institute of Refrigeration (IIR), 2016, Guideline for life cycle climate performance. http://www.cold.org.gr/library/downloads/Docs/Guideline%20for%20life%20cycle%20climate%20performance.pdf (Accessed 15.11.2021)

[10] International Institute of Refrigeration (IIR), 2018, IIR-LCCP-Calculation-Tool-V1.3-Feb2018.xls. (Software)

[11] IPU, 2021, Pack Calculation Pro 5.0. User's guide.

[12] IPU, 2022, Pack Calculation Pro Version 5.1.1.0 64-bit. https://www.ipu.dk/products/pack-calculation-pro/

[13] KPC (2021): Auflistung der Wärmepumpen, die den Mindestanforderungen der EHPA-Gütesiegelkriterien Abschnitt 2.1 „Technical Conditions" der EHPA regulations for granting the international quality label for electrically driven heat pumps in der Version 1.7 vom 07.06.2018 entsprechen. https://www.umweltfoerderung.at/fileadmin/user_upload/media/umweltfoerderung/Uebergeordnete_Dokumente/UEbersicht_Waermepumpen_EHPA.pdf (Accessed 22.12.2022)

[14] Papasavva, S., Hill, W. R., Andersen, S. O., 2010, GREEN-MAC-LCCP: A Tool for Assessing the Life Cycle Climate Performance of MAC Systems.

https://fdocuments.in/reader/full/green-mac-lccp-a-tool-for-assessing-the-life-cycle-climateperformance-of (Accessed 28.12.2021)

[15] Umweltbundesamt, 2022, Berechnung von Treibhausgas (THG)-Emissionen verschiedener Energieträger. https://secure.umweltbundesamt.at/co2mon/co2mon.html (Accessed 13.12.2022)

[16] Zhang, M., Muehlbauer, J., Aute, V., Radermacher, R., 2011, Life Cycle Climate Performance Model for residential heat pump systems. https://www.ahrinet.org/App_Content/ahri/files/RESEARCH/Technical%20Results/AHRTIRpt-09003-01.pdf (Accessed 28.12.2021)

[17] Zottl, A. 2016. GreenHP Final report. https://www.ait.ac.at/fileadmin/mc/energy/downloads/TES/Final_report_GreenHP.pdf (Accessed 13.01.2023).